Modeling and analysis of an ecosystem of bacteria and phages to minimize sludge expansion and foam formation in activated sludge water treatment

María Alejandra Vesga Barón

Pontificia Universidad
Católica de Valparaíso
Facultad de Ingenierías
Escuela de Ingeniería
Bioquímica
Valparaíso, Chile

Université de Mons

Faculté Polytechnique
SECO lab

Mons, Belgique

2025

Modeling and analysis of an ecosystem of bacteria and phages to minimize sludge expansion and foam formation in activated sludge water treatment

María Alejandra Vesga Barón

In partial fulfillment of the requirements for the degree of
Docteur en Sciences de l'Ingénieur et Technologie and
Doctorado en Ciencias de la Ingeniería mención Ingeniería Bioquímica

Supervisors
Prof. Rolando Chamy
Prof. Alain Vande Wouwer

Pontificia Universidad Católica de Valparaíso
Facultad de Ingenierías
Escuela de Ingeniería Bioquímica
Valparaíso, Chile

Université de Mons
Faculté Polytechnique
SECO lab
Mons, Belgique

2025

Members of the Jury

Prof. David Jeison (PUCV), president
Dr. Laurent Dewasme (UMONS), secretary
Prof. Philippe Bogaerts (ULB)
Prof. Sylvain Brohez (UMONS)
Dr. Gilberte Gaval (SUEZ)
Prof. Rolando Chamy (PUCV), supervisor
Prof. Alain Vande Wouwer (UMONS), supervisor

To the little dreamer

Acknowledgments

First, I would like to extend my sincere gratitude to my esteemed advisors, Prof. Alain Vande Wouwer and Prof. Rolando Chamy, whose support, encouragement, and patience led to the satisfactory completion of this thesis. Their willingness to bind practical work and modeling to develop tools for biological treatment based on bacteriophages to wastewater treatment.

I am also pleased to thank Vincent, Laurent, Valentin, Jesus, Maxime, Camilo, Jorge, and Perla, my peers and colleagues from the systems, estimation, control, and optimization lab (SECO) at Mons University.

Special gratitude to my lovely husband. Both of us had the courage to undertake this experience apart, encouraging us with love and making this journey possible together from miles of kilometers of distance between us.

I would also like to express my deepest gratitude to my parents, siblings, and parents-in-law, whose love and support were paramount in developing the thesis. Apart from my family, I want to express my gratitude to my dear "mon cousin qui n'est pas mon cousin" Juan Manuel and Albert, who welcomed me with open arms and gave me the warmth of home, my Belgian family. Finally, I would like to extend a special thank you to my dear friend Paula, whose remarkable strength and steadfast support were fundamental to the successful completion of this work.

Additionally, I would like to thank the Agencia Nacional de Investigación y Desarrollo (ANID) for the grant "Doctorado Nacional" number 21190950 (Chile), the bilateral cooperation project with Wallonia-Brussels International (WBI, Belgium) for financing the three stays at UMONS, and the PUCV grants for the research internship, attendance at conferences, and thesis completion.

Finally, this thesis is dedicated to my future family. When I set out

on this path, I prioritized my dreams, goals, and personal aspirations. I hope that when you read this in the future, we can share the anecdotes that this adventure left me and encourage you to achieve your dreams.

Abstract

Biological wastewater treatment has gained increasing prominence in global environmental concerns. Its operation presents more complex challenges than classical industrial processes, highlighting the need for efficient control strategies. Despite the ever-increasing advanced automation of wastewater treatment processes, open issues still require more analysis and the deployment of new control strategies. Interest in phages' ability to control bacterial populations has extended from medical applications into agriculture, aquaculture, and the food industry. Specifically, several studies have proposed bacteriophages as a promising alternative to control foaming and bulking in wastewater treatment systems. This strategy has shown successful results at the laboratory scale. However, this technology is still in development, and several challenges must be overcome before bacteriophages can be widely used to control foaming and bulking in pilot or larger-scale treatment plants. Bacteriophage treatment for foaming control might be the basis for a more efficient, economical, and sustainable control than the current practice based on chemical treatments.

Assays at the pilot scale involve specifically targeted bacteria. The real-life scenario includes a complex community of microorganisms and certain environmental stress factors that might affect the performance of bacteriophages employed for phage therapy. To include these factors, a thorough study of the treatment plant parameters and microbial community involvement must be performed to implement a large-scale study of phage therapy. Computational modeling is necessary to start phage-based implementation of treatment against bulking and foaming caused by an overgrowth of filamentous bacteria. Several models of the infection mechanisms in individual bacteria-phage pairs have been reported, i.e., for controlled systems with only one bacterial species in the presence of

one phage species. However, activated sludge treatment systems broadly differ from this situation.

This research begins with a literature review on the modeling, analysis, and application of phage-bacteria systems, emphasizing the importance of rigorous model formulation. Mathematical models play a key role in the development process, and the next chapter offers an overview of the proposed models, their structure, advantages, and disadvantages. Then, a candidate model of bacteria and phage populations is proposed that is simple enough to describe experimental results in the context of wastewater treatment and serve as a basis for process control.

The model is evaluated for essential system properties such as stability, identifiability, and observability—key prerequisites for process prediction, monitoring, and dynamic optimization. The development of software sensors based on the model would allow significant advances in monitoring important biological variables, such as the time evolution of filamentous bacteria concentration. It would alleviate the lack of online hardware sensors to achieve such tasks. The well-known Extended Kalman Filter (EKF) is implemented, achieving satisfactory reconstruction of nonmeasured variables.

Moving forward in exploiting the model, optimal control is developed to evaluate the critical parameters of phage therapy, such as phage doses and concentrations. This study demonstrates the feasibility of controlling bacteria that cause operational problems, such as bulking and foaming, in wastewater treatment with an activated sludge system.

The final component of this work integrates the proposed model into a broader framework based on the Activated Sludge Model No. 1 (ASM1), providing a more realistic context for evaluating bacteriophage-based biocontrol strategies within full-scale wastewater treatment operations.

In conclusion, this doctoral research substantially advances the scientific basis for phage therapy as a solution to bulking and foaming in activated sludge systems. The outcomes offer practical tools and insights for implementing phage-based treatments, positioning them as a viable, cost-effective, and environmentally sustainable alternative to traditional chemical controls. By incorporating ecological and physiological system dynamics, this study lays a solid foundation for the future deployment of bacteriophage-based control strategies.

Keywords: Bacteria-Phage model, Extended Kalman Filter, Opti-

mal control, ASM1, activated sludge water treatment.

Resumen

Modelación y análisis de un ecosistema de bacterias y fagos para minimizar la expansión de lodos y la formación de espuma en el tratamiento de aguas con lodos activos

El tratamiento biológico de aguas residuales ha adquirido una importancia cada vez mayor en el ámbito mundial. Su operación no está exenta de problemas más complejos que los procesos industriales clásicos, destacando la necesidad de estrategias de control eficientes. A pesar de que en los procesos de tratamiento de aguas residuales la automatización es cada vez mayor, aún existen problemas que requieren más análisis y la implementación de nuevas estrategias de control. El interés por la habilidad de los fagos para controlar las poblaciones bacterianas se ha extendido desde las aplicaciones médicas a la agricultura, la acuicultura y la industria alimentaria. En particular, varios autores han propuesto el uso de bacteriófagos como método alternativo para controlar la formación de espuma y el abultamiento en el tratamiento de aguas residuales. Esta estrategia ha mostrado resultados satisfactorios a escala de laboratorio. Sin embargo, esta tecnología aún se encuentra en desarrollo y deben superarse varios desafíos antes de que los bacteriófagos puedan utilizarse ampliamente para controlar la formación de espuma y el abultamiento en plantas de tratamiento piloto o de mayor escala. El tratamiento con bacteriófagos para el control del bulking y foaming podría ser la base para un control más eficiente, económico y sostenible en comparación a los tratamientos actuales basados en tratamientos químicos.

Los ensayos a escala piloto se han realizado para bacterias específicas, sin embargo, el escenario de la vida real incluye una comunidad compleja de microorganismos y ciertos factores de estrés ambiental que podrían afectar el rendimiento de los bacteriófagos empleados para la terapia con fagos. Para incluir estos factores, se debe realizar un estudio exhaustivo

de los parámetros de la planta de tratamiento y la participación de la comunidad microbiana para implementar un estudio a gran escala de la terapia con fagos. El modelado computacional es necesario para comenzar la implementación del tratamiento basado en fagos contra el bulking y foaming causados por un crecimiento excesivo de bacterias filamentosas. Se han descrito varios modelos de los mecanismos de infección para el par bacteria-fago, es decir, para sistemas controlados con una sola especie de bacteria en presencia de una especie de fago. Sin embargo, los sistemas de tratamiento con lodos activados difieren ampliamente de esta situación.

Este trabajo comienza con una revisión de la literatura sobre modelado, análisis y aplicaciones de sistemas con fagos y bacterias. Los modelos matemáticos desempeñan un papel fundamental en este proceso de desarrollo, y el siguiente capítulo ofrece una descripción general de los modelos propuestos, su estructura, ventajas y desventajas. Luego, se propone un modelo candidato de poblaciones de bacterias y fagos que es lo suficientemente simple para describir resultados experimentales en el contexto del tratamiento de aguas residuales y servir como una base para el control de procesos.

El modelo se evalúa en cuanto a sus propiedades, como estabilidad, identifiabilidad y observabilidad, que son esenciales para la predicción, control y optimización de procesos. El desarrollo de sensores de software basados en el modelo permitiría avances significativos en el monitoreo de variables biológicas importantes, como la evolución temporal de la concentración de bacterias filamentosas. Aliviaría la falta de sensores de hardware en línea para lograr tales tareas. Se implementó el conocido filtro de Kalman extendido (EFK, por sus siglas en inglés), logrando una reconstrucción satisfactoria de variables no medidas.

Avanzando en el aprovechamiento del modelo, se desarrolla un control óptimo para evaluar los parámetros críticos de la terapia con fagos, como las dosis de fagos y concentraciones. Este estudio demuestra la factibilidad de controlar las bacterias que causan problemas operacionales, como el bulking y foaming, en el tratamiento de aguas residuales con un sistema de lodos activados.

El paso final de la tesis es la inclusión del modelo en un modelo completo de lodos activados, según ASM1, con el fin de proporcionar una visión más realista del uso de bacteriófagos como estrategia de biocontrol.

Palabras clave: Modelo bacteria-fago, Filtro de Kalman Extendido, Control óptimo, ASM1, Tratamiento de aguas con lodos activos.

Motivation and Contribution

This work is part of a context of technological and scientific innovation in industrial biotechnologies, the environment, biological water purification, and sustainable development through the development of processes with optimized operation (in particular, eliminating the phenomena of sludge expansion and foam formation in biological water purification processes). This research axis is in line with environmental and energy policies worldwide. Activated Sludge (AS) is a technique widely used in the public and industrial sectors. In addition, this process plays an important role in biorefineries.

Despite the high efficiency of aerobic treatment systems, one of the most critical operational challenges is the proliferation of filamentous bacteria, which can occur for various reasons, including low dissolved oxygen concentration, low nutrient-to-biomass ratio, or nitrogen and phosphorus deficiencies. The growth of filamentous bacteria can prevent the sludge from settling properly (sludge bloom) or can generate persistent foams, up to 1 m thick in extreme cases, covering the aeration basins. As a result, some of the sludge may leave the sedimentation system, contaminating the treated water. Various methods can control filamentous organisms, such as adding chlorine or hydrogen peroxide, changing the dissolved oxygen concentration in the aeration basin, adding growth factors, inorganic talc, or coagulating polymers. However, these strategies have not proven effective in all cases, have high associated costs, and can affect effluent quality.

A biological method is an attractive control technique compared to chemical treatments. The AS processes involve the interaction of countless microorganisms that work together to purify water. Among the microorganisms present, the presence of bacteriophages (viruses that infect and lyse bacteria) can be highlighted, which, although their concentration

is low compared to bacteria, are present in the system. Bacteriophage treatment for foaming control in wastewater systems has been effective in some experimental studies. However, given the complexity of the AS system, the full understanding of the system and the phenomena involved remains unknown.

Applying phage therapy to wastewater treatment requires a better understanding of the dynamics and interactions of the microbial community in wastewater. A mathematical model could describe the temporal evolution of bacterial and bacteriophage populations and the infection phenomenon, making it an attractive tool for study. A dynamic model is helpful in an industrial context because it helps operate the plant and allows for optimizing the production of phages on an industrial scale, ensuring the treatment's economic viability.

This study aims to include an infection mechanism in the existing AS models for a system with foaming and bulking problems. The model will be developed as an extension of existing activated sludge models commonly used in industry. The general goal is to develop a mathematical model that describes the interaction between bacteria and their predators (phages). It could be used for process control, providing non-measured variables and critical system parameters in foaming and bulking treatment in domestic wastewater.

As a contribution of this work, the mathematical model for the pair bacteria-phage allows the recreation of non-measured variables from implementing the state observer EFK. Besides, phage doses and concentration, critical parameters for phage therapy implementation, could be evaluated from a simple optimal control.

All this work is possible thanks to a collaboration between PUCV (Chile) and UMONS (Belgium). This scientific cooperation was an opportunity to link a biological solution to a current industrial problem with modeling tools to contribute to its application at the industrial level, where the Belgian and Chilean teams worked together effectively. In addition to the contribution of this work, the following conferences were presented.

- November, 2024. Vesga, M; Chamy, R; Vande Wouwer. Uso de bacteriófagos en PTAS: desarrollo de observador EFK y control óptimo mediante modelos matemáticos. XXXIX Congreso Interamericano AIDIS 2024. Lima, Perú.

- November, 2023. Vesga, M; Chamy, R; Vande Wouwer. Uso de bacteriófagos en PTAS: Análisis de observabilidad y desarrollo de observador de estado clásico (EFK). XXV Congreso Chileno de Ingeniería Sanitaria y Ambiental (AIDIS). Coyhaique, Chile. (Oral)

- November, 2022. Vesga, M; Chamy, R; Vande Wouwer. Uso de bacteriófagos en PTAS: Determinación de los parámetros de operación en la producción de bacteriófagos. XXXVIII Congreso Interamericano AIDIS 2022. República dominicana. (Oral)

- November, 2021. Vesga, M; Chamy, R; Vande Wouwer, A. Uso de bacteriófagos en PTAS: Evaluación mediante modelos matemáticos. XXIV Congreso chileno de ingeniería sanitaria y ambiental. Santiago, Chile (Virtual). (Oral)

Additionally, this work led to the publishing of

- Vesga-Baron, Alejandra; Chamy, Rolando; Vande Wouwer, Alain. et al. (2022). Minimizing foaming and bulking in activated sludge with bacteriophage treatment: a review of mathematical modeling. Processes, 10(8), 1600.

Contents

List of Figures

List of Tables

List of acronyms

ABAC Ammonia-Based Aeration Control

ARB Antimicrobial Resistant Bacteria

ARG Antimicrobial Resistance Gene

AS Activated Sludge

ASM1 Activated Sludge Model No. 1

ASM2d Activated Sludge Model No. 2d

ASP Activated Sludge Process

BDF Backward Differentiation Formula

BOD Biological Oxygen Demand

BWT Biological Wastewater Treatment

CFU Colony Forming Unit

COD Chemical Oxygen Demand

DDE Delay Differential Equations

DO Dissolved Oxygen

DT Digital Twin

EKF Extended Kalman Filter

F/M Food to Microorganism ratio

FISPO Full Input-State-Parameter Observability

FOG Fats, Oil, and Grease

GAO Glycogen Accumulating Organisms

ISE Ion Selective Electrode

MOI Multiplicity of Infection

MHE Moving Horizon Estimation

MPC Model Predictive Control

ODE Ordinary Differential Equation

PAO Polyphosphate Accumulating Organisms

PFR Plug Flow Reactor

PFU Plaque Forming Unit

PI Proportional–Integral

PID Proportional–Integral–Derivative

SBR Sequencing Batch Reactor

SEM Scanning Electron Microscope

SRT Solid Retention Time

TOC Total Organic Carbon

TSS Total Suspended Solids

UV Ultraviolet

VSI Sludge Volume Index

VSS Volatile Suspended Solids

WWT Wastewater Treatment

WWTP Wastewater Treatment Plant

List of parameters and symbols

Greek symbols

β	Burst size (phage or particulate, ASM1)
γ	Death rate of bacteria
δ	Adsorption rate (infection rate constant)
η	Lysis rate of infected bacteria
η_g	Anoxic growth correction factor (heterotrophs, ASM1)
η_h	Anoxic hydrolysis correction factor (ASM1)
λ	Weighting factor in cost function
λ_i	Eigenvalue (Jacobian, local stability)
μ	Specific growth rate
μ_{max}	Maximum specific growth rate (general; or for ASM1 as μ_H, μ_A)
μ_H	Maximum specific growth rate of heterotrophs (ASM1)
μ_A	Maximum specific growth rate of autotrophs (ASM1)
ν_P	Decay/inactivation rate of free phages
ν_S	Yield coefficient (substrate to biomass)
ρ	Recovery rate of infected bacteria (literature review)
σ	Sensitivity coefficient
τ	Latency period (delay parameter in DDE)
ϕ	Natural phage decay rate (alternative notation)

Latin symbols

$\mathbf{A}$	Jacobian matrix (local stability analysis)
b_A	Decay rate of autotrophic biomass (ASM1)
b_H	Decay rate of heterotrophic biomass (ASM1)
$\mathbf{D}$	Dilution rate
D_P	Phage dilution rate (input flow)
f_P	Fraction of biomass yielding particulate products (ASM1)
$\mathbf{F}$	Total flow (substrate + phage)
F_P	Phage flow (input)
F_S	Substrate flow (input)
k_a	Ammonification rate (ASM1)
k_x	Decay rate constant (biomass)
k_d	Decay rate constant (general)
k_h	Hydrolysis rate constant (ASM1)
$K_L a$	Volumetric oxygen transfer coefficient (ASM1)
K_M	Half-saturation coefficient (Monnod)
K_{NH}	Half-saturation for NH_4^+–N (ASM1)
K_O	Half-saturation constant for oxygen
K_{OA}	Oxygen half-saturation for autotrophs (ASM1)
K_{OH}	Oxygen half-saturation for heterotrophs (ASM1)
K_{NO}	Nitrate half-saturation (ASM1)
K_S	Substrate half-saturation
K_X	Hydrolysis half-saturation (ASM1)
$\mathbb{m}$	Maintenance rate of infected bacteria
$\mathbf{P}$	Free phage concentration
P_{in}	Phage concentration in input (optimal control)
Q_{in}	Influent flow rate (ASM1)
Q_r	Recirculation flow rate (ASM1)
Q_w	Waste flow rate (ASM1)
$\mathbf{S}$	Substrate concentration
S_{ALK}	Alkalinity (ASM1)
S_I	Soluble inert organic matter (ASM1)
S_{in}	Influent substrate concentration
S_{ND}	Soluble biodegradable organic nitrogen (ASM1)
S_{NH}	Ammonium plus ammonia nitrogen (ASM1)
S_{NO}	Nitrate and nitrite nitrogen (ASM1)

S_O	Dissolved oxygen (ASM1)
S_{Osat}	Oxygen saturation concentration (ASM1)
S_S	Readily biodegradable substrate (ASM1)
t	Time
V_R	Reactor volume (ASM1)
V_S	Settler volume (ASM1)
$\mathbf{x}$	State vector (e.g., x = [X_S, X_I, P, S])
$\overline{x}$	Equilibrium state vector
X	General bacteria concentration
X_{BA}	Active autotrophic biomass (ASM1)
X_{BH}	Active heterotrophic biomass (ASM1)
$X_{BH,NS}$	Non-susceptible heterotrophic biomass (phage-modified ASM1)
$X_{BH,S}$	Susceptible heterotrophic biomass (phage-modified ASM1)
$X_{BH,I}$	Infected heterotrophic biomass (phage-modified ASM1)
X_I	Infected bacteria concentration
$X_{I,ASM}$	Inert particulate organic matter (ASM1)
X_{max}	Carrying capacity (logistic model)
X_{ND}	Particulate biodegradable organic nitrogen (ASM1)
X_P	Particulate products from biomass decay (ASM1)
X_S	Susceptible bacteria concentration
$X_{S,ASM}$	Slowly biodegradable substrate (ASM1)
X_T	Total bacteria concentration
Y_H	Yield coefficient for heterotrophs
Y_A	Yield coefficient for autotrophs

Chapter 1

Introduction

Clean, accesible water for all is an essential part of the world we want to live in, and there is enough freshwater on the planet to achieve this. However, more than 2 billion people are living with the risk of reduced access to freshwater resources, and by 2050, at least one in four people is likely to live in a country affected by chronic or recurring shortages of freshwater. Although water use efficiency has risen by 9%, water stress and water scarcity remain a concern in many parts of the world. In 2020, 2.4 billion people lived in water-stressed countries. Also, the challenges are compounded by conflicts and climate change. Drought afflicts some of the world's poorest countries, worsening hunger and malnutrition (United Nations, 2019, 2023).

Substantial progress has been achieved over the past decade in improving access to safe drinking water and sanitation. Currently, more than 90% of the global population benefits from improved drinking water sources (United Nations, 2019). Between 2015 and 2022, the proportion of the world's population with access to safely managed drinking water services increased from 69 to 73 %; safely managed sanitation services increased from 49 to 57 %; and basic hygiene services increased from 67 to 75 % (United Nations, 2023).

Despite significant progress, billions of people still lack universal coverage with access to safe drinking water, sanitation, and hygiene. Achieving by 2030 will require a substantial increase in current global rates of progress: sixfold for drinking water, fivefold for sanitation, and threefold for hygiene (United Nations, 2023).

Data from 2017–2020 indicate that 60 % of assessed water bodies

in 97 countries with robust monitoring systems had good ambient water quality. However, a lack of data poses a risk to more than 3 billion people living in areas where freshwater quality is unknown. Agriculture and untreated wastewater are significant threats to water quality, with nitrogen and phosphorus measurements frequently failing to meet targets. Efforts are needed to improve farming practices and wastewater treatment, especially in regions with high population growth (United Nations, 2023).

Progress towards the target of halving the proportion of untreated wastewater by 2030 is limited. Based on data from 140 countries and territories, about 58 % of household wastewater was safely treated in 2022. However, wastewater statistics are lacking in many countries, and reporting is low, especially from industrial sources (United Nations, 2023). It is estimated that more than 80% of wastewater resulting from human activities is discharged into rivers or sea without any pollution removal, which generates concern (United Nations, 2019).

Therefore, wastewater treatment, which removes contaminants from wastewater or sewage and converts it into an effluent that can be returned to the water cycle with minimum environmental impact or directly reused, is receiving increasing interest.

1.1 Activated sludge system

The Activated Sludge (AS) process has been used to treat industrial and municipal wastewater for nearly a century and is currently the most widely implemented wastewater treatment method. The AS is a natural biological treatment process that imports many microorganisms. It is a complex mix of microbiology and biochemistry.

The infrastructure of a basic Activated Sludge Process (ASP) (Figure 1.1) consists of (Hreiz et al., 2015):

- A single bioreactor operated continuously, where suspended microorganisms consume the colloidal and dissolved organic matter. The reactor is aerated to provide dissolved oxygen (DO) for aerobic biodegradation. Bacteria consume one part of the colloidal and dissolved carbonaceous compounds to satisfy their energetic needs (catabolism), and synthesize another part – along with a small proportion of ammonium and phosphorus – into new cellular tissues (anabolism).

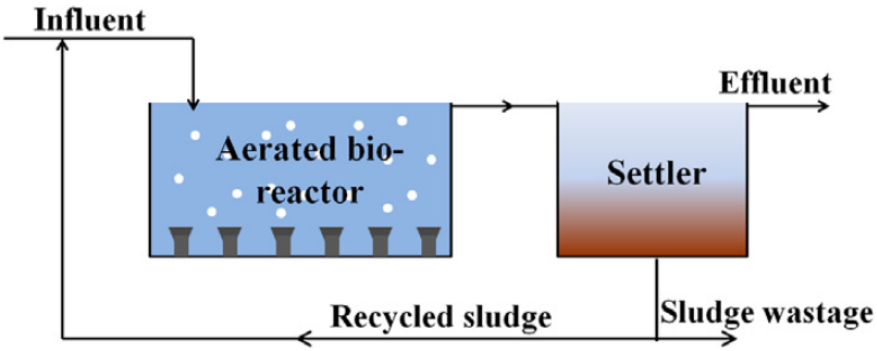

Figure 1.1: The basic ASP.

- A settling tank (referred to as secondary settler or clarifier) where activated sludge (flocculated biomass) is gravitationally separated from the treated wastewater. The effluent overflows into the receiving water body, but in some Wastewater Treatment Plants (WWTPs), it may undergo additional treatments (e.g., filtration and disinfection) before being discharged. A minimum solid retention time (SRT, also referred to as 'sludge age') of about 3 days is required for bacteria to aggregate into flocs (bio-flocculation) so as to enable their gravitational separation.

- A sludge recycle line returns most of the settled sludge to the bioreactor, maintaining a high bacterial concentration in the reactor and intensifying the biological nutrient removal.

- A sludge wastage line at the bottom of the clarifier, from where a small fraction of sludge is withdrawn in order to stabilize the biomass concentration in the bioreactor and to fix an adequate SRT. The excess sludge withdrawn is then treated separately.

The basic principle in the process consists of contacting the wastewater with a mixed population of microorganisms in the form of a floc suspension in an aerated, agitated system. Suspended and colloidal material is quickly eliminated from the wastewater by adsorption and agglomeration in the microbial flocs. The oxidative process provides the energy required for the adsorption and assimilation processes. Once the desired

treatment level is reached, the microbial floc mass, i.e., the "sludge," is subsequently separated from the water by sedimentation. The breakdown of organic material via the aerobic pathway is divided into three major phases: the hydrolysis of complex organic molecules into their respective monomers; the decomposition of these monomers into common intermediates, and, finally, the introduction of these intermediates into the Krebs cycle and the respiratory chain, where the final electron acceptor is molecular oxygen, forming water as the final product along with carbon dioxide and ammonia. AS systems can reach organic material removal rates between 85% and 98% at the end of secondary treatment (Wang et al., 2010).

1.2 Activated sludge microbiology

The AS process purifies water through the oxidation of organic material present in the wastewater by diverse aerobic microorganisms, transforming this material into a more stable form, thereby lowering the organic load. Microscopic examination of this sludge reveals that it is formed from a heterogeneous population of microorganisms, which change continuously due to variations in wastewater composition and environmental conditions. The microorganisms that constitute the AS are protozoans, fungi, algae, filamentous organisms, viruses, and bacteria, the latter ones being the dominant group responsible for the more significant part of the process (90% to 95%) (Fan et al., 2017). More than 300 species of bacteria have been isolated from AS systems. The main bacterial populations operating in AS systems are heterotrophs, nitrifiers, denitrifiers, polyphosphate, and glycogen-accumulating organisms (PAO and GAO, respectively). These microorganisms are important in terms of both their function and competition with filamentous bacteria, which often cause serious problems in the AS process (Tandoi et al., 2017).

The bacteria responsible for the oxidation of organic material and nutrient transformation produce polysaccharides and other polymeric materials that aid biomass flocculation. The principal genera are: *Zooglea, Pseudomonas, Flavobacterium, Alcaligenes, Bacillus, Corynebacterium, Achromobacter, Comomonas, Brevibacterium, Acineto bacter*, filamentous organisms (*Sphaerotilus, Beggiatoa*), autotrophic nitrifying bacteria (*Nitrosomonas and Nitrobacter*), and phototrophic sulphur bacteria

(*Rhodospirillaceae*). Some bacteria are capable of connecting with each other to form flocs, an important characteristic of ASs that allows for a highly efficient secondary sedimentation process and, therefore, greater transparency and higher quality in the final effluent. Filamentous bacteria are also common in ASs, and a moderate presence of these organisms contributes to proper consistency in the flocs; the main foaming genera are: *Corynebacterium, Dietzia, Gordonia, Skermania, Mycobacterium, Nocardia, Rhodococcus, Microthrix* y *Tsukamurella* and the principal bulking genera are *Microthrix parvicella* and *Sphaerotilus natans* (Jiang et al., 2008; Yang et al., 2017). Viral communities in the AS systems are incredibly diverse. Compared to bacterial community analysis, research on viral communities in wastewater or wastewater treatment systems is limited. There is an estimated amount of 108-109 phages genotypes in 1 mL of actived sludge, which is a number comparable to or greater than the number of phages found in most of the aquatic systems (Suttle, 2007). In general, the prevailing conditions in an AS system do not favour the growth of fungi. However, under some circumstances, filamentous fungi are observed. Fungal growth can be favoured under low pH, toxicity, and in nitrogen-deficient effluents. Protozoans are organisms belonging to the *Protistaç* kingdom and are bacteria predators. The main groups are: *Ciliates, flagellates, rhizopods*, and *amoeboids*. Rotifers are multicellular organisms that have sizes between 100 and 500 microns. Those present in ASs belong to two principal orders: *Bdeloidea* (*Philodina* and *Habrotocha*), and *Monogononta* (*Lecane* and *Notomata*). The role of rotifers in ASs is to remove the suspended bacteria outside the flocs and contribute, though their wastes, to floc formation (Moeller et al., 2018).

1.3 Activated Sludge problems

Despite the significant efficiency of AS treatment, the process is not without problems. The most critical operational difficulties are bulking and foaming, caused by the increase in the growth of filamentous bacteria. An increase in filamentous bacteria can prevent the sludge from settling appropriately (sludge bulking) or can generate persistent foams, up to 1 m thick in extreme cases. This growth can occur for various reasons, including low dissolved oxygen concentration, the low ratio of food to a unit of biomass (F/M ratio), and nutritional deficiency (nitrogen or

phosphorus) (Richard et al., 2003; Wu et al., 2015).

In the bulking process, the sludge in the aeration basin does not settle and develops a biological foam on the surface. Bulking can be caused by the growth of filamentous organisms that do not settle and filamentous organisms that form foams due to the large volumes of water assimilated in their cellular structure (figure 1.2)(Jenkins et al., 2004). In the foaming process, the foam is characterized as persistent, viscous, and brown in color. Due to these problems, the effluent is contaminated, the aeration basin population drops because the sludge cannot be recirculated, and noxious odors are formed when the foam (which contains organic material) is degraded outside of the AS system (Madoni et al., 2000; Ding et al., 2015).

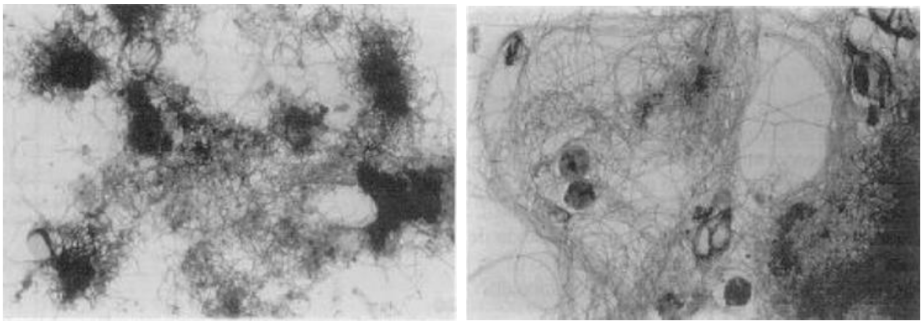

(a) Filamentous organisms that do not settle

(b) Filamentous organisms that form foams

Figure 1.2: Characteristic examples of filamentous organisms that can develop in the AS process and affect the sedimentation of the suspended solids in the mixed liquor.

Filamentous organisms may be controlled through various methods, including the addition of chlorine or hydrogen peroxide to the recycled AS, regulating dissolved oxygen concentration in the aeration basin; alteration of the waste influent points in the aeration basin, to modify the F/M ratio; addition of principal nutrients (such as nitrogen and phosphorus); addition of trace metals, nutrients, and growth factors; and, more recently, addition of inorganic talc or coagulating polymers. Non-specific methods have a temporary effect. They are useful when the cause of the filamentous bacteria cannot be determined immediately and when

a rapid resolution of the problem is needed. Nevertheless, specific control methods are usually more desirable because only when the cause is addressed can the plant be operated with limited filament proliferation (Tandoi et al., 2017).

Examining the problem's causes is necessary to approach the problem correctly. In activated sludge processes characterized by a low F/M ratio ($0.05-0.10\,kg_{COD}\,kg^{-1}\,VSS\,d^{-1}$), the concentration of Chemical Oxygen Demand (COD) in the aerobic tank is very low, especially in the case of a completely mixed tank reactor. At these low substrate concentrations, the growth of filaments is favored with respect to floc-forming bacteria. In this sense, because lower F/M values are associated with higher COD removals, the bulking associated with low substrate concentration is also linked to a good activated sludge performance. In order to solve (or avoid) the problem without affecting substrate removal in the plant, the most useful strategy is to create a substrate concentration gradient inside the aeration tank reactor (or at least the presence of zones with different substrate concentrations). To achieve this goal, it would be necessary to modify the activated sludge process configuration, which would increase the cost and the complexity of the operation (Tandoi et al., 2017).

One of the most frequent causes of filamentous bulking is low dissolved oxygen (DO) concentration in the aeration tank. Similar to the low F/M (Food to Microorganism ratio) case. A correlation between organic loading and minimum DO concentration is needed to avoid filamentous accumulation. Values of DO concentrations required to avoid filament proliferation should be calculated, which involves a proper aerator design (Tandoi et al., 2017).

The term 'nutrient' in activated sludge systems usually refers to chemical elements other than carbon, oxygen, sulfur, and nitrogen that are essential for biomass synthesis. Nutrients needed in major amounts are nitrogen (N) and (P) phosphorus. Domestic wastewater is normally rich in nutrients (hence, N and P often have to be removed by additional processes). Previous reports (Wagner (1982); Richard et al. (1985); Simpson et al. (1991); Switzenbaum et al. (1992)) showed that filament growth is enhanced with respect to floc-former growth when N and P levels are low. When the problem can be definitely related to nutrient deficiency, the control method is to add the deficient nutrient, and it is easily implemented (Tandoi et al., 2017).

Microthrix parvicella is a filamentous bacterium that causes either bulking or severe foaming problems in domestic WWTPs worldwide. Its growth is particularly difficult to prevent. Most of the work performed on this bacterium shows that it is enhanced by low temperatures and the presence of long-chain fatty acids in the influent. Studies have also shown that it can only grow under aerobic or microaerophilic conditions. The most frequently used technique for controlling *M. parvicella* has been the use of anoxic selectors. Moreover, the addition of polyaluminium chloride was proposed, which interferes strongly with the growth of the filament*M. parvicella* by causing either a flocculating or a specific toxic effect. This strategy is now largely adopted worldwide (Eikelboom, 1991; Tandoi et al., 2017).

The factors leading to sludge bulking are often unidentified, so non-specific control methods are widely used. These methods can be the first method of controlling bulking before a cause-and-effect relationship is found and a specific control method is implemented. Nonspecific control methods usually consist of adding chemicals, such as oxidizing agents (chlorine, ozone, hydrogen peroxide), weighting and flocculating agents (salts of iron and aluminum, lime, polymers, and talc), and specific biocide (Tandoi et al., 2017).

The most widely used biocide agent is Cl_2. It is also the oldest control measure against bulking. The amount of chlorine fed to activated sludge systems varies in the range of 1–15 $g\,Cl_2\,kg^{-1}\,VSS\,d^{-1}$. The aim of oxidizing agents (biocides) is to kill filamentous organisms without affecting floc-formers. Because of its potentially deteriorative effects on floc-formers, the correct choice of addition point and of the amount of toxicant added should be carefully chosen. The best performance is usually obtained by adding the toxicant to the return sludge stream because of the higher amount of solids that are exposed to it. In addition to the daily dosage of the biocide, other important parameters in the dosage strategy are the concentration of the biocide at the dose point and the frequency of exposure of activated sludge to the chlorine dose. The addition of chlorine to AS systems has caused some concerns about possible effluent quality deterioration due to the formation of halogenated organic compounds (Tandoi et al., 2017).

Although several technical strategies exist for controlling bulking and foaming problems, e.g., the addition of chlorine or hydrogen peroxide to

the recycled AS, regulating dissolved oxygen concentration or the waste inflow in the aeration basin to modify the F/M ratio, the addition of principal nutrients (such as nitrogen and phosphorus) or trace metals and growth factors, and, more recently, the addition of inorganic talc or coagulating polymers, they have not been proven effective in all cases. Their associated costs are relatively high, and their use affects the effluent quality, even when they are effective (Shao et al., 1997; Roels et al., 2002; Nielsen et al., 2005; Paris et al., 2005; Noutsopoulos et al., 2006; Mamais et al., 2011). At the industrial level, large amounts of chlorine are used. Adding chlorine is effective in 63% of cases. Still, it can potentially create toxic chlorinated organic compounds in low concentrations and, therefore, can be counterproductive to the water treatment process. Manipulation of the sludge recycling flow and increasing the aeration to control filamentous bacteria have associated operational costs and have not been shown to be effective considering the complexity of the treated influent (Madoni et al., 2000; Séka et al., 2001; Wu et al., 2015).

1.4 Biological treatment

The addition of microbial and enzymatic preparations to control filamentous bacteria has been significantly more limited compared to the use of biocides and flocculating agents. Some authors have demonstrated the elimination of selectively filamentous bacteria through this form of 'Biological Control.' A new and promising field involves the use of phages (viruses) that specifically target filamentous bacteria. This approach seems quite promising as a form of 'Biological Control' without any chemical additives, but currently, there are no full-scale applications (Tandoi et al., 2017).

Bacteriophages are viruses that infect and lyse bacteria. Interest in the ability of phages to control bacterial populations has extended from medical applications into the fields of agriculture, aquaculture and the food industry. Figure 1.3 shows the exponential growth in the studies related to phages over the years and how their interest in wastewater treatment has been increasing in recent years. Phage treatments have the potential to control environmental wastewater process problems such as foaming and bulking in activated sludge plants(Abedon et al., 2011a; Kotay et al., 2011; Endersen et al., 2014; Madhusudana Rao and Lalitha,

2015; Yang et al., 2017; Buttimer et al., 2017; Doss et al., 2017; Sharma et al., 2017; Plaza et al., 2018; Svircev et al., 2018; García et al., 2019; Sieiro et al., 2020; Nachimuthu et al., 2021).

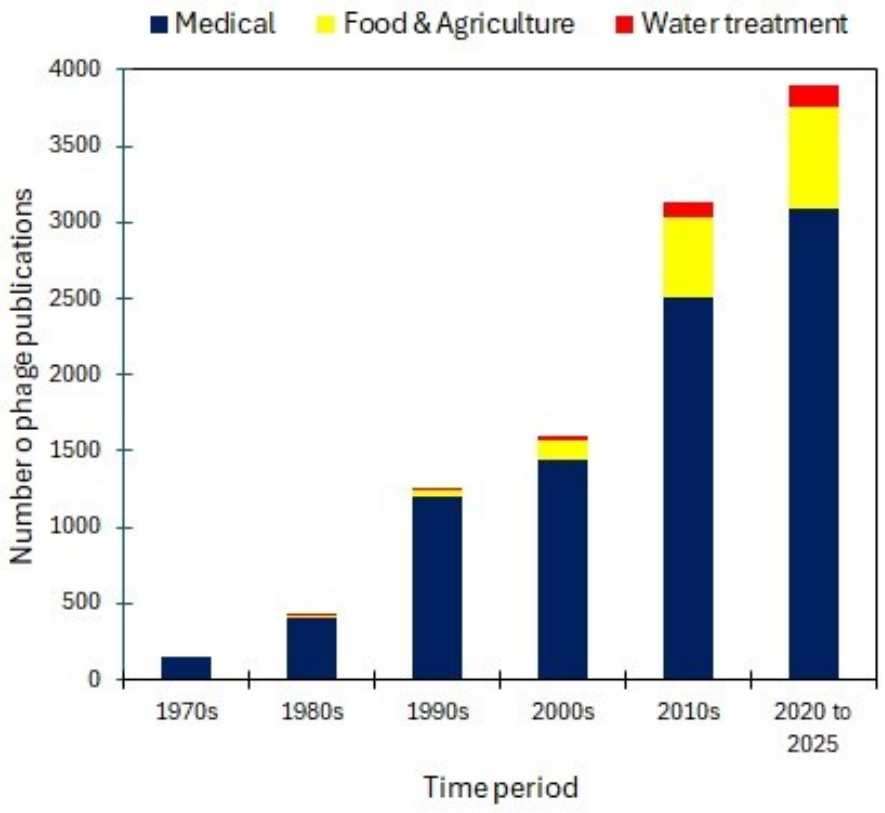

Figure 1.3: Exponential increase in phage application-related publications over the past decades. NCBI PubMed results for the number of yearly publications from 1970 to 2025.

Bacteriophages are usually prepared at a laboratory scale in shake flasks. These protocols are adjusted to batch cultures with low cell densities and regulatory conditions, producing low phage concentrations. Despite the low phage density generated in batch mode, when a higher bacteriophage concentration is required, the shake flasks are replaced by bioreactors operating in batch mode (Abedon et al., 2011a; Buttimer

et al., 2017; Plaza et al., 2018; Endersen et al., 2014). Although batch mode is operationally simpler than continuous mode, sterile conditions at higher cell densities entail increased cost (Podgornik et al., 2015). The potential application of phage techniques in wastewater treatment systems to improve effluent and sludge emissions into the environment has not been well studied. Phage treatments have the potential to control environmental wastewater process problems such as foaming and bulking in activated sludge plants (Kotay et al., 2011; Yang et al., 2017).

Viral communities in the AS systems are incredibly diverse. Compared to bacterial community analysis, research on viral communities in wastewater or wastewater treatment systems is limited. There is an estimated amount of 108-109 phage genotypes in 1mL of activated sludge, which is a number comparable to or greater than the number of phages found in most aquatic systems (Suttle, 2007). Therefore, using phage to control environmental wastewater processes such as foaming and bulking in activated sludge plants could improve effluent and sludge emissions into the environment (Choi et al., 2011; Yang et al., 2017).

There are several academic studies where the use of bacteriophages is proposed to treat bulking or foaming in activated sludge plants as a biological control, unlike the traditional chemical treatment. In these studies, the use of bacteriophages has been validated to eliminate the foaming-producing filamentous bacteria, such as *Haliscomenobacter hydrossis, Sphaerotilus natans, Tetrasphaera jenkinsii, Gordonia, Beggiatoa, Nocardia*, and *Nostocoida limícola*. The lytic phages for these bacteria can be isolated from active sludge systems such as the GTE7 phage (*Siphoviridae* family) that has lytic activity on the Gordonia species and some Nocardia species, which reduces the number of bacterial cells causing foaming below the threshold required for a stable foam to occur. As we can see in Table 1.1, bacteriophages can infect a single or multiple hosts (Choi et al., 2011; Petrovski et al., 2011).

However, the successful application of phage therapy to wastewater treatment does require further understanding of wastewater microbial community dynamics and interactions. Success would also depend on the accurate identification of problem bacteria, effective isolation and unbiased enrichment of phages, and the ability of phages to penetrate flocs and remain infective in situ. Strategies to counter host cell resistance must also be developed. Furthermore, safety considerations, such as risk

Table 1.1: Bacteriophages capable of lysing filamentous bacteria model.

Filamentous bacteria model	**Bacteriophage**	**Authors**
Haliscomenobacter hydrossis, Sphaerotilus natans	SN-phage	Choi et al. (2011)
Gordonia terrae, Gordonia malaquae, Gordonia australis, Gordonia amictia and Nocardia nova, Nocaridia asteroides	GTE7	Petrovski et al. (2011) Liu et al. (2015)
Skermania piniformis Sphaerotilus natans	SPI1	Dyson et al. (2015)
Haliscomenobacter	Phage from *Myoviridae* family	Kotay et al. (2011)

of pathogen emergence through transduction, must be assessed together with the cost–benefit and reliability of treatments. Thus, substantial research is required before the phage therapy can be applied successfully to wastewater treatment plants. With a greater understanding of the microbial ecology of wastewater treatment systems, phages may become effective solutions to wastewater treatment problems and optimization (Withey et al., 2005; Cairns et al., 2009; Liu et al., 2015).

Chapter 2

Reported applications of bacteriophages

2.1 Origins of bacteriophages - First Applications

In 1896, Ernest Hankin observed that the Ganges and Jumna rivers in India exhibited antibacterial properties. He hypothesized that these properties contributed to a reduced incidence of gastrointestinal infections, particularly cholera, in villages near the rivers. Building upon these observations, Frederick Twort first identified bacteriophages in 1915. His research aimed to cultivate filterable viruses in vitro using a variety of bacterial cultures and media. Independently, in 1917, Félix d'Herelle also discovered bacteriophages while investigating pest control in Mexico through the bacterium *Coccobacillus sauterelles*. He observed clear zones on bacterial cultures, which he attributed to an infection by an "ultramicrobe" (Hankin, 1896; Twort, 1961; d'Herelle, 1961; Abedon et al., 2011b; Maura and Debarbieux, 2011; Harper et al., 2021)

The historical development of bacteriophage research can be divided into three phases. The first phase began with d'Herelle's work, who believed that phages played a central role in the recovery from infectious diseases. In his studies on patients recovering from dysentery and typhoid, he noted an increase in phage titers and concluded that this was due to the adaptation and multiplication of lytic phages, which lysed the causative pathogens. Based on these findings, he proposed the use of

phages as therapeutic and prophylactic agents in a wide range of bacterial infections, leading to the foundation of "phage therapy", involved the application of phage-based treatments to diseases affecting the skin, intestines, respiratory, and genital systems, resulting in the commercialization of several therapeutic formulations and attracting pharmaceutical interest (d'Herelle, 1961; Kutter and Sulakvelidze, 2004; Dublanchet and Fruciano, 2008; Maura and Debarbieux, 2011).

Initial veterinary applications demonstrated phage efficacy in managing avian typhosis and *Bacillus gallinarum* infections in chickens, significantly reducing mortality rates and epidemic duration. Field trials against hemorrhagic septicemia in water buffaloes (barbone)—a highly fatal disease—produced similarly encouraging results. These successful applications in veterinary medicine prompted further trials in human healthcare (Harper et al., 2021).

Phage therapy was also used in the management of cholera. In India, cholera-specific phage preparations were added to drinking water supplies as a preventative measure. Patients treated orally with these phages experienced reductions in disease severity, symptom duration, and mortality. In several WHO-sponsored studies during the 1970s, phage therapy was found to be comparable to tetracycline in some clinical aspects of cholera control (d'Herelle, 1925; Marčuk et al., 1971; Monsur et al., 1970; Kutter and Sulakvelidze, 2004).

For nearly a century, clinical trials of phage therapy were conducted in Eastern Europe, particularly at the Eliava Institute of Bacteriophage. The institute extensively explored the preclinical and clinical application of phages against common bacterial pathogens including *Staphylococcus aureus, Escherichia coli, Streptococcus spp., Pseudomonas aeruginosa, Proteus spp., Shigella dysenteriae, Salmonella spp.*, and *Enterococcus spp.*(Lin et al., 2017).

However, early trials suffered from methodological flaws due to limited understanding of phage biology and inadequate protocols, leading to inconsistent outcomes. With the advent of antibiotics in the 1940s, phage therapy was largely abandoned in Western medicine, although it remained in use in Eastern Europe and the former Soviet Union, particularly for antibiotic-resistant infections involving *Staphylococcus, Pseudomonas, Klebsiella*, and *E. coli* (Carlton, 1999; Weber-Dąbrowska et al., 2001; Lin et al., 2017).

Beyond medical applications, bacteriophages have proven useful in agriculture, aquaculture, and food safety, especially where bacterial contamination presents a persistent risk. These broader applications began to emerge in the 1940s, with both successful and unsuccessful results reported. Phages are now studied for their ability to control foodborne pathogens on processing surfaces, reducing contamination and enhancing food safety. Unlike chemical sanitizers, which may be corrosive or toxic, phages offer a biologically selective and environmentally benign alternative (d'Herelle, 1926; Kutter and Sulakvelidze, 2004; Maura and Debarbieux, 2011).

Phages have been shown to reduce *Salmonella enteritidis* contamination on poultry skin through high-titer phage sprays, effectively eliminating detectable bacterial loads (Goode et al., 2003; Withey et al., 2005; Harper et al., 2021). Various companies have developed phage-based disinfectants targeting *Salmonella, E. coli*, and *Listeria monocytogenes*. Future applications are expected to expand throughout the food production chain, including agricultural and aquacultural settings, where phages may mitigate losses from bacterial pathogens (Buttimer et al., 2017; García et al., 2019)

The second phase of phage research, initiated in the 1940s, was marked by fundamental contributions to molecular biology. Phages became model organisms in studies of viral replication, genetic recombination, and host interactions (Summers, 1999; Maura and Debarbieux, 2011). Max Delbrück's pioneering work on phage adsorption, burst size, and host lysis led to the establishment of the T-phage series as standard research models, facilitating reproducibility and comparability in phage studies (Ellis and Delbruck, 1939; Delbrück, 1940a,b; Sharp, 2001).

The study of phage genetics began with the construction of recombinational maps and was followed by the discovery of phenotypic mixing. Subsequently, studies about the structural analysis of the regions in phage T4 enabled others to make a closer analysis of the phage replication cycle (Hershey and Rotman, 1949; Benzer, 1955; Epstein et al., 1963; Sharp, 2001)

The different sequence specificities of the host endonucleases from different strains enabled the development of site-specific DNA cleavage and laid the foundation for the development of gene cloning. Highlighting the ability of temperate bacteriophages to insert their genome into that

of the host formed the basis of the development of genetic tools in microbiology (Arber and Dussoix, 1962; Gefter et al., 1966; Shapiro et al., 1969; Sharp, 2001; Maura and Debarbieux, 2011).

Until the 1990s, phage research primarily supported the development of molecular biology techniques and the study of gene expression regulation and protein structure (Maura and Debarbieux, 2011).

The third phase, beginning in the 1990s, shifted toward understanding the ecological roles of phages and their environmental applications. In aquatic and terrestrial ecosystems, phages are now recognized as key regulators of microbial populations. In aquaculture, they have been studied for the control of bacterial infections in fish and plants, and for the mitigation of harmful algal blooms caused by cyanobacteria (Withey et al., 2005; Maura and Debarbieux, 2011).

Cyanobacterial blooms (cyanoHABs) pose an increasing threat to freshwater systems, impacting ecosystem health and drinking water safety. These blooms cause hypoxia, disrupt food webs, and produce potent toxins. Cyanophages—viruses that specifically infect cyanobacteria—are being investigated as tools to prevent or mitigate cyanoHAB events during early bloom stages (Grasso et al., 2022; Krausfeldt et al., 2024).

Phages are also abundant in soils, and in the gastrointestinal tracts of humans and animals, making them common in feces and sewage. The microbial communities in sewage are predominantly of human origin, and phages have been proposed as indicators or tracers for pathogenic bacteria in wastewater systems (Withey et al., 2005).

Biological sludge from wastewater treatment processes contains a complex array of pathogenic microorganisms. As the use of sludge in agriculture grows, concerns about pathogen transmission have intensified. In this context, phages could be employed to reduce the presence of *E. coli* and *Enterobacteria*, minimizing the health risks associated with sludge application (Withey et al., 2005).

Although the role of phages in wastewater treatment microbial communities remains poorly understood, they are believed to influence community composition and dynamics, particularly in anaerobic digesters. Additionally, phages may enhance sludge dewaterability and digestibility (Withey et al., 2005).

2.2 Applications in WWTP

Much of the study on phage-bacteria interactions has been based on pure rather than applied concerns. However, the use of phage therapy has expanded to the field of wastewater treatment. Shivaram et al. (2023) presents an overview of the use of bacteriophages to control bulking, foaming, and biofilm formation in a wastewater treatment plant (WWTP). They indicate that most of the bacterial species responsible for this problem have been identified, and their respective phages are isolated to control their growth. However, the most difficult step would be to upscale and implement current laboratory and pilot-scale studies to a large scale and assess the economic feasibility of the process. Currently, removing only unwanted (pathogen) bacteria in the biological unit of the WWTP is not possible using chemical methods. Therefore, strategies must be developed to implement phage therapy in combination to reduce the use of chemicals in the immediate future followed by the implementation of phage therapy as a clear-cut solution for biological treatments in WWTPs. This is a possible cause for reinvestments in system equipment and can result in the formation of harmful byproducts. Hence, strategies must be developed to implement phage therapy in combination to reduce the use of chemicals in the immediate future, followed by the implementation of phage therapy as a clear-cut solution for biological treatments in WWTPs.

In another case, bacteriophages have been used as novel tools in water pollution control, such as monitoring pathogens, tracking pollution sources, treating pathogenic bacteria, infecting bloom-forming cyanobacteria, and controlling bulking sludge and biofilm pollution in wastewater treatment systems. However, a challenge in activated sludge is decreased phage concentration owing to off-target adsorption. This may be a common problem faced by phage-based technology in practical applications. It is, therefore, that before phage-based technology can be applied to wastewater treatment, further research is needed on the community structure and interaction mechanisms of microorganisms in wastewater (Ji et al., 2021).

Another function of the bacteriophages in wastewater treatment systems is addressed to the phages, which could also serve as monitoring tools and performance indicators. Detecting and identifying specific phages can reveal insights regarding the health and stability of the bac-

terial community and aid in predicting disturbances based on the population dynamics of phage-host systems (Aw et al., 2014; Stefanakis et al., 2019). Therefore, phages are potential indicators of effluent quality (Silverman et al., 2013; Yahya et al., 2015; Boehm, 2019). Additionally, correlating a phage ecogenomic fingerprint with treatment configuration and operation can develop into a tool for monitoring and controlling Biological Wastewater Treatment (BWT) more quickly and reliably, shifting from a health-related assessment to a process and engineering perspective (Runa et al., 2021).

Wastewater treatment plants (WWTPs) harbor a considerable diversity of antibiotic remnants and a high bacterial load in the same space for an extended period, facilitating the emergence of antimicrobial-resistant bacteria (ARB) and antimicrobial resistance genes (ARGs). Existing treatment methods are unable to completely eliminate ARB and ARGs, which are ultimately released into the aquatic environment (Reisoglu and Aydin, 2023). Pallavali et al. (2023) isolated the multidrug-resistant bacterium *Aeromonas spp.* and its lytic phage from livestock WWTP. They found that the phage effectively reduced the bacterial population from 65.7 to 20% after 24 hours of incubation. Then, the dose of phage in mixed cultures could mitigate the population of a target bacterium, which can spread antibiotic traits to wastewater treatment processes and receiving water basins. Therefore, these results indicate that lytic phages can be an alternative method to reduce antibiotic resistance in wastewater without the presence of chemical byproducts. Nevertheless, further studies on the use of phage cocktails and accurate ARB monitoring of phage treatment will be required to enhance the efficacy and stability of ARB control in wastewater treatment systems.

Last, bacteriophages can be beneficial in controlling biofouling in wastewater systems that harbor unwelcome microorganisms, disrupting the bioreactor treatment process. While membrane bioreactor systems are advanced wastewater treatment strategies and known for their higher elimination capacity than the traditional ones, biofouling as an environmental and medical problem resulting from the augmented antibiotic resistance in biofilms is an inescapable challenge in membrane bioreactor systems, and it hampers the working of the system (Zhen et al., 2019). An example of phage application in solving membrane biofouling problems is indicated by Ayyaru et al. (2018). They have monitored the

effect of lytic phages on membrane biofouling by isolating a bacterium and its respective phage from municipal wastewater. When they investigated the impact of bacterium and phage suspension using permeability flux and SEM, they reached out to the success of lytic phage on bacterial inhibition and elimination of biofilm formation (Reisoglu and Aydin, 2023).

2.3 Experimental results

Most reports on the use of phages in wastewater treatment focus on isolating phages from Wastewater Treatment (WWT) and proposing their possible use; however, none of them have proven this potential. The PUCV group studied the control of bulking and foaming through phage therapy and conducted some previous experimental work on this subject. A Chilean WWTP with foaming and bulking problems was studied. The results of the sequencing analysis allowed the identification and quantification of the abundance of filamentous bacteria present. The identified filamentous bacteria belong to the genera *Thiothrix, Sphaerotilus* and *Gordonia*. In this study, it was concluded that the bulking problem was caused by an average increase of 48% in the proportion of *Thiothrix*. Meanwhile, an increase in the proportion of *Gordonia* was observed in all foam samples, confirming that this bacteria is responsible for the appearance of foam in the reactor (Lafitte, 2019).

Subsequently, assays were conducted to determine treatment effectiveness and the optimal dosage. A complete factorial design with three bacteriophage concentration levels ($1.19{\cdot}10^7$, $1.19{\cdot}10^8$, and $2.25{\cdot}10^7 PFU g_{TSS}^{-1}$), and three daily dosage levels (1, 2, and 3 per day) were used for the experiments. The response variable evaluated was the Gordonia percentage reduction in the sludge. It was found that the best treatment occurred with the lowest number of doses and at the highest concentration. Thus, it was concluded that the behavior of bacteriophages is not linear with respect to their lytic power and concentration but rather obeys an optimal relationship between the bacterial metabolism that they attack and the number of bacteriophages capable of adhering to the bacteria without destroying them before they replicate within them. $1.19 \cdot 10^8 PFU g_{TSS}^{-1}$ was estimated as the minimum concentration required to eliminate foaming by reducing at least 50% of *Gordonia* present in the reactors (Lafitte,

2019).

In addition, the disappearance of the foam was qualitatively evaluated, and the existence of any change at the microscopic level in the configuration of the flocs in the sludge; these results can be observed in figures 2.1 and 2.2. Figure 2.1 shows the 40x Gram-stained microscopic photographs before and after the phage application treatment. The decrease in Gordonia after the phage was applied to the system is clearly evident. Figure 2.2 shows the continuous activated sludge system before and after the phage application. It is clear that foam reduction was complete within 24 hours of phage application.

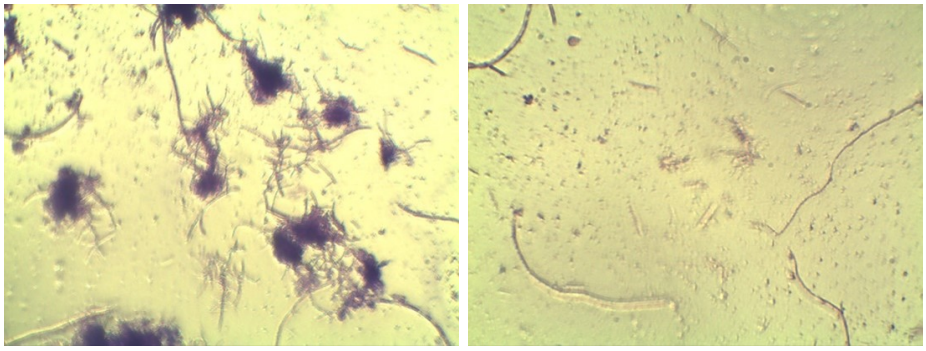

(a) Before the phage dose (b) After the application of phage doses

Figure 2.1: *Gordonia*. Microscope photographs at 40x. Images taken from Lafitte (2019).

This study met its objectives and opened the door to new research into the control of bulking and foaming with bacteriophages. However, a major challenge, which has not been resolved to date, is the difficulty of culturing a large proportion of the phages present in WWTP. Thus, a study of the kinetic parameters made sense at this point.

The following study was focused on determining the kinetic and infection parameters of the bacteria-phage pair. In this study, *Gordonia rubripertincta* and its respective phage *GRU1* were used. Depending on the supplemented medium, a specific growth rate (MIU) was determined between 0.036 and 0.24 h-1. Despite multiple efforts to obtain lysis plaques with *G. rubripertincta* phages, obtaining a homogeneous culture and lawn of *Gordonia* was difficult. Once these difficulties were

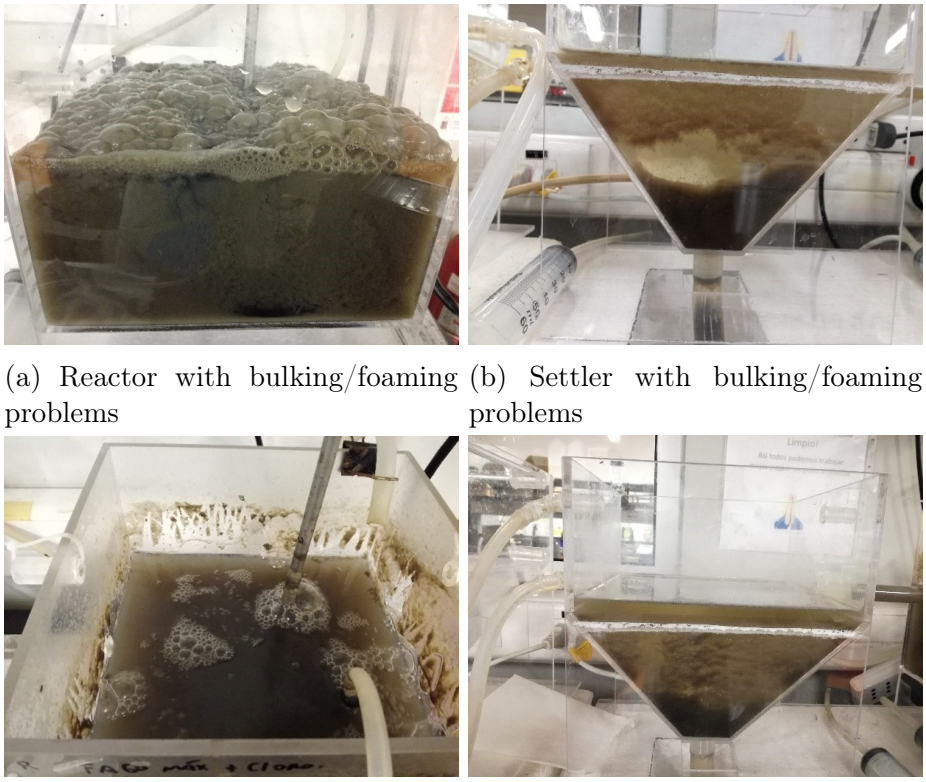

(a) Reactor with bulking/foaming problems

(b) Settler with bulking/foaming problems

(c) Settler before the application of phage doses

(d) Settler after the application of phage doses

Figure 2.2: Continuous activated sludge system. Images taken from Lafitte (2019).

overcome, lysis plaques were obtained. However, once the phage was characterized and despite repeated one-step assays for almost 7 hours (sufficient time for eclosion to take place), it was not possible to observe the release of viral particles, that is, the eclosion (Toledo, 2022).

Parameter estimation is probably the biggest challenge, given the difficulty of collecting informative experimental data. Process modeling plays a fundamental role in this regard, as it allows us to study a process in silico with less laboratory experience.

Mathematical modeling of microbial populations has a long history of application in ecology and biology. Although the field has considered modeling bacterial populations affected by phage activity, this has not

been a major focus, particularly in wastewater treatment. Models have tended to focus more on ecological and evolutionary issues than on the effectiveness of a particular phage treatment in controlling a bacterial population (Cairns et al., 2009). A mathematical model can help control the process on a large scale, and the inclusion of a predation mechanism is a new addition to the existing activated sludge models (Moussa et al., 2005).

2.4 Modelling challenges

Monitoring bacterial growth kinetics could be based on the relations presented in the previous sections, obtaining the parameters associated with logistic and Monod laws (specific growth rate, carrying capacity, etc.). This approach is mostly useful in pure cultures where it is easy to collect data, but it is much more delicate, or even impossible, in full-scale operation, with consortia of micro-organisms.

On the other hand, infection parameters can be determined with additional tests. For instance, latent period and burst size can be determined by one-step growth assays, and the adsorption constant can be determined according to a standard published protocol Hyman and Abedon (2009). However, it is also observed that these parameters could be time-varying and that additional modeling effort is required (Hadas et al., 1997; Abedon et al., 2001; Golec et al., 2014; Santos et al., 2014; García et al., 2019).

de Leeuw et al. (2017) used microtiter plates (which served as multiple micro-scale eco-systems) and studied the predator-prey relationship between bacteria and phage isolated from wastewater treatment bioreactors. The shifts in the bacterial population were monitored through the optical readings from the plate reader, and a mathematical model incorporating phage-bacteria interactions was developed and calibrated using Matlab. However, only the total bacterial population was observed, whereas monitoring the phage population and substrate concentrations would be valuable, and represents an actual challenge in monitoring and controlling wastewater treatment.

Nabergoj et al. (2018) investigated how dilution rate, defining bacterial growth rate in continuous culture, affects adsorption constant, latent period, and burst size and consequently also bacteriophage population

growth rate. They used a well-studied phage T4 and *E. coli* K-12 as a host in a chemostat. The authors demonstrated that bacterial growth rate had an important influence on three phage growth parameters, e.g., adsorption constant, latent period, and burst size, determining the bacteriophage population growth rate. Also, bacteriophage population growth rate as a function of dilution rate was found to be accurately described by a simple Monod equation. From these results, the question emerges if these changes in infection parameters are general or depend on the choice of a phage-host system, which adds to the difficulties of parameter estimation.

Another challenge for the application of bacteriophage treatment at the industrial level is the large number of phages that should be produced, so that cost-effective and scalable methods for phage production are required to meet the demand. In this connection, computational models could also assist the optimization of such production processes, and are an open research avenue. In this connection, Krysiak-Baltyn et al. (2018) proposed a model for a two-stage, self-cycling process, which was successfully operated without showing evidence of resistant bacteria. The model developed for a setup with multiple reactors provided simple cost estimates as a function of operational parameters such as substrate concentration, feed volume, and cycling times. They concluded that the approach is flexible and could be used to optimize phage production at a laboratory or industrial scale by minimizing costs or maximizing productivity.

2.5 Practical applications of computational models in activated sludge processes

Single reactor models have been essential to increasing our understanding of some aspects of the system dynamics, but these models may not be adequate to simulate the spread and propagation of phages in the complex and varied configurations of real-world systems, including the sewage pipes and wastewater treatment plants. In that sense, few authors have studied phage treatment. One of the first foaming studies was accomplished by Blackall et al. (1985), who analyzed the onset of foam formation and subsequent persistence of foaming in terms of a mathe-

matical model for *Nocardia amarae* (filamentous bacteria) described by two balance equations.

Using experimental data, the authors determined that the foam acted as a significant source for continued bacteria growth in the mixed liquor, which would make it difficult for the microorganisms to wash out. Also, activated sludge systems are sensitive to changes in key variables that could lead to the onset or disappearance of foam. They concluded that such a model is helpful, but that there are difficulties in obtaining meaningful values for some parameters, especially if more than one filamentous organism is dominant (Soddell and Seviour, 1990).

Hao et al. (2011) presented a model to simulate a sequencing batch reactor (SBR) system enriching polyphosphate-accumulating organisms (PAOs). For this purpose, they proposed extending the Activated Sludge Model No. 2d (ASM2d) to incorporate predation and viral infection processes. In order to include predation and viral infection, the decay process in ASM2d was split into three individual processes, e.g., predation-induced decay, viral infection-induced decay, and other factors-induced decay (e.g., toxic substances, natural cell death, etc.). Correspondingly, the stoichiometric matrix and kinetic rate expressions related to predation and viral infection were added to the extended ASM2d.

For foaming treatment, Liu et al. (2015) isolated Gordonia species from activated sludge of a commercial wastewater treatment plant, and four isolated phages were applied to sludge, resulting in a reduction of Gordonia host levels in a wastewater sludge model by approximately 10-fold as compared to non-phage-treated reactors. In addition to controlling Gordonia levels in activated sludge, phage-treated sludge at the end of the experiment showed better settling properties and lower foaming potential in the supernatant after settlement compared to the control. They concluded that phages applied for bio-control could survive during sludge aeration, providing significant potential for phage application in controlling Gordonia-associated foaming and bulking during wastewater treatment (Liu et al., 2015).

Recently, Krysiak-Baltyn et al. (2017) proposed a model incorporating phage dynamics in wastewater treatment for two reactor configurations, SBR (Sequencing Batch Reactor) and PFR (Plug Flow Reactor), to investigate the potential use of phages as a tool to reduce foaming or bulking. The model couples wastewater treatment dynamics within the

commercial software GPS-X (Hydromantis Inc.) with phage dynamics through a newly developed add-on called PhageDyn. Simulations predict that immediately after phage dosing, there is a lag period during which no apparent changes are observed, followed by a sudden and quick increase in the phage concentration and reduction in foaming biomass. 'Normalization' without foaming is achieved within 1–2 weeks after dosing. The system may subsequently relapse to foaming, requiring additional phage dosing, or be "cured" such that the added phages keep the problematic foaming biomass indefinitely at bay. The behavior described by Krysiak-Baltyn et al. (2017) has been the closest to reality, although the Delay Differential Equations (DDE) system had to be reformulated into a set of Ordinary Differential Equations (ODEs) due to computational challenges. They concluded that the kinetic parameters describing the behavior of the phages and reactor configuration are vital determinants of the outcome.

Chapter 3

Bacteria–Phage Population Model

3.1 An overview of bacteria-phage population models

To introduce dynamic models of bacteria-phages systems, a good approach is to introduce the concept of compartments, representing the different components of the system, and to go from simple to more detailed models.

As a start, the growth of bacteria, which can be represented by different kinetic laws, has to be described. The kinetic expressions that have been most commonly used in modeling bacterial growth include the Malthusian (Malthus, 1798)

$$\frac{dX}{dt} = \mu_{max} X, \tag{3.1}$$

and Logistic (Verhulst, 1838)

$$\frac{dX}{dt} = \mu_{max}(1 - \frac{X}{X_{max}})X, \tag{3.2}$$

expressions, where X is the concentration of bacteria, μ_{max} the maximum specific growth rate and X_{max} is the carrying capacity of the environment. The Malthusian model is appropriate to describe the early exponential growth, but has limited applicability. The logistic model has

the interesting added feature that it provides an equilibrium state at the carrying capacity, which represents the maximum population that can be sustained by the resources of the environment.

The next logical level is to explain the growth by the consumption of a limiting substrate (S) as represented by the Monod law (Monod, 1950)

$$\frac{dX}{dt} = \mu_{max}(\frac{S}{K_S + S})X, \tag{3.3}$$

where K_S is the half-saturation coefficient.

However, attempts to fit the growth of filamentous organisms in activated sludge with simple models such as those mentioned above have not been successful, due to interactions between microorganisms. Microbial growth in an activated sludge plant occurs in the presence of a diversity of organisms, among which antagonistic and symbiotic relationships exist. To take account of the interaction with a predator, it is necessary to turn to predator-prey models as proposed in the seminal work of (Lotka, 1925; Volterra, 1926). This corresponds to a 2-compartment model

$$\frac{dX}{dt} = \mu_1(P)X = (\alpha - \delta P)X, \tag{3.4a}$$

$$\frac{dP}{dt} = \mu_2(X)P = (-\varphi + \eta X)P, \tag{3.4b}$$

where X and P are the prey and predator populations, respectively, $\mu_1(P)$ and $\mu_2(X)$ are specific growth rates with parameters α, δ, φ and η describing the natural growth or decay and the interaction between the two species. This model can be modified in various ways, for instance by introducing logistic growth, limited predation, the consumption of a limiting substrate following a Monod law, etc.

Campbell (1961) proposed such a model, under the assumption that a bacterium can only be infected by one phage and the burst size, i.e., the average number of newly synthesized phages released from a single infected bacterium, is constant. In a batch (no in- and outflow) reactor, the model of the system could be first written as follows

$$\frac{dX}{dt} = \mu(X)X - \delta XP = \mu_{max}(1 - \frac{X}{X_{max}})X - \delta XP, \tag{3.5a}$$

$$\frac{dP}{dt} = -\delta XP + \beta\delta X(t-\tau)P(t-\tau) - \nu_p P, \tag{3.5b}$$

where the susceptible bacteria population X grows at a specific rate $\mu(X)$ in the form of a logistic equation and decays according to the phage infection rate δXP, where δ is the adsorption rate which describes the number of phages that bind to the bacterium (Shao and Wang, 2008). The number of free phage particles decays accordingly at the rate $-\delta XP$, in addition to the natural phage inactivation $-\nu_p P$, and increases in proportion to the production of infected cells with the burst size β. The production of new phages is not an instantaneous phenomenon, but takes place after a latency phase τ.

Remark 1. *The consideration of a latency phase τ results in a Delay Differential Equation (DDE) system, which is significantly more difficult to solve and to analyze.*

To better understand the concept of the latency phase, it is necessary to delve into its principles. The latent period τ represents the time elapsing from the instant of infection, i.e., when the content of the virus head is injected inside the bacterium, to the instant of the bacterium cell wall lysis, at which a number of copies of assembled phages are released in solution (Beretta and Kuang, 1998). The processes that occur during the latent period include (Weitz, 2016):

- translocation of viral genetic material from the periplasm into the cytoplasm,
- replication of genetic material and production of virus particle components,
- packaging of viral genomes into viral heads,
- disruption of the cell surface and release of viral progeny.

In this time span, the eclipse period E is the time it takes for intact virus particles to appear (Wang et al., 1996), and the moment at which cellular lysis would lead to the potential continuation of a viral infection. The maturation rate R represents the increase in phage progeny per unit of time, occurring in the lapse of time $\tau - E$, and the burst size β determines the number of phages released in the event of bacterial lysis

or rupture (Abedon et al., 2001, 2003). The relationship between these variables is described by the following equation.

$$\beta = (\tau - E)R \tag{3.6}$$

Burst size and the phage generation time are controlled by the phage latent period, with a directly proportional relation between burst size and latent period, i.e., greater burst sizes associated with longer latent periods (Abedon et al., 2001).

Levin et al. (1977) extended the previous model by considering two distinct bacterial populations, i.e., the susceptible bacteria X_S and the infected bacteria X_I, both feeding on a limiting resource S (see equation 3.7d). They also pointed out that Campbell's model did not take the removal of infected bacteria due to dilution in a continuous process into account. The proposed model takes the following form

$$\frac{dX_S(t)}{dt} = \mu(S)X_S(t) - \delta X_S(t)P(t) - DX_S(t), \tag{3.7a}$$

$$\frac{dX_I(t)}{dt} = \delta X_S(t)P(t) - e^{D\tau}\delta X_S(t-\tau)P(t-\tau) - DX_I(t), \tag{3.7b}$$

$$\frac{dP(t)}{dt} = -\delta X_S(t)P(t) + \beta e^{D\tau}\delta X_S(t-\tau)P(t-\tau) - \nu_p P(t) - DP(t), \tag{3.7c}$$

$$\frac{dS(t)}{dt} = D(S_{in} - S(t)) - \nu_s \mu(S)X_T(t), \tag{3.7d}$$

$$X_T(t) = (X_S(t) + X_I(t)). \tag{3.7e}$$

where D is the dilution rate and the factor $e^{(-D\tau)}$ represents the dilution effect on a time span τ (the delayed populations should therefore be divided by this factor) and S_{in} is substrate concentration in the feed. The growth rate $\mu(S)$ could follow various laws, e.g., Monod law.

Remark 2. *The substrate consumed by a cell is used for: (i) growth, including substrate incorporated into biomass and used to generate energy for biosynthesis; (ii) maintenance of cellular viability, where substrate is utilized to produce energy for non-growth-related functions such as nutrient transport, osmotic balance, and others; and (iii) producing*

extracellular metabolites, which may or may not occur depending on the microorganism (Pirt, 1965; Acevedo et al., 2004). Since, in an infected bacterium, the phage seizes control of the cellular machinery to produce new viral particles, cell growth is arrested. Consequently, substrate consumption by X_I is solely attributed to maintenance metabolism and/or phage production. Levin's model assumes that the total bacteria population X_T consumes substrate at a rate proportional to μ, implicitly assuming that the maintenance rate of X_I would be equal to μ.

Anderson and May (1981) developed a population model of microparasites and invertebrate hosts. This model extends the previous by considering a death phenomenon affecting the susceptible and infected individuals, a recovery of infected individuals to susceptible ones, and a lysis of infected cells.

$$\frac{dX_S(t)}{dt} = \mu(X_S(t) + X_I(t)) - \delta X_S(t)P(t) - \gamma X_S(t) + \rho X_I(t), \quad (3.8a)$$

$$\frac{dX_I(t)}{dt} = \delta X_S(t)P(t) - \eta X_I(t) - \gamma X_I(t) - \rho X_I(t) \quad (3.8b)$$

$$\frac{dP(t)}{dt} = -\delta X_S(t)P(t) + \eta X_I(t), \quad (3.8c)$$

where γ is the death rate of the susceptible and infected bacteria. η is the lysis rate giving rise to the release of phages, and ρ is the recovery rate

Remark 3. *This model does not consider a limiting substrate nor dilution effects. It assumes that both susceptible and infected bacteria grow and die at the same rates, μ and γ, respectively. Interestingly, it relates the lysis and phage production directly to the infected bacteria population, avoiding the explicit consideration of a latency period applied to the susceptible and phage populations. Mathematically speaking, the delay τ is replaced by a time constant $1/\eta$, which has two advantages: (a) the model equations are simple ordinary differential equations and (b) the lysis rate can be different from the infection rate. However, the model assumes that the production of phages also occurs at the same rate η.*

Later on, Beretta and Kuang (1998) considered a similar model, with a logistic factor for the growth phenomenon (where X_{max} is the carrying

capacity), no recovery rate, but a parameter β for the production of phages.

$$\frac{dX_S(t)}{dt} = \mu_{max}(1 - \frac{X_S(t) + X_I(t)}{X_{max}})X_S(t) - \delta X_S(t)P(t), \tag{3.9a}$$

$$\frac{dX_I(t)}{dt} = \delta X_S(t)P(t) - \eta X_I(t), \tag{3.9b}$$

$$\frac{dP(t)}{dt} = -\delta X_S(t)P(t) + \beta\eta X_I(t) - \nu_p P(t). \tag{3.9c}$$

On the other, Payne and Jansen (2001) considered a slightly different structure, where both bacteria populations are growing at the same rate μ.

$$\frac{dX_S(t)}{dt} = \mu X_S(t) - \delta X_S(t)P(t), \tag{3.10a}$$

$$\frac{dX_I(t)}{dt} = \mu X_I(t) + \delta X_S(t)P(t) - \eta X_I(t), \tag{3.10b}$$

$$\frac{dP(t)}{dt} = -\delta X_S(t)P(t) + \beta\eta X_I(t) - \nu_p P(t). \tag{3.10c}$$

Remark 4. *The latter models no longer consider a latency phase, and have the advantage of being described by ordinary differential equations. They differ mostly in the expression of the growth, infection, recovery, lysis, and phase production rates.*

Siekmann et al. (2008) extended the model of Beretta and Kuang (1998) by adding an evolution equation for viruses $P_I(t)$ that are confined in their host.

$$\frac{dX_S(t)}{dt} = \mu_{max}(1 - \frac{X_S(t) + X_I(t)}{X_{max}})X_S(t) - \delta X_S(t)P(t), \tag{3.11a}$$

$$\frac{dX_I(t)}{dt} = \delta X_S(t)P(t) - \eta X_I(t), \tag{3.11b}$$

$$\frac{dP_I(t)}{dt} = \mu_{max}P_I(t) - c\frac{P_I^2(t)}{X_I} - \alpha\eta P_I(t) + \delta X_S(t)P(t) \tag{3.11c}$$

$$\frac{dP(t)}{dt} = \alpha\eta P_I(t) - \delta X_S(t)P(t) - \nu_p P(t), \tag{3.11d}$$

where $0 \leq \alpha \leq 1$.

Remark 5. *This model assumes a logistic growth of the susceptible bacteria (carrying capacity X_{max}) and of the host viruses (carrying capacity X_I). It is, however, questionable why the same unlimited growth rate μ_{max} applies to both X_S and P_I, since P_I is related to X_I, which has no growth.*

In systems where infection occurs, the possibility exists that the pathogen becomes resistant to the treatment (e.g., bacteria may become resistant to antibiotics, which must then be administered in certain doses for a certain time to prevent the occurrence of this phenomenon). Similarly, the susceptible bacteria could become resistant to the phage treatment due to natural mutation. Cairns et al. (2009) included a mutation rate ε from susceptible $X_S(t)$ to resistant bacteria $X_R(t)$, leading to

$$\frac{dX_S(t)}{dt} = \mu X_S(t) - \delta X_S(t)P(t) - \varepsilon X_S(t), \tag{3.12a}$$

$$\frac{dX_I(t)}{dt} = \delta X_S(t)P(t) - \delta X_S(t-\tau)P(t-\tau), \tag{3.12b}$$

$$\frac{dX_R(t)}{dt} = \mu X_R(t) + \varepsilon X_S(t), \tag{3.12c}$$

$$\frac{dP(t)}{dt} = -\delta X_S(t)P(t) + \beta\delta X_S(t-\tau)P(t-\tau) - \nu_p P(t). \tag{3.12d}$$

Santos et al. (2014) slightly modified the previous model by including a limiting substrate as in some of the earlier models (Levin et al., 1977),

$$\frac{dX_S(t)}{dt} = \mu(S)X_S(t) - \delta X_S(t)P(t), \tag{3.13a}$$

$$\frac{dX_I(t)}{dt} = \delta X_S(t)P(t) - \delta X_S(t-\tau)P(t-\tau), \tag{3.13b}$$

$$\frac{dX_R(t)}{dt} = \mu(S)X_R(t), \tag{3.13c}$$

$$\frac{dP(t)}{dt} = -\delta X_S(t)P(t) + \beta\delta X_S(t-\tau)P(t-\tau), \tag{3.13d}$$

$$\frac{dS(t)}{dt} = -\nu_s \mu X_T(t) = -\nu_s \mu (X_S(t) + X_I(t) + X_R(t)). \tag{3.13e}$$

where $\mu(S)$ is a Monod law.

Having presented an overview of existing models, the objective of the next section is to propose a simple model that contains most of the distinctive features highlighted in previous studies and would be appropriate to describe bacteria-phages system in the context of wastewater treatment.

3.2 A candidate model of bacteria and phage populations

A simple model, which would be suitable to describe experimental results in the context of wastewater treatment, could take the following factors into account:

- the bacteria-phage populations develop in a bioreactor with a limiting substrate and dilution rate (which can be set to zero for batch operation);
- the growth kinetics $\mu(S)$ of the susceptible bacteria can take various forms, notably the Monod law;
- the infected bacteria do not grow but instead maintain metabolism and/or produce phage using the same substrate at a rate m (a feature that has not been described in earlier models, which either assume growth or maintenance at the same rate);
- the infection rate is proportional to $X_S(t)P(t)$ with a rate δ;
- η is the lysis rate (the lysis and release phenomena are represented by rate equations rather than by introducing a delay, which is a mathematical idealization complexifying the model structure) ;
- β is the release rate of new phages;
- ν_P is the natural decay of the free phages;
- natural decay rates of the susceptible and infected bacteria (which should probably be set to different values in contrast with the earlier models) could be easily introduced but are not taken into consideration, as probably negligible with respect to the other phenomena.

The resulting model equations are given by:

$$\frac{dX_S(t)}{dt} = \mu(S)X_S(t) - \delta X_S(t)P(t) - DX_S(t), \tag{3.14a}$$

$$\frac{dX_I(t)}{dt} = \delta X_S(t)P(t) - \eta X_I(t) - DX_I(t), \tag{3.14b}$$

$$\frac{dP(t)}{dt} = -\delta X_S(t)P(t) + \beta\eta X_I(t) - \nu_p P(t) - DP(t), \tag{3.14c}$$

$$\frac{dS(t)}{dt} = -\nu_s(\mu(S)X_S(t) + mX_I(t)) + D(S_{in} - S(t)). \tag{3.14d}$$

This model has the advantage of being in the form of a first-order Ordinary Differential Equation (ODE) system, thus amenable to a classical state-space representation.

$$\dot{x} = f(x, u) \tag{3.15a}$$

$$y = Cx \tag{3.15b}$$

with the following definitions corresponding to equations 3.14

$$x = \begin{bmatrix} X_S \\ X_I \\ P \\ S \end{bmatrix}, \quad f(x) = \begin{bmatrix} f_{X_S}(x) \\ f_{X_I}(x) \\ f_P(x) \\ f_S(x) \end{bmatrix} \tag{3.16}$$

The vector $y(t)$ represents the set of measurements that can be collected either for parameter identification purposes or for the design of software sensors monitoring the bioreactor. The matrix C describes the selection or linear combination of specific state variables. Note that this matrix C can be different in the two above-mentioned tasks. Indeed, parameter estimation can be based on off-line and on-line measurements, whereas software sensors can only use on-line measurements.

3.3 Model simulations

As noted earlier, the proposed model offers the advantage of being a system of ordinary differential equations (ODEs), which simplifies both numerical implementation and analytical manipulation. ODE-based models are preferred in engineering applications due to their compatibility with standard numerical solvers and state-space representation.

Some authors—such as Anderson and May (1981); Beretta and Kuang (1998); Payne and Jansen (2001); Siekmann et al. (2008)—have employed delay differential equations (DDEs) to account for the latency period between infection and lysis. The inclusion of a delay parameter τ, reflects biological reality but increases the mathematical and computational complexity of the model. By contrast, other researchers—such as Campbell (1961); Levin et al. (1977); Cairns et al. (2009); Santos et al. (2014)]—have opted for ODE-based formulations, modeling lysis with an exponential rate η instead of an explicit delay. Both approaches have demonstrated validity across diverse domains, including phage therapy and aquatic disease modeling.

All simulations presented here were performed using MATLAB (The MathWorks, Natick, MA, USA), employing the *ode15s* solver. This solver is well-suited for stiff ODE systems and utilizes a variable-order backward differentiation formula (BDF). Stiffness may arise in phage–bacteria models when the system exhibits both slow dynamics (e.g., substrate depletion) and rapid transients (e.g., lysis bursts or infection spikes). Stiffness arises explicitly when hydrodynamic and biological time constants coexist within a model. Moreover, the bacteria–phage model becomes stiff when it incorporates fast viral infections (e.g., minutes) relative to slow bacterial growth (e.g., hours). This stiffness is further exacerbated by the inclusion of very fast hydrodynamic processes (e.g., seconds). The substantial disparity in time scales renders the system numerically stiff, requiring specialized solution techniques. In such cases, *ode15s* is more efficient than explicit solvers like *ode45*, which require prohibitively small time steps to meet error tolerances.

The parameter values used in the simulations are listed in Table 3.1. Key parameters such as the maximum bacterial growth rate μ_{max}, adsorption rate δ, and burst size β beta were experimentally estimated for the pair *Gordonia westfalica* and its lytic phage, previously isolated and characterized in foaming samples from PUCV laboratories (Lafitte, 2019; Toledo, 2022). These values are within the range of values reported in the literature (Abedon et al. (2001); Wang (2006); Shao and Wang (2008)). The laboratory analyses carry out only allowed the estimation of some parameters (μ_{max}, δ, and β); however, to perform full parameter identification and estimate the remaining unknown parameters using the model 3.14, monitoring of infection kinetics under varying

conditions is required. Previous research did not include such data, as it was not the objective of the study; hence, the remaining parameters were sourced from established models Payne and Jansen (2001); Cairns et al. (2009); Santos et al. (2014).

Table 3.1: Model parameter values.

Parameter		**Value**
Bacteria	$\mu_{max}(h^{-1})$	0.4298
growth	$K_M(mg\,mL^{-1})$	0.39
Bacteriophages	$\delta(mL\,CFU^{-1}PFU^{-1}\,h^{-1})$	$3.02 \cdot 10^{-9}$
proliferation	$\beta(PFU\,CFU^{-1})$	110
(Infection)	$\eta(h^{-1})$	0.5
Other	$\nu_S(mg\,CFU^{-1})$	$1.23 \cdot 10^{-6}$
parameters	$\nu_P(h^{-1})$	0.01032
	$m(h^{-1})$	$1 \cdot 10^{-6}$
Operational	$S_{in}(mg\,mL^{-1})$	4
parameters	$D(h^{-1})$	0.1

To assess the model's behavior, we simulated the impact of three critical infection-related parameters: the burst size β, the lysis rate η, and the adsorption rate δ.

Figure 3.1 illustrates the effect of increasing burst size β on population dynamics. The burst size, which represents the number of phages released per lysed bacterium, is an intrinsic property of the phage–host interaction. Literature reports average values of 60 PFU per cell, with ranges spanning from a few units to over 200.

In all cases, it is evident that phage release affects bacterial control, as the bacteria do not continue their characteristic exponential growth. Therefore, regardless of the number of phages released, the development of *Gordonia* is slowed.

Our simulations demonstrate that higher burst sizes intensify bacterial suppression and introduce oscillatory behavior as the system approaches equilibrium (a phenomenon that will be explored in the next chapter). Oscillations emerge for $\beta \geq 100$, which suggests a dynamic balance between infection and recovery cycles.

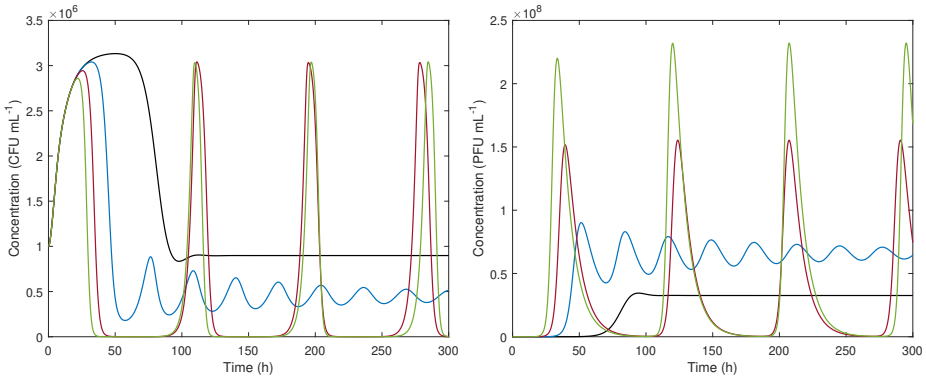

(a) Susceptible bacteria (b) Infected bacteria

Figure 3.1: Time evolution for different burst sizes. Initial conditions $X_{S0} = 1 \cdot 10^6\ CFU\ mL^{-1}$, $X_{I0} = 0$, $P_0 = 1 \cdot 10^2\ PFU\ mL^{-1}$ and $S_0 = 0.1\ mg\ mL^{-1}$. Burst size in order black, blue, red, and green are $50, 100, 150, 200\ PFU\ CFU^{-1}$.

Regardless, the burst size is an intrinsic property of a bacteriophage; this parameter is determined by the phage's genetic makeup and its interaction with the host, making it a specific trait of that phage-host pair. In this sense, a correct selection of the bacterial-phage pair is crucial for the effective application of phage therapy as a control.

Figure 3.2 explores the effect of varying the adsorption rate δ. This parameter reflects the rate at which phages encounter and successfully attach to host cells. Its value depends on phage and host concentrations, environmental conditions (e.g., temperature, pH), and intrinsic viral properties. Typical values fall within the range of 10^{-8} to $10^{-10} ml min^{-1}$ for different phages.

Simulations show that faster adsorption rates accelerate bacterial decline and enhance phage proliferation. The adsorption rate is influenced by phage concentration, bacterial concentration, and the phage's intrinsic adsorption rate constant. However, operational parameters such as temperature or pH have a significant effect on the adsorption rate constant (Jeon and Ahn, 2021; Pradeep et al., 2022; Abedon, 2023).

The phage lysis rate, η is directly associated with the lysis time, which is typically measured in minutes. Some studies have found optimal lysis times between 60 and 100 minutes. Other research has identified lysis times that range from as short as 30 minutes to as long as 120 minutes

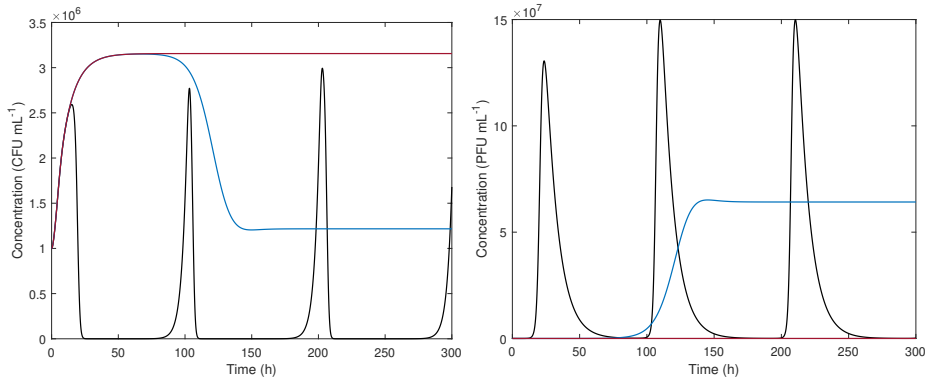

(a) Susceptible bacteria (b) Infected bacteria

Figure 3.2: Time evolution for different absorption rates. Initial conditions $X_{S0} = 1 \cdot 10^6\ CFU\ mL^{-1}$, $X_{I0} = 0$, $P_0 = 1 \cdot 10^2\ PFU\ mL^{-1}$ and $S_0 = 0.1\ mg\ mL^{-1}$. Absorption rate in order black, blue, and red are $1 \cdot 10^{-8}, 1 \cdot 10^{-9}, 1 \cdot 10^{-10}\ mL\ CFU^{-1} PFU^{-1}\ h^{-1}$.

(Shao and Wang, 2008; Payne and Jansen, 2001; Kannoly et al., 2022). Figure 3.3 analyzes the influence of the lysis rate η, which determines the average time between infection and cell lysis.

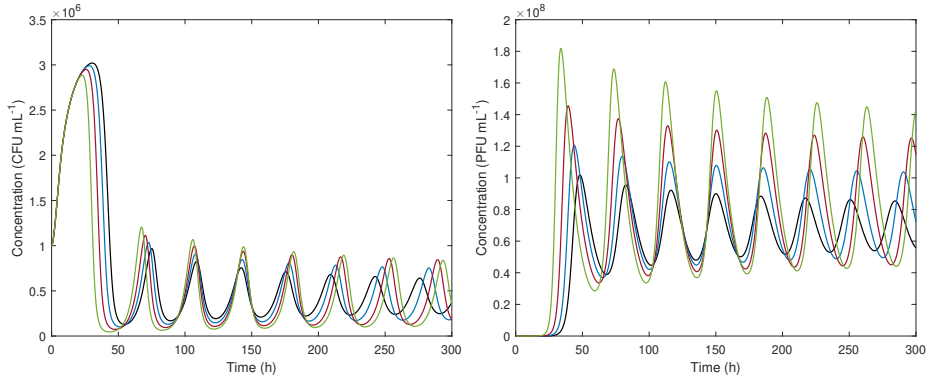

(a) Susceptible bacteria (b) Infected bacteria

Figure 3.3: Time evolution for different lysis rates. Initial conditions $X_{S0} = 1 \cdot 10^6\ CFU\ mL^{-1}$, $X_{I0} = 0$, $P_0 = 1 \cdot 10^2\ PFU\ mL^{-1}$ and $S_0 = 0.1\ mg\ mL^{-1}$. Lysis rates in order black, blue, red, and green are $0.5, 0.67, 1, 2\ h^{-1}$.

Shorter lysis times (higher η) result in faster phage production and more rapid bacterial control. Our results indicate that variations in η primarily affect phage concentration and infection timing, rather than altering the overall qualitative behavior of the system. The optimal lysis time for maximum phage progeny production can vary depending on the phage, host, and growth conditions.

These preliminary simulations confirm that the model captures essential features of bacteria–phage population dynamics and highlights the sensitivity of the system to infection parameters. In the following chapters, the relevance and influence of these factors on the model will be explored in greater depth.

3.4 Discussion

The proposed model shares conceptual similarities with the classical SIR model used in epidemiology, where individuals transition between Susceptible (S), Infected (I), and Recovered (R) compartments. In our case, susceptible bacteria (X_S) become infected (X_I) upon contact with phages, and ultimately lyse, contributing to the free phage population (P). This structure, while simplified, is versatile and widely used in disease modeling and ecological studies.

The historical models discussed in Section 3.1 were developed in diverse fields. The first models presented (Malthus (1798); Verhulst (1838); Monod (1950); Lotka (1925); Volterra (1926)) , were developed to model the population growth of the age and/or ecological purpose. Verhulst (1838) used the model to study population growth in Belgium, London, and Paris, among others. Meanwhile, Lotka (1925) had been studying chemical reactions, and Volterra (1926) the fish population when they arrived at the same mathematical expression. While not all were originally designed for wastewater treatment or phage therapy, they provide foundational insights into population interactions and resource dynamics.

Many of these models have not been validated experimentally, often due to limitations in available data or methodological complexity. For example, Campbell (1961) formulated a nonspecific model focusing on infection properties, this model was developed from a consideration of the biology of the interacting species, but was not very specific about the nature of the habitat and took no account of the relationship between

prey growth and the availability of primary resources. Although this model was not explicitly validated, many authors took Campbell's model as a basis for their models. Similarly, Beretta and Kuang (1998) and Siekmann et al. (2008) developed models to describe viral dynamics in marine plankton communities, without direct empirical validation.

In contrast, Payne and Jansen (2001) formulated a model for phage therapy, examining the outcomes of phage therapy and antibiotics. They found that there are situations in which earlier inoculation can be less efficacious, and simultaneous inoculation with antibiotics can be detrimental to phage therapy. Their therapeutic responses were made using formulae dependent on biologically meaningful parameters. Therefore, they suggested that experimental measurement of the parameters should be a prerequisite for applying the model to particular study systems.

Validated models are more common in phage therapy, where systems can be controlled in laboratory or clinical settings. For instance, Levin et al. (1977) conducted experiments with *E. coli* B and K12, and the virulent bacteriophage T2, to examine the appropriateness of the theory developed in their model of the phage-bacteria interaction. In the study of a one-resource, two-prey, and one-predator system, although the equilibrium predicted by the model was a reasonable analogue of the experimental system, the behavior of the laboratory populations deviated from the theoretical predictions in one significant way. Nevertheless, the Levin et al. (1977) model was the basis for the development of other models, such as the Santos et al. (2014) model.

Despite their long history, phage therapies have been overshadowed by chemical antibiotic therapies over time. However, in recent years, renewed attention has been given to this phenomenon; accordingly, interest has shifted to validating such models with data from a variety of bacterial species and virulent phage strains. There is some interest in *Campylobacte Jejuni*, as a human pathogen that ranks among the major causes of infectious gastroenteritis (campylobacteriosis). However, phage therapy against *C. jejuni* is not only crucial in human medicine, but is also relevant to agricultural and veterinary applications. e.g., phage therapy of poultry before slaughter or of meat before packaging could potentially prevent campylobacters from entering the food chain. Cairns et al. (2009) focused their work on the *C. jejuni*-phage system, fitting the model to time series data to estimate thresholds and rate constants

directly, finding that their simple model fits the data surprisingly well (Cairns et al., 2009).

Additionally, Santos et al. (2014) developed a mathematical model that can predict and explain the basic behavior of phage-bacteria population dynamics. The authors studied a *Salmonella enterica serovar* strain S1400 and its *Salmonella* phage PVP-SE1 as therapeutic use. The experimental validation of the model was performed using data from phage-interaction studies conducted in a 5 L bioreactor, and the model's output was found to match the experimental data closely (Santos et al., 2014).

These examples illustrate the progressive convergence of theoretical and empirical modeling in recent years, particularly in medical, agricultural, and food safety applications. The relevance of such models to wastewater treatment—specifically, to activated sludge systems—is supported by analogous population dynamics and environmental conditions. However, adaptation of these models to the complexities of AS systems requires further development.

Our proposed model incorporates both theoretical structure and experimental observations. It is intended to support diverse applications: predicting system evolution, estimating unmeasured variables, assisting control strategies, and guiding future experiments. Before deployment, the model must be analyzed, including equilibrium points, stability, identifiability, and observability, which are paramount in the future exploitation of the model. The next chapter focuses on this mathematical characterization.

Chapter 4

Model analysis

The theoretical analysis focuses on three aspects: operational conditions, parameters, and states. In the following, we focus attention on the model analysis, including equilibrium points, stability, identifiability, and observability, which are of paramount importance in the future exploitation of the model. This analysis was conducted for the parameter values given in Table 3.1, which were shown in the previous chapter.

4.1 Equilibrium points

The equilibrium points are the solution of the nonlinear system of algebraic equations

$$f(\bar{x}) = 0, \tag{4.1}$$

where $\bar{x} \in \mathbb{R}$ is an equilibrium point.

The analysis reveals that there are three possible equilibrium points, whose location and stability may depend on the value of the dilution rate:

- point 1 is the trivial equilibrium where there is no bacteria and no phage (all populations are extinct);
- point 2 corresponds to a population of bacteria with no phage and no infection, feeding on a substrate (this situation corresponds to a reactor with no phage treatment);

- points 3 represents the possible coexistence between the different populations, which is a priori the equilibrium point of interest for our analysis.

The equilibrium points are presented in Figure 4.1 as a function of the dilution rate.

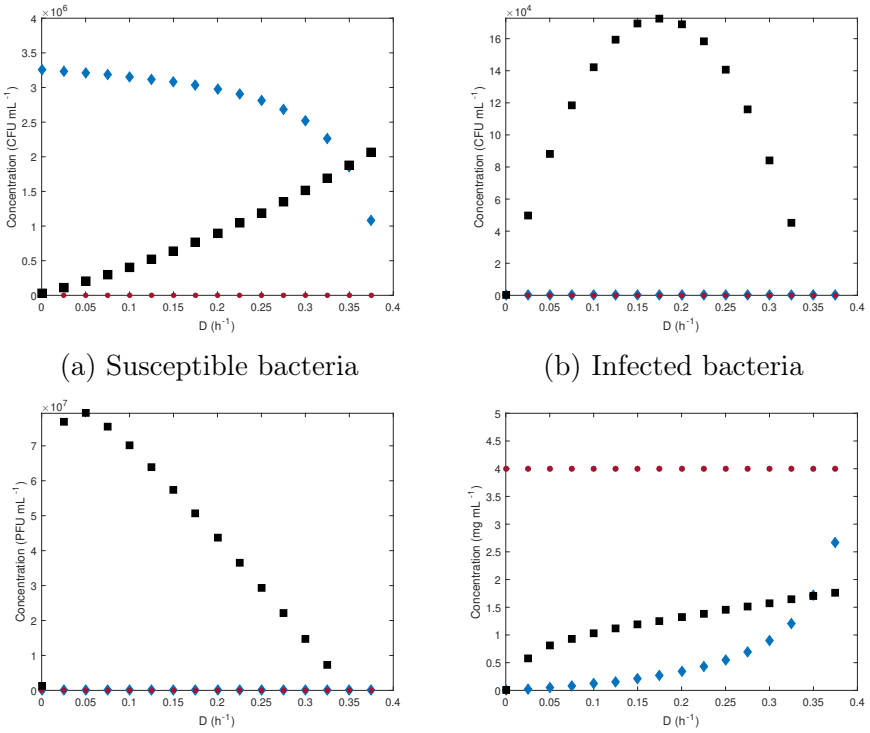

(a) Susceptible bacteria (b) Infected bacteria

(c) Phages (d) Substrate

Figure 4.1: Equilibrium points. Red dot: trivial point, blue diamond: point 2, black square:point 3 .

The evolution of the equilibrium point 2 shows that the wash-out occurs when $D > \mu(S)$ (around D = 0.3901 h^{-1}).

Points 3 is interesting to study, as it corresponds to the phage treatment and the coexistence of the several populations. At low dilution rates, the susceptible bacteria population is much smaller than with no treatment. The infected bacteria population is washed out for dilution rates larger than $0.3451h^{-1}$.

4.2 Stability

The several equilibrium points have to be analyzed with respect to their stability. An equilibrium point which is locally stable will attract trajectories starting from initial conditions located in a close neighborhood (this neighborhood is called the region of attraction of the equilibrium point).

Local stability is studied by evaluating the Jacobian matrix

$$A = \begin{bmatrix} \frac{\partial f_{X_S}}{\partial X_S} & \frac{\partial f_{X_S}}{\partial X_I} & \frac{\partial f_{X_S}}{\partial P} & \frac{\partial f_{X_S}}{\partial S} \\ \frac{\partial f_{X_I}}{\partial X_S} & \frac{\partial f_{X_I}}{\partial X_I} & \frac{\partial f_{X_I}}{\partial P} & \frac{\partial f_{X_I}}{\partial S} \\ \frac{\partial f_P}{\partial X_S} & \frac{\partial f_P}{\partial X_I} & \frac{\partial f_P}{\partial P} & \frac{\partial f_P}{\partial S} \\ \frac{\partial f_S}{\partial X_S} & \frac{\partial f_S}{\partial X_I} & \frac{\partial f_S}{\partial P} & \frac{\partial f_S}{\partial S} \end{bmatrix} \tag{4.2}$$

at the equilibrium point under consideration. The eigenvalues were calculated with the Matlab command *eig*, which returns a column vector containing the eigenvalues of the square matrix A.The eigenvalues of A are represented as a function of D in Figure 4.2.

The two first equilibrium points are saddle points, i.e., points characterized by real positive and negative eigenvalues. This reflects the fact that a small perturbation in the population will generate the onset of bacteria, phages, and infection. The third equilibrium point is characterized by two negative real eigenvalues (stable), and two complex conjugate eigenvalues, which are real negative for $D > 0.0951h^{-1}$. For smaller dilution rates ($D < 0.0951h^{-1}$), the real part of these latter eigenvalues is positive, yielding an unstable spiral.

Figure 4.3 presents phase plane plots for $D = 0.05\ h^{-1}$ (subfigures (a) and zoom (b)) and $D = 0.2\ h^{-1}$ (subfigure (c)) for different initial conditions and the parameters given in Table 3.1, in order to have a deeper insight in the system trajectories. For $D = 0.05\ /h^{-1}$, the trajectories form diverging spirals which collide into limit cycles, whereas for $D = 0.2\ /h^{-1}$, the trajectories form converging spirals towards the equilibrium point 3.

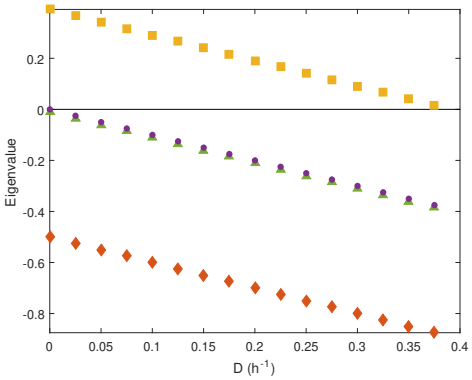

(a) Trivial point

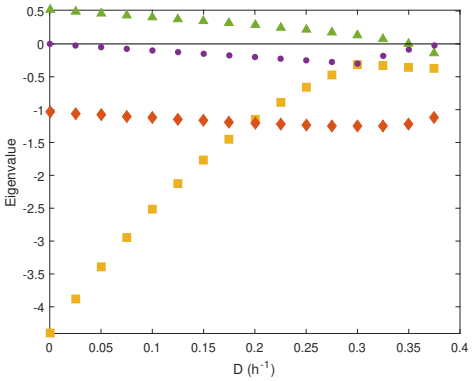

(b) Point 2

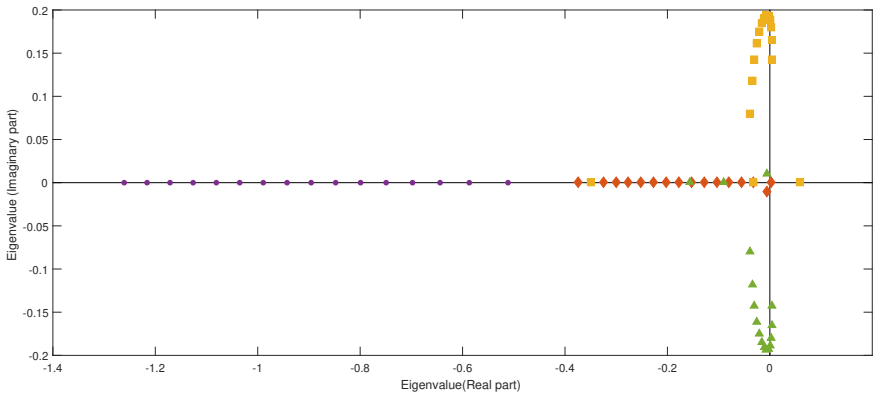

(c) Point 3

Figure 4.2: Stability. Violet dot: eigenvalue 1 (λ_1), orange diamond: eigenvalue 2 (λ_2), green triangle: eigenvalue 3 (λ_3), and yellow square: eigenvalue 4 (λ_4).

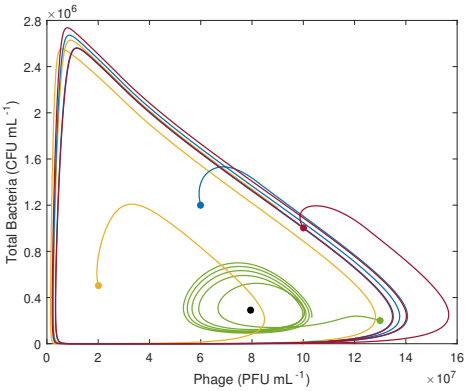

(a) $D = 0.05\, h^{-1}$

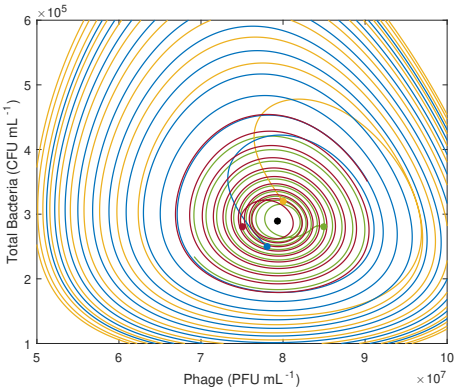

(b) $D = 0.05\, h^{-1}$

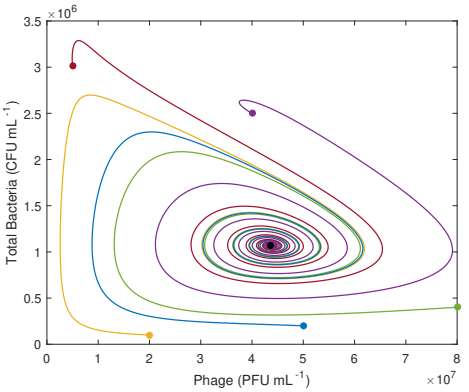

(c) $D = 0.2\, h^{-1}$

Figure 4.3: Phase plane. Black point: equilibrium point; colored points: initial conditions.

Figure 4.4 presents time evolution for $D = 0.1\ h^{-1}$, when a phage concentration of $1 \cdot 10^2\ PFU\ mL^{-1}$ is initially added. As expected, the response converges towards equilibrium point 3 while oscillating. The phage addition is successful from the point of view of controlling the population of unwanted bacteria, since even though not all bacteria are eliminated, their excessive growth is mitigated.

Finally, figure 4.5 focuses attention on the bacteria populations for four different dilution rates, e.g., 0.05, 0.2, 0.3, and 0.42 $^{-1}$, respectively. In the first case, equilibrium point 3 is unstable and the populations present sustained oscillations. In the second and third cases, the equilibrium point is stable and the populations get to equilibrium values, while in the last case, wash-out conditions are achieved.

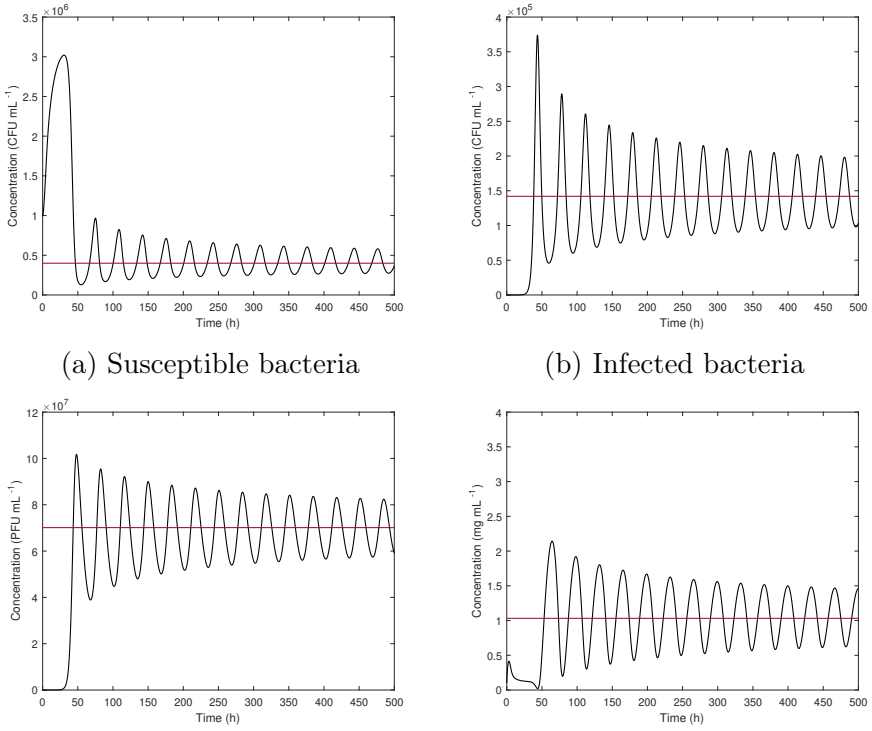

(a) Susceptible bacteria

(b) Infected bacteria

(c) Phages

(d) Substrate

Figure 4.4: Time evolution. Initial conditions $X_{S0} = 1 \cdot 10^6\ CFU\ mL^{-1}$, $X_{I0} = 0$, $P_0 = 1 \cdot 10^2\ PFU\ mL^{-1}$ and $S_0 = 0.1\ mg\ mL^{-1}$. Dilution rate: $D = 0.1 h^{-1}$.

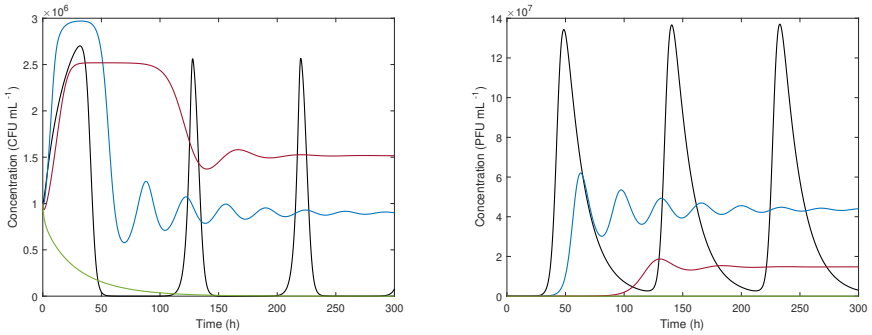

(a) Susceptible bacteria (b) Infected bacteria

Figure 4.5: Time evolution for different dilution rates. Initial conditions $X_{S0} = 1 \cdot 10^6\ CFU\ mL^{-1}$, $X_{I0} = 0$, $P_0 = 1 \cdot 10^2\ PFU\ mL^{-1}$ and $S_0 = 0.1\ mg\ mL^{-1}$. Dilution rate in order black, blue, red, and green are $0.05, 0.2, 0.3, 0.42\ h^{-1}$.

4.3 Identifiability

Once a model structure is adopted, the next step in the model derivation is the estimation of the parameter values from experimental data. A natural question arises on whether this is feasible with the data at hand. This question is usually studied in two steps: (a) structural identifiability and (b) practical identifiability. While practical identifiability refers to quantifying the uncertainty in parameter values when estimated from sampled noisy measurements, structural identifiability considers an ideal situation where the data is available in continuous time and with no noise or errors whatsoever (Ljung and Glad, 1994; Audoly et al., 2001; Hong et al., 2020; Lam et al., 2022). Of course, structural identifiability is a prerequisite, which, if not achieved, should imply questioning about the model structure and parametrization, and possibly a reformulation of the model.

4.3.1 Structural identifiability analysis

In this study, structural identifiability is assessed referring to the concept of observability as suggested by Villaverde (2019). Indeed, structural identifiability can be seen as a particular case of observability if the pa-

rameters are considered as constant state variables, and it is possible to simultaneously analyze the observability and structural identifiability of a model using the conceptual tools of differential geometry(Villaverde, 2019).

The structural identifiability analysis is carried out for model 3.14, regarding the vector of eight parameters (p).

$$p = \begin{Bmatrix} \mu_{max} & K_M & \delta & \beta & \eta & m & \nu_S & \nu_P \end{Bmatrix} \tag{4.3}$$

and various possible measurement configurations, i.e., matrix C in equations 3.15. Operational parameters, S_{in}, and D are known as they are under the control of the operator.

This study is achieved using STRIKE-GOLDD (Villaverde et al., 2019), a MATLAB toolbox that analyses the local structural identifiability and observability of nonlinear dynamic models with multiple time-varying and possibly unknown inputs. The algorithm adopts a differential geometry approach, recasting the identifiability problem as an observability problem. Essentially, the observability of the model variables (states, parameters, and inputs) is determined by calculating the rank of a generalized observability-identifiability matrix, which is built using Lie derivatives. Unobservable variables exist when the matrix is rank deficient. If these variables are parameters, they are called (structurally) unidentifiable. The procedure determines the subset of identifiable parameters, observable states, and observable (also called reconstructible) inputs, thus performing a Full Input-State-Parameter Observability (FISPO) analysis. This approach is directly applicable to many models of small and medium-sized systems; larger systems can be analyzed using additional features of the method (Villaverde et al., 2019).

Table 4.1 shows the results of the identifiability study with the STRIKE-GOLDD toolbox. This analysis is first performed assuming that p is completely unknown, x and x_0 wholly known; this scenario is called "4 measurements" since the four states can be measured. Afterwards, depending on the known states, other measurement configurations with 3, 2 or 1 measurement are also considered.

Table 4.1: Structural identifiability analysis.

States	**Parameters**								**¿Identifiable?**
	μ_{max}	K_M	ν_S	δ	β	η	ν_P	**m**	
					4 measurements				
X_S, X_I, P, S	x	x	x	x	x	x	x	x	Yes
					3 measurements				
X_S, X_I, P	x	x	x	x	x	x	x	x	Yes
X_S, X_I, S	x	x	x	x	x	x	x	x	Yes
X_S, P, S	x	x	x	x	x	x	x	x	Yes
X_I, P, S	x	x	x	x	x	x	x	x	Yes
X_T, P, S	x	x	x	x	x	x	x	x	Yes
					2 measurements				
X_S, X_I	x	x	x	x	x	x	x	x	Yes
X_S, P	x	x	x	x	x	x	x	x	Yes
X_S, S	x	x	x	x	x	x	x	x	Yes
X_I, P	x	x	x	x	x	x	x	x	No
X_I, P	✓	✓	x	x	x	x	x	x	Yes
X_I, P	x	x	x	✓	✓	x	x	x	Yes
X_I, S	x	x	x	x	x	x	x	x	Yes
P, S	x	x	x	x	x	x	x	x	Yes
X_T, P	x	x	x	x	x	x	x	x	Yes
X_T, S	x	x	x	x	x	x	x	x	Yes
					1 measurement				
X_S	x	x	x	x	x	x	x	x	No
X_S	✓	✓	x	✓	✓	x	x	x	Yes
X_I	x	x	x	x	x	x	x	x	No
X_I	✓	✓	x	✓	✓	x	x	x	Yes
P	x	x	x	x	x	x	x	x	No
P	✓	✓	x	✓	✓	x	x	x	Yes
S	x	x	x	x	x	x	x	x	No
S	✓	✓	x	✓	✓	x	x	x	Yes
X_T	x	x	x	x	x	x	x	x	No
X_T	✓	✓	x	✓	✓	x	x	x	Yes

x unknown ✓ known.

It is apparent that all the measurement configurations with 4 and 3 measurements (including also the situation where the total biomass $X_T = X_S + X_I$ can be measured) lead to a FISPO system. On the other hand, the choice of measured variables becomes critical when only 2 measurements are available, and the system is not identifiable with only 1 measurement.

Unidentifiable scenarios are therefore re-evaluated, assuming that some of the parameters are a priori known and do not require further identification. In practice, some preliminary experimental results may sometimes be available beforehand which could be exploited to fix some of the parameters, e.g., μ_{max} and K_M could be estimated experimentally based on a growth curve, δ through an adsorption curve, and β from a one-step test (Hyman and Abedon, 2009). Then, a few 1- and 2-measurement configurations lead to a structurally identifiable system, where it would be possible to estimate the remaining unknown parameters.

4.3.2 Practical identifiability: Parametric sensitivity analysis

Practical identifiability focuses on the information content of the data and the influence of sampling and noise. Here, the analysis is performed in simulation and is restricted to a local parameter sensitivity analysis around the equilibrium point corresponding to the conditions in Table 3.1.

The sensitivity coefficient was calculated as follows (Zambrano et al., 2016):

$$\sigma_{\hat{y}}^{\Delta p} = \frac{1}{T_s} \int_0^{T_s} \frac{\hat{y}(p + \Delta p, t) - \hat{y}(p, t)}{\hat{y}(p, t)} \, dt \tag{4.4}$$

where $\hat{y}(p, t)$ is the model value $\hat{y}$ at time t using the parameter p, $\hat{y}(p + \Delta p, t)$ is the model value $\hat{y}$ at time t evaluated under a change in the parameter by Δp from its reference value p, and T_s is the simulation time. To calculate the sensitivity coefficient for each model parameter, one must change that parameter while keeping the remaining parameters at their reference values. Since X_S, X_I, P, and S profiles are available, a sensitivity factor $\sigma_{\hat{y}}^{\Delta p}$ was calculated for each of them and evaluated by

changing the reference parameter values by 5%. The outputs model were integrated, and the sensitivity coefficients were normalized to facilitate the comparison between the parameters and the different model outputs. The results are presented in Figure 4.6.

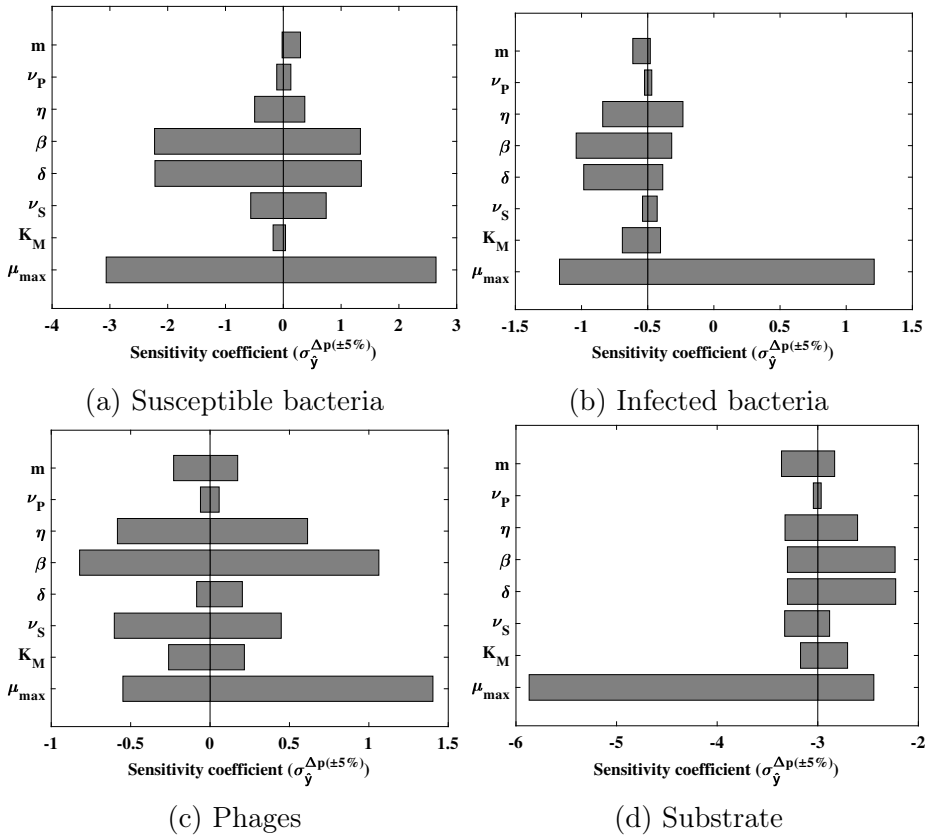

(a) Susceptible bacteria (b) Infected bacteria

(c) Phages (d) Substrate

Figure 4.6: Parametric sensitivity análisis. Normalized values of $\sigma_{\hat{y}}^{\Delta p}$ for the model outputs for a change of 5% in the parameters described in Table 3.1.

This analysis confirms that if all the variables are measured, information is a priori available to estimate all the parameters. The less sensitive parameters are ν_P and K_M. The natural phage inactivation coefficient ν_P accounts for the stability of the phage over time, a very important physical parameter in the infection, but that does not depend on the operational parameters. Classically, the half-saturation coefficient K_M is more delicate to estimate if the feed to the reactor is not varied enough

to get in the appropriate range of substrate concentrations (too high concentrations hide this parameter, while too low concentrations make it linearly dependent on μ_{max}). These aspects have to be explored based on the a posteriori estimates of the uncertainty on the actual identification results, for instance on the basis of the Fisher Information Matrix.

4.4 Observability

Observability is the next interesting model property in view of the design of state estimators or observers, or, in a more technical language, software sensors, dedicated to the reconstruction of non-measured variables. This is particularly important in real case applications, where online instrumentation is limited and the deployment of software sensors is a key asset to monitor the plant at minimal costs. Software sensors blend, or fuse, the predictive information of a dynamic model of the process together with the measurement information from available hardware sensors. A wide range of such state estimators, including the extended Kalman filters, are available (see for instance, Bogaerts and Wouwer (2003); Goffaux and Vande Wouwer (2005) for more details and references).

The concept of observability describes the theoretical possibility of inferring the state vector of a system from observations of the output vector. Observability considers only the dynamic equations of the model, including the definition of inputs and outputs, but not the actual characteristics of the experimental measurements, such the noise level.

Local observability can be easily evaluated by calculating the rank of an observability matrix, which is built as follows.

Consider a linear time-invariant system with n state variables given by

$$\dot{x} = Ax + Bu, \quad y = Cx \tag{4.5}$$

where A, B and C are respectively the state transition, input and output matrices . In the case of a nonlinear system, these matrices can be obtained by computing Jacobian matrices at the point under consideration (for instance matrix A has been evaluated for our model in Equation 4.2).

The observability matrix is defined by

$$O = \begin{bmatrix} C \\ CA \\ CA^2 \\ \vdots \\ CA^n \end{bmatrix} \tag{4.6}$$

and the system is locally observable if and only if this matrix is full row-rank (the rank calculation can be easily carried out in Matlab using the sequence $rank(obsv(A, C))$).

This local analysis reveals that the model is observable around equilibrium 3 for all possible combinations of the measurements, including X_s, X_i, the total biomass $X_T = X_s + X_i$, P, and S, starting with a single measurement of one of these variables. In practice, the availability of more measurement signals will allow improving the convergence and robustness of the software sensor. It will also avoid loosing observability in the case where the measured signal vanishes, provided the additional measurement signals do not vanish at the same time of course.

Table 4.2: Structural observability analysis.

States				**¿Observable?**
X_S	X_I	P	S	
✓	✓	✓	x	Yes
✓	✓	x	✓	Yes
✓	x	✓	✓	Yes
✓	✓	x	x	Yes
✓	x	✓	x	Yes
✓	x	x	✓	Yes
x	✓	✓	x	Yes
x	✓	x	✓	Yes
x	x	✓	✓	Yes
✓	x	x	x	Yes
x	✓	x	x	Yes
x	x	✓	x	Yes
x	x	x	✓	Yes

x unknown ✓ known.

The results of this local analysis are confirmed by the use of the Matlab toolbox STRIKE-GOLDD, introduced earlier for the identifiability analysis. The advantage of this tool is that it considers the original nonlinear model and provides a global analysis. Table 4.2 shows the results. In conclusion, with at least one measured state (no matter which one), the system is observable, and all state variables can be estimated with an appropriate software sensor.

4.5 Model identification and discussion

In the previous sections, a detailed theoretical study was conducted. The results obtained from the identifiability and observability analyses yielded several possible scenarios; however, not all of them are experimentally feasible. The difficulties in performing some measurements, coupled with the lack of instrumentation and/or methodologies to determine all the parameters and/or states, limit our ability to study only some of the possible scenarios. We have compiled experimental data from partner research groups and will evaluate which scenarios are actually possible based on what can be achieved experimentally.

It is clarified that the Grupo IDIN y Servicios de Tecnología Ltda. (Chile) provided the following data under confidentiality agreement conditions, solely for use in an academic setting. Therefore, we will refer to the "bacteria" and the "phage" without specifying their identities. The primary aim of this data was to control Salmonella in the agricultural sector. This information is presented to exemplify what data can be determined experimentally and what tests are performed for this purpose. Data are shown in figures 4.7 and 4.8.

From the data presented in figure 4.7, it has been possible to obtain the parameters: maximum growth rate $\mu_{max} = 1.208\ h^{-1}$, doubling time $t_D = 34\ min$ from the bacterial growth curve, burst size $\beta = 387\ PFU\ CFU^{-1}$, and latency period $\tau = 10\ min$ from the one-step analysis; absorption rate $3.3 \cdot 10^{-10}\ mL\ CFU^{-1}\ min^{-1}$ from the adsorption curve. Figure 4.8 shows the infection curve, from which it is possible to observe that the bacterial concentration decreases after phage application.

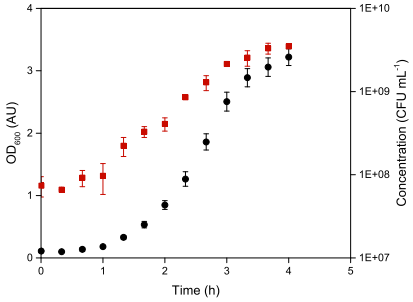

(a) Bacteria growth curve

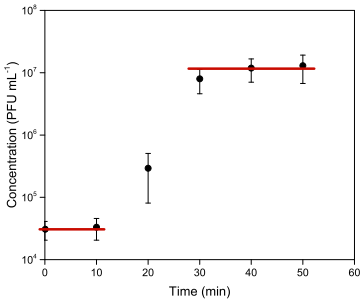

(b) One-step curve

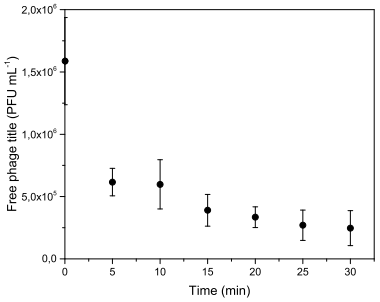

(c) Adsorption curve

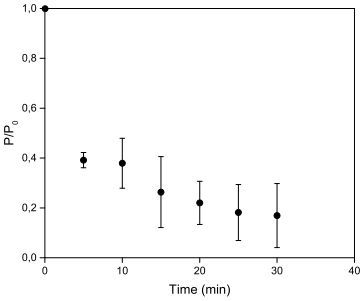

(d) Adsorption curve

Figure 4.7: Experimental data provided by IDIN group. (a) Left axis: black dot, right axis: red square.

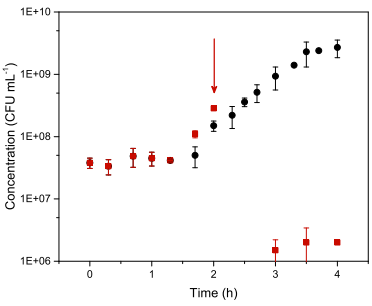

Figure 4.8: Infection curve, black dot: control curve, red square: infection curve, red arrow indicates phage inoculation.

Assuming that the data provided corresponds to the bacteria-phage pair of interest for foaming and bulking control, out of the eight parameters considered in the model, three of them (μ_{max}, δ, and β) can be estimated through specific tests. Additionally, for a Monod-type kinetics, a parameter identification can be made from the microbial growth curve, obtaining the value of K_M. Furthermore, as presented in 4.8, it is possible to monitor the states of X_T and P over time. With this information, and according to the scenarios studied in section 4.3, only three of the twenty proposed scenarios would be possible: the scenario corresponding to two measurements (X_T and P),), and the scenarios corresponding to one measurement (X_T or P), with known values of μ_{max}, K_M, δ and β.

On the other hand, we were able to obtain different phage infection kinetics for some vibrios; Dr. Roberto Bastías's group at PUCV provided us with these datasets. The data are associated with various research articles and publications (Bastías et al. (2010); Kalatzis et al. (2016); Plaza et al. (2018); Kokkari et al. (2018). The data show different kinetics for *Vibrio parahaemolyticus* and *Vibrio alginolyticus* and their respective phages. The vibrios studied are associated with aquatic environments, especially marine ecosystems. *V. parahaemolyticus* is a species found in the sea and estuaries, which, when ingested, can cause gastrointestinal illness in humans. *V. alginolyticus* is a marine bacterium of medical importance, as it causes otitis and wound infections. It is also present in animals such as pufferfish, where it is responsible for the production of the potent neurotoxin tetrodotoxin.

Figures 4.9, 4.11, and 4.10 show the different kinetics of vibrios under varying phages and MOIs (Multiplicity of Infection - ratio of the number of viral particles to the number of host cells in a specific infection medium). The data indicate that the objective of the studies was to produce high phage concentrations rather than bacterial control. In these cases, bacteria were used solely for phage propagation.

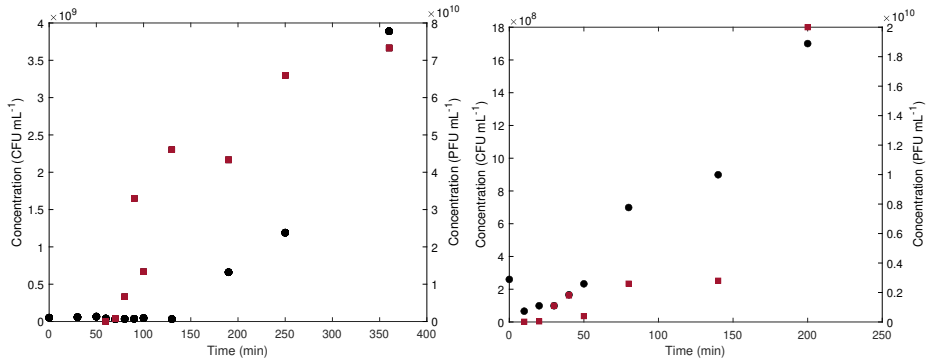

(a) MOI 10 (b) MOI 1

Figure 4.9: Infection curves for *V. parahaemolyticus* and VP93 phage. Black dot: bacteria, red square: phage (a) $X_0 = 5 \cdot 10^7\ CFU\ mL^{-1}$, $P_0 = 4 \cdot 10^7\ PFU\ mL^{-1}$, and $MOI = 10$, (b) $X_0 = 2.6 \cdot 10^8\ CFU\ mL^{-1}$, $P_0 = 1.8 \cdot 10^7\ PFU\ mL^{-1}$, and $MOI = 1$.

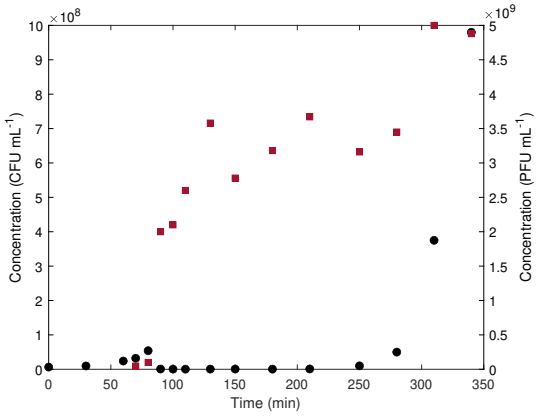

Figure 4.10: Infection curves for *V. parahaemolyticus* and kvp40 phage. Black dot: bacteria, red square: phage. $X_0 = 6.4 \cdot 10^6\ CFU\ mL^{-1}$, $P_0 = 4.7 \cdot 10^7\ PFU\ mL^{-1}$, and $MOI = 10$.

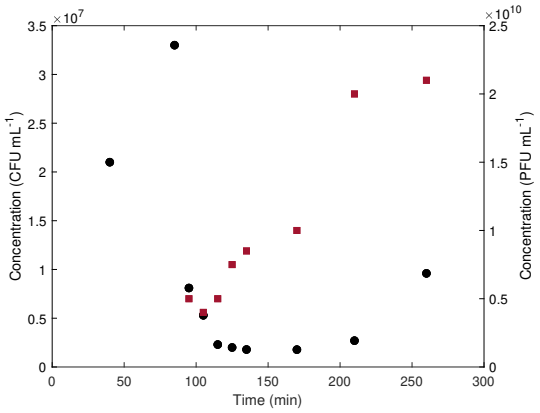

Figure 4.11: Infection curve for *V. alginolyticus* and ven2 phage. Black dot: bacteria, red square: phage. $X_0 = 2.1 \cdot 10^7\ CFU\ mL^{-1}$, and $P_0 = 5 \cdot 10^9\ PFU\ mL^{-1}$.

Again, the available experimental data correspond to concentrations of X_T and P. The fact that the state S is not measured, despite its quantification not being particularly complex, leads us to consider that the model could be modified to assume a different growth pattern, such as using a logistic equation. In that case, the parameter K_M would be replaced by X_{max}, and the parameters ν_S and m should be reconsidered. These changes could enable the use of published experimental data to validate our model. However, with the data currently available, having only the total bacterial concentration quantified—without distinguishing between the states X_S and X_I—necessitates a reduction of our model to such an extent that it would not be possible to estimate the missing parameters. In this context, it would be more appropriate to analyze the data using more general models, such as the Monod or logistic models.

Taking into account the experimental data provided and discussed, to determine the kinetic parameters, the following tests are recommended:

- **Growth curve:** The bacteria's growth in a phage-free environment should be recorded over time. Ideally, if this growth is associated with a specific substrate, or if growth can be determined in terms of carbon availability—such as chemical oxygen demand (COD)—the variation in substrate (COD) over time should also be recorded.

- **Adsorption curve:** The loss of free phages, in units of volume of the infection medium per unit of time, should be monitored over time.

- **One-step:** An assay in which the phages released from a host cell infected by a phage are counted. The latent period is initially observed, and then it can be assessed.

On the other hand, the infection assays are performed under conditions of a complex, well-enriched medium, which ensures no limitation by substrate, thereby not affecting bacterial growth. Therefore, only measurements of the total bacteria and free phage states are taken over time. However, it is recommended that COD measurements be taken over time in future assays so that these data can be used within a wastewater treatment system.

It is also recommended to perform infections with different initial conditions, not only with MOI equal to 1 or 10, but also with initial conditions that allow validation of the equilibrium behaviors presented in section 4.2.

The theoretical studies developed in this chapter have been relevant in determining the operational conditions that favor the improved performance of phage therapy. Similarly, determining that the model meets the properties of identifiability and observability is crucial for control. The next chapter will explore in more depth how the observable nature of the model enables it to be used for reconstructing unmeasured variables (state observers) and optimal control.

Chapter 5

State estimation and control

In wastewater treatment plants (WWTPs), variables such as dissolved oxygen (DO), nitrates (NO_3^-), ammonia (NH_4^+), phosphorus (P), chemical oxygen demand (COD), and total suspended solids (TSS) are monitored to ensure efficiency and compliance with environmental regulations (Hongyang et al., 2018). More precisely, these variables are monitored and controlled in the following way:

- DO is measured online using optical sensors, enabling automated adjustments to the air supply.
- NO_3^- is utilized in anoxic zones for denitrification and is monitored using online ISE or UV sensors, ensuring optimal removal efficiency.
- NH_4^+ is controlled in the aerobic stage. Online ISE (Ion Selective Electrode) sensors enable dynamic strategies, such as Ammonia-Based Aeration Control (ABAC).
- Phosphorus is removed biologically or chemically. Online analyzers provide real-time data for chemical dosing, complemented by laboratory colorimetric tests for detection.
- COD is primarily measured offline due to the complexity of standard methods, although soft sensors and UV-based estimations are also employed.
- TSS is calculated using online turbidity sensors and gravimetric methods in the lab.

Despite the variety of sensors currently available on the market, in many industrial cases, the measurement of specific compounds of interest, such as ammonium or phosphorus, is performed offline in the laboratory using spectrophotometry or standard colorimetric methods. Figure 5.1 shows a WWTPs schematically, indicating where some of the sensors are located.

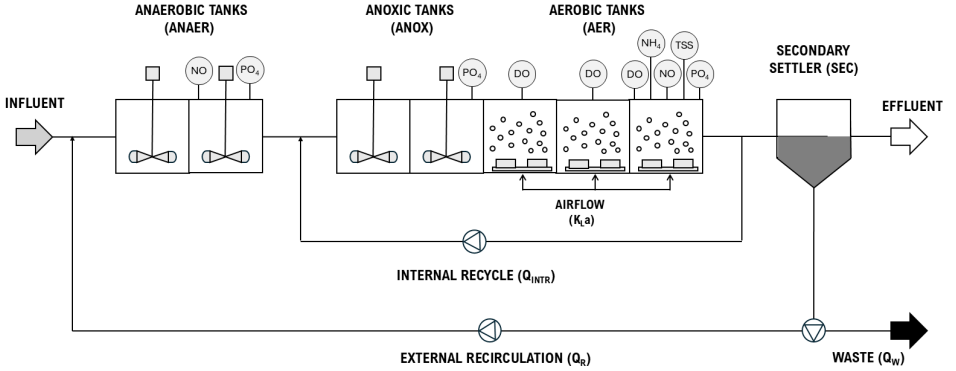

Figure 5.1: WWTPs scheme. Adapted from Ostace et al. (2013)

WWTPs employ traditional PI/PID loops and advanced strategies, such as Model Predictive Control (MPC), fuzzy logic, and hierarchical control, depending on the system's complexity. PI/PID control is widely used in industry for controlling DO, sludge recirculation, and clarifier levels. Ostace et al. (2013) demonstrated multiple PI loops for DO, NO_3^-, and P control, achieving robust performance under variable conditions.

Moreover, cascade control systems, such as ABAC, adjust DO setpoints based on NH_4^+ readings, thereby optimizing aeration. Hierarchical schemes, such as those proposed by Tejaswini et al. (2020), combine fractional PI controllers with fuzzy or MPC supervisors, thereby improving tracking and reducing costs. Revollar et al. (2020) controlled dissolved oxygen (DO) using the N/E index ($NremovedperkWh$), thereby balancing energy efficiency and effluent quality.

Model Predictive Control (MPC) anticipates future process behavior to optimize control. Applied by Hongyang et al. (2018) to nitrogen and phosphorus loops in BSM1-P, MPC outperformed PI controllers under variable loads. Although effective, real-world implementation remains

limited due to modeling complexity. Also, fuzzy logic control allows decision-making based on heuristic rules. Santín et al. (2023) applied it to minimize N_2O emissions, improving effluent quality. Sheik et al. (2022) developed SOPCA, combining fuzzy control and override logic, enhancing phosphorus removal by 28.5% and lowering costs. Bertanza et al. (2020) documented a fuzzy DO controller in a real plant, achieving up to 50% energy savings.

More classical is chemical dosing control. Garikiparthy et al. (2016) evaluated strategies for polymer dosing to control total phosphorus, finding that advanced feedback control was most effective in minimizing chemical use and meeting discharge limits. In the same way as a chemical product is added, bacteriophages can be administered to the system as a concentrated phage solution.

However, many of these new control strategies have not yet been applied in the industry; most WWTPs use PI/PID loops and cascade schemes. ABAC has proven energy savings, and fuzzy controllers are finding application in DO control. MPC adoption is growing in large-scale systems, but it remains rare due to its complexity.

Precise control of critical variables is essential in wastewater treatment plants (WWTPs), and the control strategies employed are diverse. Modern instrumentation enables real-time data for automated control, and techniques have evolved from PI loops to advanced hybrid schemes (Chen et al., 2021). Although real-world application of advanced control is limited, literature shows that intelligent supervisory layers over traditional controls can enhance process stability, efficiency, and sustainability. This chapter will examine two distinct phage control strategies: the development of an EKF and the application of optimal control in phage therapy.

5.1 State Observer

In standard wastewater treatment operations, online measurements are often limited to physical-chemical parameters such as temperature, pH, dissolved oxygen, and residual chlorine. However, measurements of other variables that are highly important in monitoring WWTPs, such as Chemical Oxygen Demand (COD), Biological Oxygen Demand (BOD), Fats, Oil, and Grease (FOG), Total Organic Carbon (TOC AOX), nitro-

gen, phosphorus, solids, biomass concentrations, and products of interest, are usually the results of sampling and off-line laboratory analysis. As such, they are available at discrete times only and with relatively long sampling intervals (several hours up to 1–2 days). In recent years, online probes for measuring component concentrations have been developed, but their use is still very limited. Although some hardware sensors are readily available, they often present several drawbacks: cost, sample destruction, discrete-time measurements rather than continuous, processing delay, sterilization needs, and disturbances in the hydrodynamic conditions inside the bioreactor (Goffaux and Vande Wouwer, 2005; Bogaerts and Wouwer, 2003).

Given these limitations, there is considerable interest in implementing state observers—advanced computational algorithms designed to reconstruct the unmeasured internal states of a process in real time. Unlike basic software sensors, which may rely primarily on input-output relationships, state observers leverage a dynamic process model combined with available measurements (often sparse or asynchronous) to continuously estimate non-measured variables. The observer uses the system's mathematical representation to propagate the state forward in time, integrating available measurements to correct for model uncertainties and disturbances (Bastin and Dochain, 1990; Kadlec et al., 2009).

Software sensors are based on the theory of state observation. As mentioned in the previous chapter (chapter 4 section4.4), the system candidate model is observable with at least one measured state (regardless of which one) and, therefore, could be used to implement a state observer.

Many kinds of state observers have been proposed since the 1960s, and most of them have been applied in the field of biotechnology. Each technique has its own advantages and drawbacks depending on its ability to account for measurement errors, the necessity of using an accurate model for reaction kinetics, whether it is based on local linearization of nonlinear models or nonlinear theory, and on its convergence speed—which can be arbitrarily fixed or determined by the culture conditions (Bernard and Gouzé, 2002; Bogaerts and Wouwer, 2003).

A fundamental requirement for effective state observer design is strong model connectivity between measured and unmeasured variables. Approaches such as Luenberger observers, extended Kalman filters (EKF),

and moving horizon estimation (MHE) are widely employed in bioprocess engineering to estimate critical states such as biomass, substrate, or metabolite concentrations, which are otherwise difficult or costly to measure directly (Dochain, 2003; Kadlec et al., 2009). These observers are particularly valuable in complex and nonlinear biological systems, where real-time monitoring is essential for advanced process control and optimization.

In bioprocess applications, one of the major techniques that have emerged is Kalman filtering, and in particular, the continuous-discrete Extended Kalman Filter (EKF), which allows the use of a continuous-time dynamic model of the bioprocess together with discrete-time measurements, and which takes into account process and measurement noise. Process nonlinearity is approximately addressed through linearization along the state estimate trajectory. State and measurement noise are assumed to be normally distributed (Goffaux and Vande Wouwer, 2005; Alexander et al., 2020).

Furthermore, recent studies have shown that tailored parameter estimation procedures, specifically designed for observer-based monitoring, enhance the sensitivity of estimated (non-measured) states to the measured outputs, thereby improving the reliability of real-time state reconstruction (Bogaerts and Wouwer, 2003; Kadlec et al., 2009). State observers therefore play a crucial role in enabling effective monitoring, diagnosis, and control of bioprocesses, compensating for the inherent limitations of traditional hardware sensors.

5.1.1 Extended Kalman Filter (EKF)

The Kalman Filter is a widely used estimation algorithm in many fields. It is designed to estimate the system hidden states, even when the measurements are imprecise or uncertain. It also predicts the future system state based on past estimations. The Kalman Filter solves the estimation problem for linear systems. However, most real-life systems are nonlinear. The EKF is used in nonlinear systems since it performs analytical linearization of the model at each point in time. EKF is the most common nonlinear extension of the Kalman Filter (Bogaerts and Wouwer, 2003; Goffaux and Vande Wouwer, 2005; Rawlings et al., 2017; Alexander et al., 2023).

The EKF is a widely applied estimation technique due to its simplicity, generally robust performance, and low computational cost. The classical EKF formulation is well-documented in the literature (Bogaerts and Wouwer, 2003; Goffaux and Vande Wouwer, 2005; Rawlings et al., 2017; Alexander et al., 2023).

The EKF algorithm involves a linearization of the nonlinear state equations around the current state estimate $\hat{x}$. As a result, a group of iterative equations is obtained,

Given the following nonlinear system:

$$x_n = f(x_{n-1}, u_{n-1}) + w_n \tag{5.1}$$
$$z_n = h(x_n) + v_n \tag{5.2}$$

where x is the system states vector, u the actuation input and y the measurement output. w is the process noise (model uncertainty) and v the measurement noise (sensor errors). The EKF algorithm proceeds as follows:

- The system equation f and measurement equation h are linearized along the a posteriori estimation $\hat{x}_{n-1,n-1}$
- The state and covariance are predicted between two measurement times t_{n-1} and t_n. The covariance prediction uses the Jacobian matrix A and the process noise covariance matrix Q_{n-1}. The state prediction uses the original nonlinear dynamics

  $$\hat{x}_{n,n-1} = f(\hat{x}_{n-1,n-1}, u_{n-1}) \tag{5.3a}$$
  $$P_{n,n-1} = AP_{n-1,n-1}A^T + Q_{n-1} \tag{5.3b}$$

  where $\hat{x}_{n,n-1}$ is the a priori state estimate (based on the knowledge of the measurement in t_{n-1} and $P_{n,n-1}$ is the a priori covariance matrix. A is the Jacobian matrix computed according 4.2.
- The state and covariance are corrected at time t_n when a new measurement is available

  First, the Kalman gain matrix K is given by,

  $$K_n = P_{n,n-1}H^T(HP_{n,n-1}H^T + R_n)^{-1} \tag{5.4}$$

where H is the Jacobian of the measurement equation, and R_n is the measurement noise covariance matrix.

Then, the state and covariance update equations are

$$\hat{x}_{n,n} = \hat{x}_{n,n-1} + K_n(z_n - H\hat{x}_{n,n-1}) \tag{5.5a}$$

$$P_{n,n} = (I - K_n H)P_{n,n-1} \tag{5.5b}$$

where $\hat{x}_{n,n}$ and $P_{n,n}$ are the a posteriori state and covariance matrix estimates.

In the correction equation, the measurement z_n is compared to the a priori estimate $\hat{z}_{n,n-1} = H\hat{x}_{n,n-1}$

The algorithm can also be described by the steps displayed in Table 5.1.

Table 5.1: Steps of the extended Kalman filter algorithm

Step 1:	Assign the initial values to the system when $n = 0$: $\hat{x}_{0,0}$, $\hat{P}_{0,0}$ (best initial guesses based on the initial measurements)
Step 2:	Propagate the state in time using the nonlinear model: $\hat{x}_{n,n-1}$
Step 3:	Propagate in time the covariance matrix based on the Jacobian transition matrix and the process noise covariance Q: $P_{n,n-1}$
Step 4:	Compute the Kalman gain based on the a priori covariance matrix, the measurement noise covariance R, and the Jacobian of the measurement equation: K_n
Step 5:	Update the state using the correction matrix and the online measurement z_n: $\hat{x}_{n,n}$
Step 6:	Update the covariance matrix: $P_{n,n}$

Regarding the EKF implementation, the Jacobian matrix (equation 4.2) was calculated analytically, as the model equations are relatively simple and allow for straightforward symbolic differentiation. The expression of the resulting Jacobian is as follows.

$$A = \begin{bmatrix} \frac{\mu_{max}S}{(S+K_M)} - \delta P - D & 0 & -\delta X_S & \frac{\mu_{max}X_S}{(S+K_M)} - \frac{\mu_{max}SX_S}{(S+K_M)^2} \\ \delta P & -(D+\eta) & \delta X_S & 0 \\ -\delta P & \beta\eta & -(D+\nu_P+\delta X_S) & 0 \\ \frac{-\mu_{max}\nu_S S}{SK_M} & -m & 0 & \frac{\mu_{max}\nu_S SX_S}{(S+K_S)^2} - \frac{\mu_{max}\nu_S S}{(S+K_S)} - D \end{bmatrix} \tag{5.6}$$

To compute the Kalman gain matrix, direct matrix inversion can be numerically unstable, particularly when the state error covariance matrix (P) is rank-deficient or ill-conditioned. Such conditions frequently arise in biological or environmental systems due to the presence of noise, model uncertainties, or limited observability. To overcome this issue, Cholesky factorization is employed as a numerically robust alternative. By decomposing the innovation covariance matrix into a product of triangular matrices, Cholesky factorization enables the solution of linear systems without explicitly computing matrix inverses. This approach enhances numerical stability and prevents filter divergence, especially in EKF implementations where P may be semi-definite or poorly conditioned.

Back to the bacteriophage application, only the substrate and phage population can be measured, typically offline. In the case of bacteria, quantifying their state at any given time—whether infected or susceptible—is impossible. In the following, we will therefore study the possibility of applying EKF to the estimation of the bacteria populations using the measurements of phages and substrate, or to estimate both bacteria and phage based on the sole measurement of substrate.

When applying the EKF using both S and P measurements (figure 5.2), a notably rapid convergence of the state estimates was observed, with the filter stabilizing in less than 20 hours. This rapid convergence underscores the significant advantage of having multiple, complementary measurements, as the additional phage data provide crucial information to disambiguate the underlying system states and reduce the overall estimation uncertainty.

Conversely, in the scenario where only S measurements were available (figure 5.3), the convergence of the EKF was considerably slower compared with the previous scenario. In this case, the filter required nearly twice as long—approximately 40 hours—to reach comparable levels of convergence. This delay can be attributed to the loss of information associated with the absence of direct phage measurements, which limits the filter's ability to accurately reconstruct the full state of the system, particularly for those variables that are only indirectly related to the measured substrate.

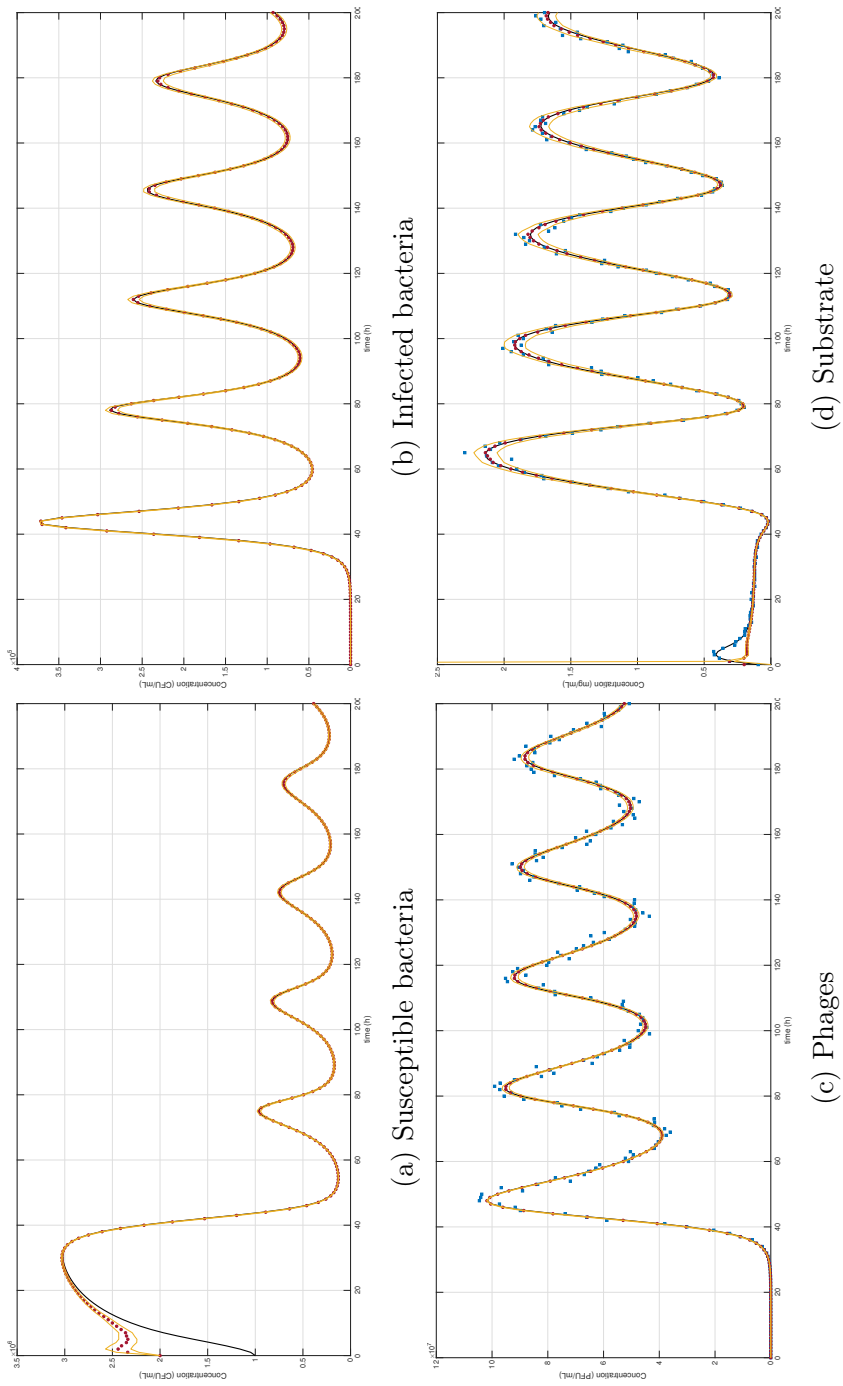

(a) Susceptible bacteria (b) Infected bacteria (c) Phages (d) Substrate

Figure 5.2: Scenario: Phage and substrate measured. Blue square: measurements, black line: model output, red dot: EKF estimation, and yellow lines: estimation confidence interval

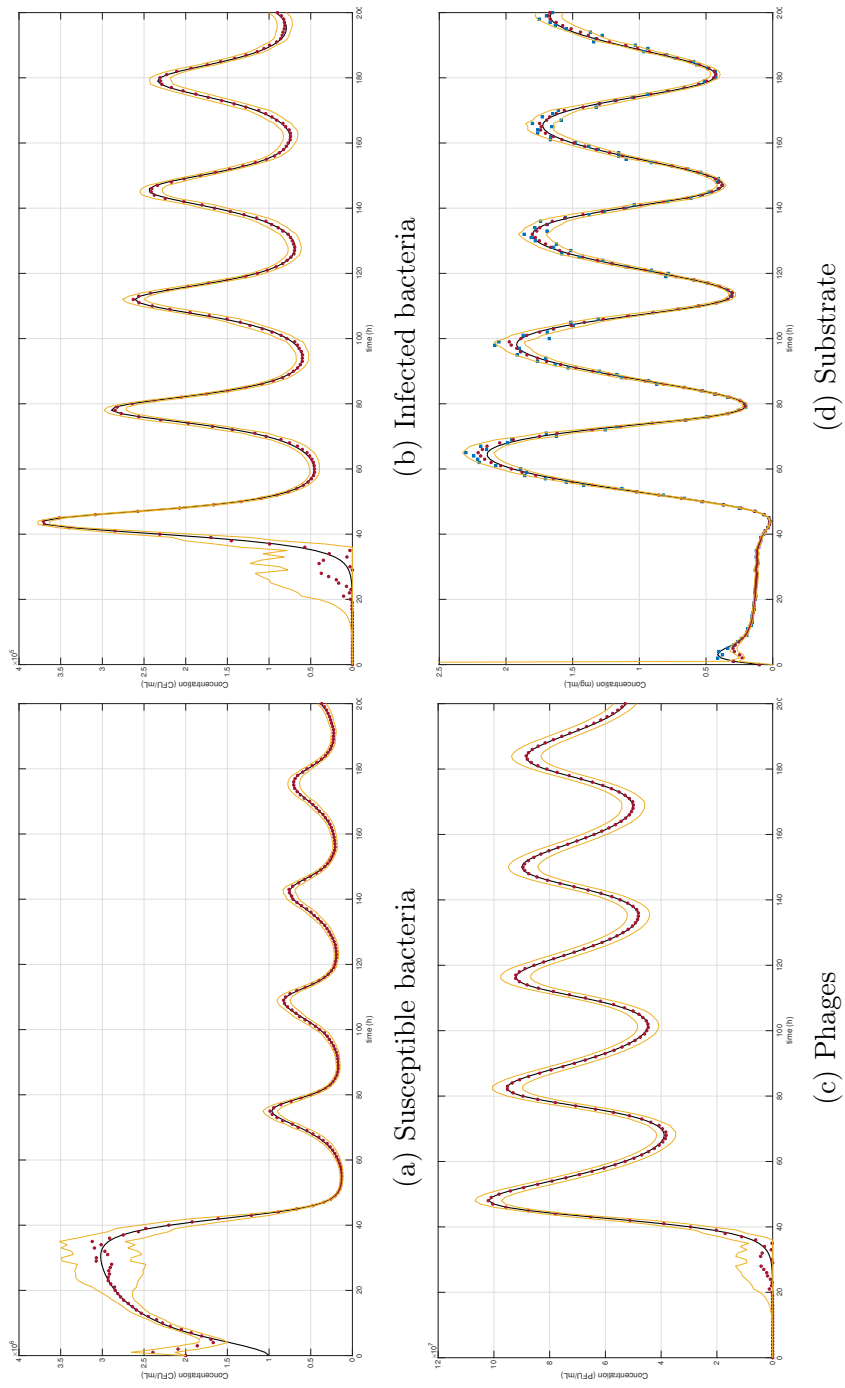

(a) Susceptible bacteria (b) Infected bacteria

(c) Phages (d) Substrate

Figure 5.3: Scenario: Substrate measured. Blue square: measurements, black line: model output, red dot: EKF estimation, and yellow lines: estimation confidence interval

These results demonstrate the importance of measurement availability and diversity in state estimation for bioprocess systems. While the EKF is capable of providing reliable estimates even with a single measurement, the estimation performance, in terms of both convergence speed and transient accuracy, is markedly improved when multiple system variables are monitored.

5.1.2 Effect of the process noise

One of the main challenges in EKF-based estimation is providing appropriate system and measurement covariance matrices Q, and R. These are often difficult to quantify, especially in processes where noise sources are not clearly defined. It is therefore common to approximate them by trial and error until satisfactory estimation results are achieved (Alexander et al., 2023).

In this study, we consider a relative error model to simplify this tuning. As an example, we consider 5 % of relative error for the measured variables and relative errors for the process model varying between 0.01 % and 1 % (corresponding to a higher trust in the model).

The impact of different values of Q is illustrated in Figure 5.4. When the process noise is set to a very low value (e.g., 0.01%), the filter places substantial trust in the model predictions and gives comparatively little weight to new measurement information. Under these conditions, the filter's state estimates closely follow the model trajectory, and the filter's ability to rapidly adapt to actual system disturbances may be limited. This can result in persistent estimation errors, especially if the actual process deviates from the assumed model dynamics. On the other hand, increasing the value of Q (e.g., to 1%) effectively reduces the filter's confidence in the model, allowing it to respond more dynamically to discrepancies revealed by the measurement data. This results in state estimates that are more sensitive to actual process variability.

These results highlight the trade-off in selecting Q, a lower process noise covariance leads to more model-driven estimates, whereas a higher covariance enables faster correction based on observed data but may also amplify measurement noise in the estimates. The use of a relative error model provides a systematic and reproducible framework for initial tuning.

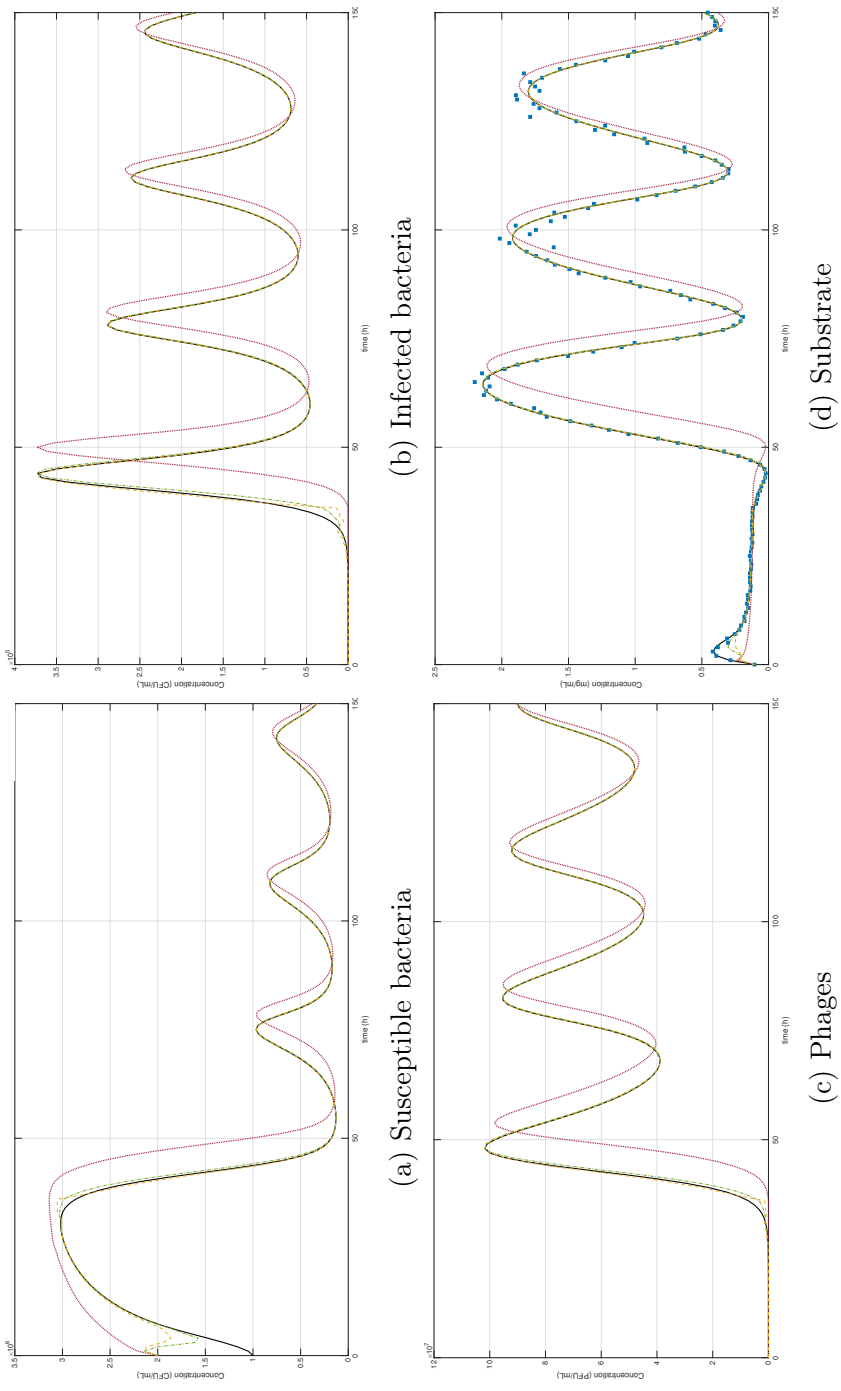

(a) Susceptible bacteria (b) Infected bacteria

(c) Phages (d) Substrate

Figure 5.4: Effect of relative errors for the process model. Blue square: measurements, black line: model output, red dots line: EKF estimation with 1 % error, green dashed dotted: EKF estimation with 0.1 % error, and yellow dashed line: EKF estimation with 0.01 % error.

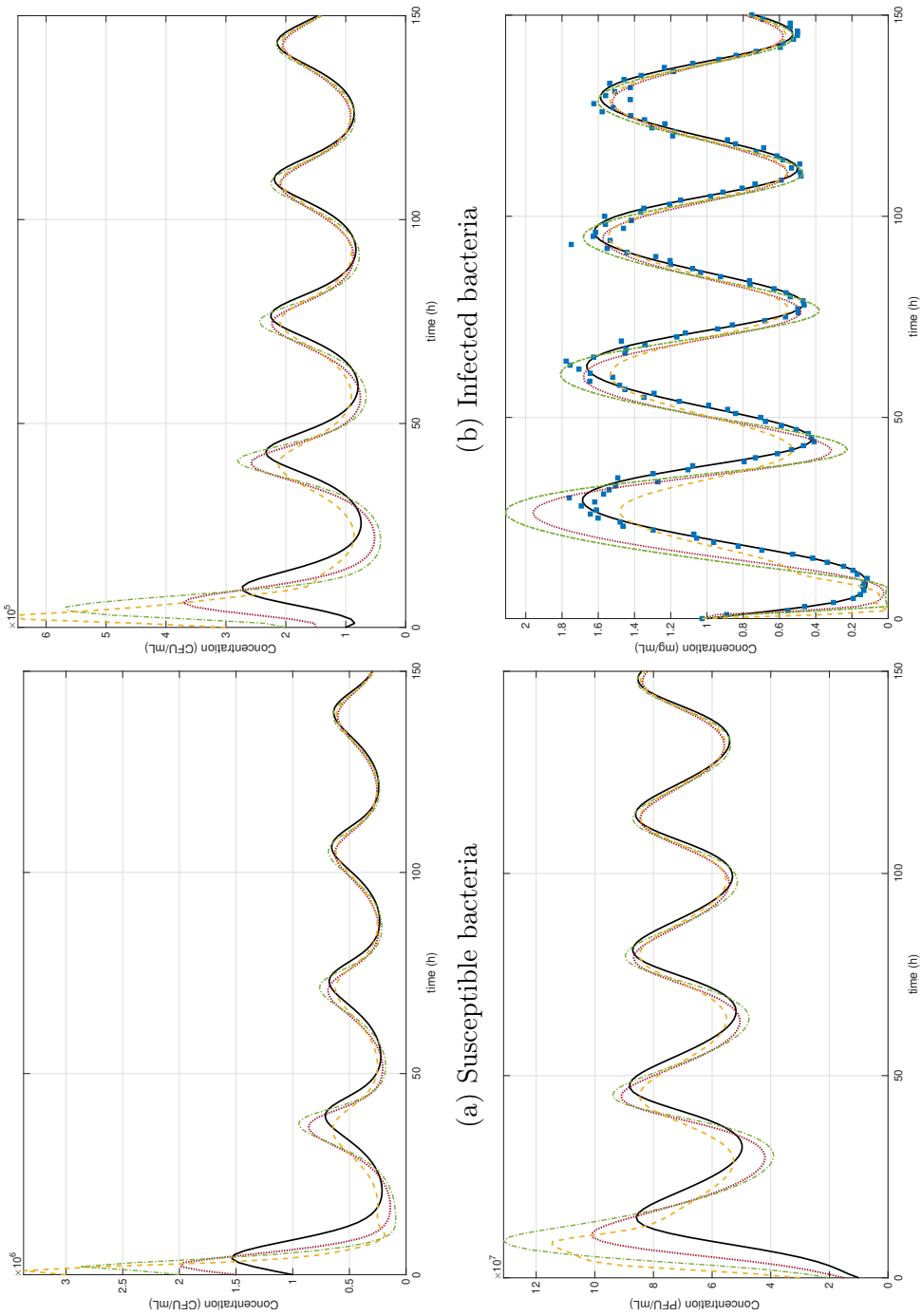

(a) Susceptible bacteria (b) Infected bacteria

(c) Phages (d) Substrate

Figure 5.5: Effect of initial errors in the state estimates. Blue square: measurements, black line: model output, red dots line: EKF estimation with 50 % error, green dashed dotted: EKF estimation with 100 % error, and yellow dashed line: EKF estimation with 200 % error.

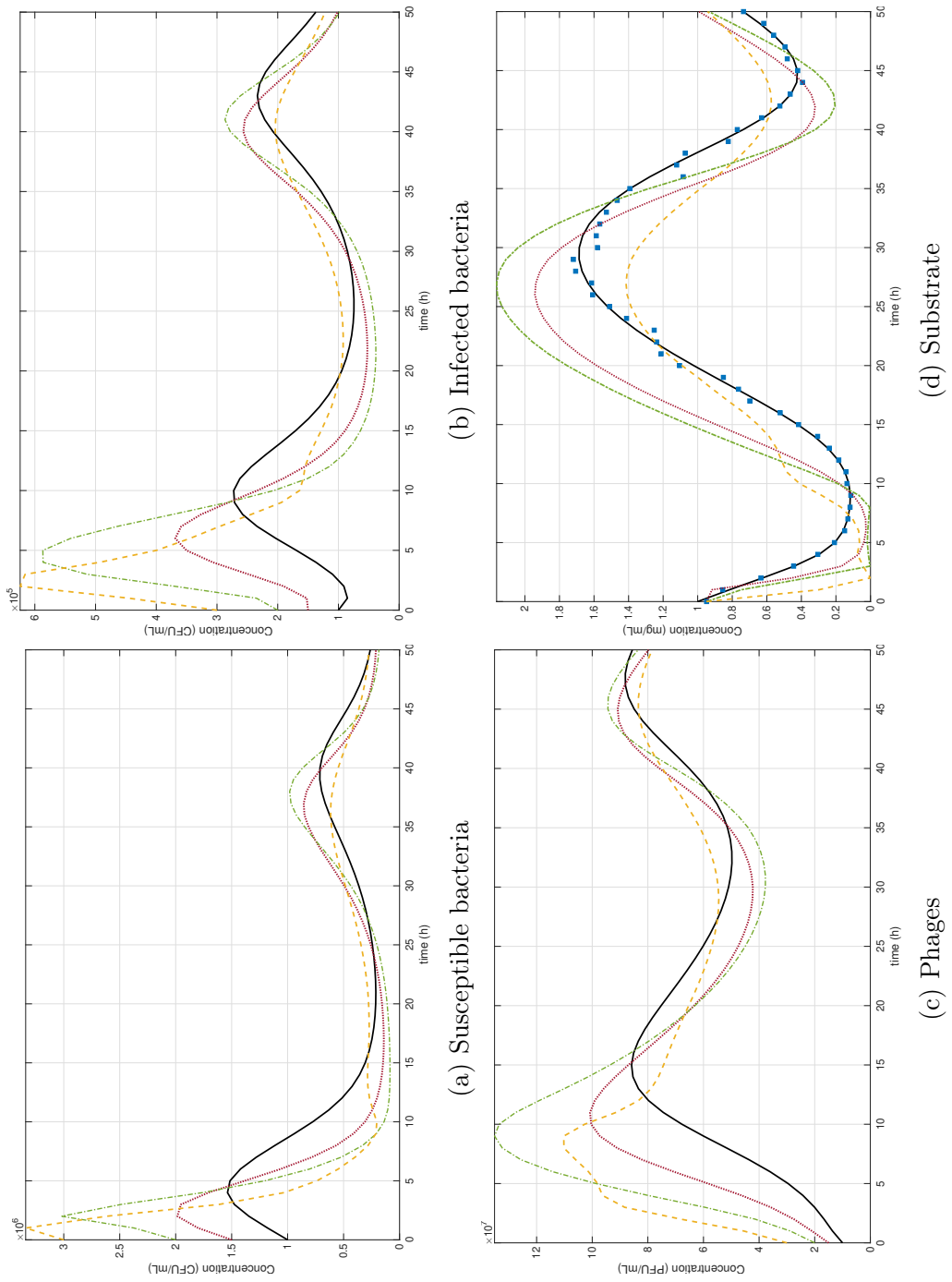

Figure 5.6: Effect of initial errors in the state estimates - Zoom. Blue square: measurements, black line: model output, red dots line: EKF estimation with 50 % error, green dashed dotted: EKF estimation with 100 % error, and yellow dashed line: EKF estimation with 200 % error.

5.1.3 Effect of initial errors in the state estimates

To evaluate the observer convergence, erroneous initial conditions are used for the nonmeasured variables, e.g., 200 % of errors are considered (the sensor output is used for the measured variables). Specifically, error magnitudes of 50%, 100%, and 200% were tested, as illustrated in Figure 5.6.

The results show that, with a 100% error in the initial state, the estimated trajectories initially overshoot above the accurate model output. In contrast, when a 200% error is applied, the estimated state trajectories initially undershoot, falling below the expected model behavior. Despite these significant discrepancies, the EKF demonstrated robust convergence properties. In both scenarios, the state estimates gradually approached the actual system values, albeit over a more extended convergence period compared to cases with accurate initializations.

The increased convergence time observed under significant initial condition errors can be attributed to the filter's need to correct for the substantial initial offset using only the available measurement updates. Nonetheless, the EKF was able to overcome these initial uncertainties and reliably estimate the true system states in the long term, indicating a high degree of robustness to poor initial knowledge of the system.

These findings highlight the EKF's practical suitability for WWTP applications, where initial state information is often uncertain or imprecise. Although larger initial errors increase the time required for the observer to stabilize, the filter's convergence is ultimately assured, provided that informative measurements are available throughout the process.

5.1.4 Effect of confidence interval

The previous results show the time trajectory of the actual variables (emulated by a model), the estimated variables (calculated by EKF), together with 99% confidence intervals. To further evaluate the uncertainty quantification provided by the filter, additional cases with 90% and 95% confidence intervals were also illustrated, as shown in figure 5.7.

The results demonstrate that the width of the confidence interval reflects the degree of statistical certainty regarding the estimated state at each time point. As expected, the 90% confidence intervals are narrower, indicating higher certainty but increased risk of excluding the true value.

In contrast, the 99% intervals are the widest, ensuring a higher probability that the true state lies within the interval, but at the cost of reduced precision.

For all confidence levels considered, the actual system trajectories remained within the predicted intervals throughout most of the simulation, confirming the reliability of the EKF's uncertainty quantification. Overall, the EKF demonstrates robust performance in capturing estimation uncertainty, with the flexibility to tailor the confidence level to the needs of the WWTP under study.

5.1.5 Effect of model parameter errors

Lastly, to evaluate the robustness of the EKF, the values of the most influential model parameters ($\mu_{max}, \delta, \beta, \eta$) were intentionally altered by 10% based on the sensitivity analysis (section 4.3). The results are shown in figure 5.8. This scenario simulates a realistic situation where parameter identification is imperfect, and the actual system parameters deviate from those used in the observer model. As anticipated, the introduction of parameter errors resulted in a deterioration of the EKF's predictive performance, as evidenced by an increase in the estimation error and a slower convergence toward the actual state values. This decline in performance is attributed to the model mismatch: the predictions generated by the observer no longer accurately represent the real system dynamics due to the parameter discrepancies.

To mitigate the negative impact of model uncertainty, the process noise covariance matrix (Q) was increased from 1% to 10% relative error for the process model, and the measurement noise covariance matrix (R) was decreased from 5% to 0.5% relative error for the measurement. This adjustment effectively reduces the filter's confidence in the predictive model and places greater emphasis on the measurement updates during the correction step. As a result, the EKF was able to compensate for the parameter-induced model errors, achieving convergence behavior and estimation accuracy comparable to the baseline scenario with perfectly identified parameters.

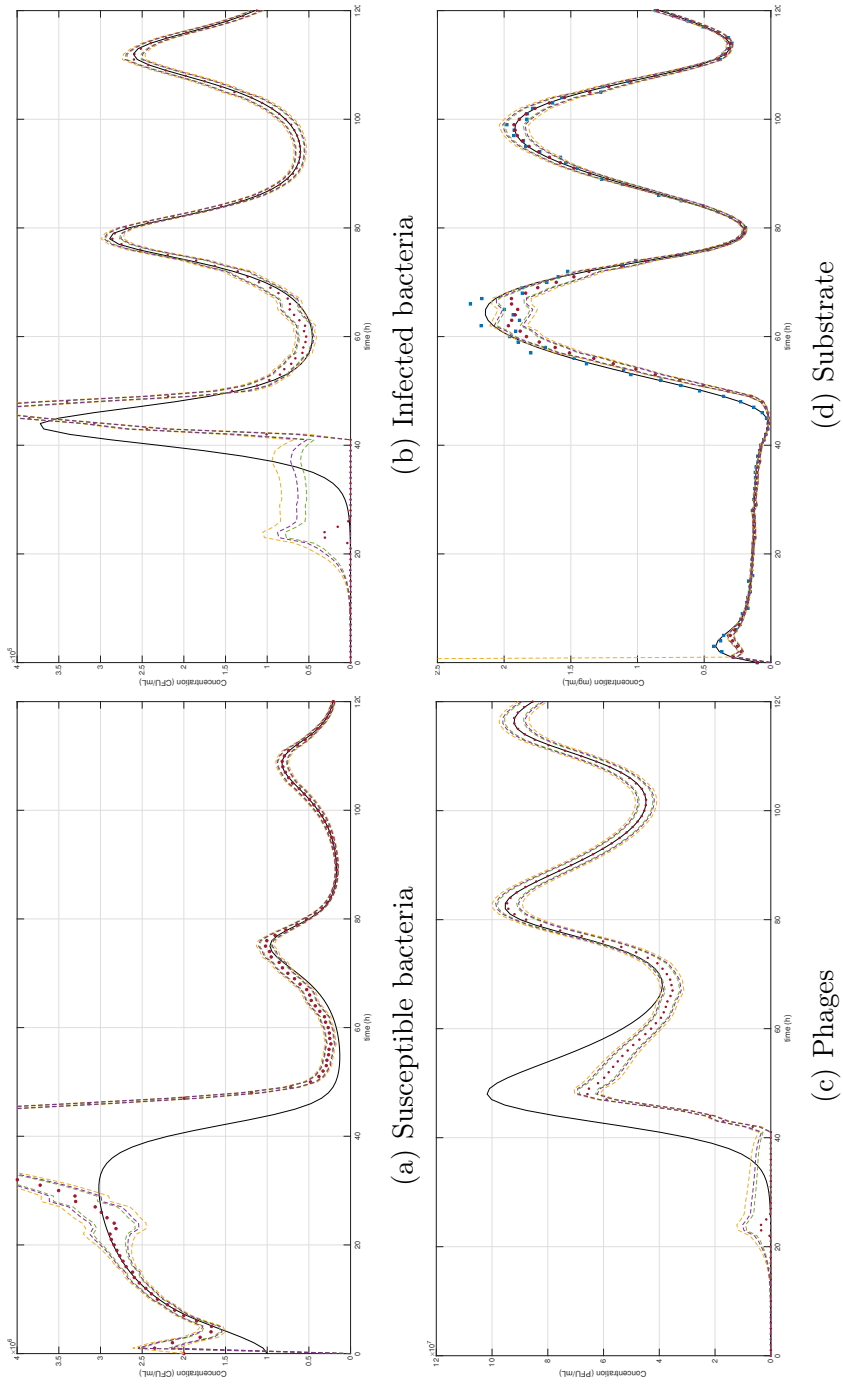

(a) Susceptible bacteria (b) Infected bacteria (c) Phages (d) Substrate

Figure 5.7: Effect of confidence interval. Blue square: measurements, black line: model output, dashed lines: Confidence interval calculated, green 90 % error, purple 95 % error, and yellow 99 % error.

Figure 5.8: Effect of model parameter errors. Blue square: measurements, black line: model output, dots: EKF estimation, red 0 % error in sensitive parameters and 1 % relative error for the process model, green 10 % error in sensitive parameters and 1 % relative error for the process model, and yellow 10 % error in sensitive parameters and 10 % relative error for the process model and 0.5% relative error for the measurements

In summary, these results demonstrate the EKF's adaptability in the presence of moderate parameter uncertainties. While the initial prediction performance is degraded under parameter mismatch, appropriately tuning the process noise covariance (Q) and the measured noise covariance (R) allows the filter to rely more heavily on available measurements, thereby restoring its ability to track the true system states effectively. This underscores the importance of carefully selecting filter parameters in practical applications, particularly when the model is subject to uncertainties inherent in the parameter identification process.

The observer estimations matched the model outputs within a reasonable time frame for all non-measured states. Note that in all cases, the response converges towards the equilibrium point while oscillating, as described in the sections 4.1, and 4.2.

The application of Extended Kalman Filter (EKF) in real-world wastewater treatment plants (WWTPs) remains somewhat limited; however, its study represents a powerful tool for future implementation. EKF forms the basis for Digital Twins (DTs), which are among the most effective tools for managing complex systems, where optimal operation, predictive maintenance, and automation are essential for addressing operational challenges. DTs integrate model-driven and data-driven approaches, relying on gray-box models and utilizing real-time data collected from a limited number of non-intrusive sensors. Digital Twin technologies are rapidly expanding across various domains, from healthcare to urban infrastructure management. In the industrial sector, DTs are applied to a wide range of tasks, including real-time monitoring and predictive control. (Baldassarre et al., 2024; Isoko et al., 2024).

Despite the positive results achieved with the EKF, implementing it using appropriate sensing technologies remains a challenge. As noted at the beginning of this chapter, chemical oxygen demand (COD) is typically measured offline; however, it can be estimated online using soft sensors and UV-based estimation techniques. Although the latter are less commonly employed, they represent a promising alternative for evaluating the feasibility of large-scale EKF implementation. In contrast, monitoring bacteria and phages presents a more complex scenario, as their accurate quantification requires the use of specialized techniques, such as those employed in molecular biology, to determine their concentrations specifically and reliably.

5.2 Optimal Control

Continuing with the architecture of the control, an optimal control in open-loop was studied. For this study, and to prevent disturbing the operation of the actual system, the addition of phage is achieved using a new input. Continuous phage production in a reservoir tank, which feeds the reactor with a constant phage concentration, is considered. Figure 5.9 illustrates the proposed theoretical control scheme. The system is limited to the AS reactor, as this is where phage therapy will be performed. It is emphasized that the control system may differ in practice; however, this approach represents a first step in investigating optimal control in an open-loop system (assuming the ideal case where everything is ideal and well known).

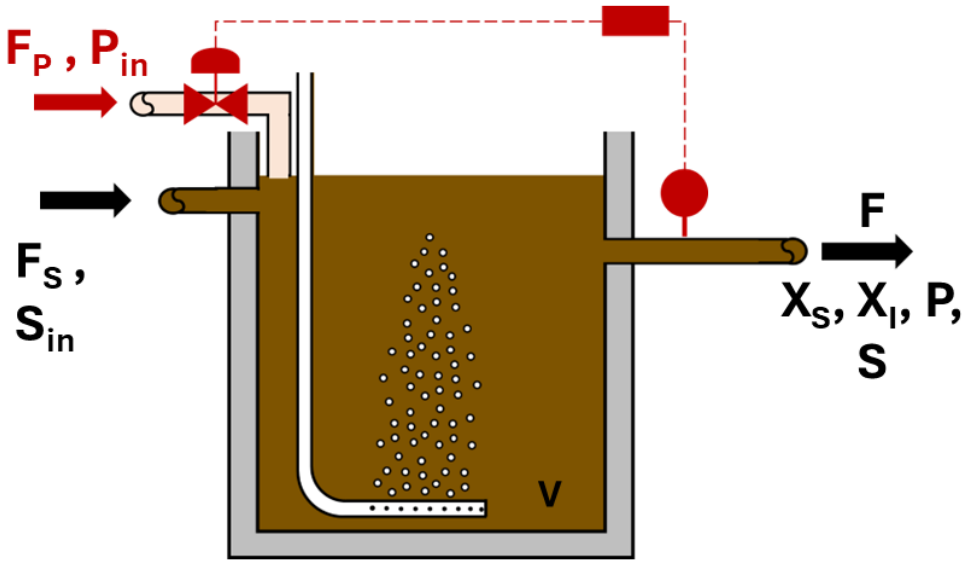

Figure 5.9: Control strategy scheme

The model was modified simply as follows.

$$\frac{dX_S(t)}{dt} = \mu(S)X_S(t) - \delta X_S(t)P(t) - DX_S(t), \tag{5.7a}$$

$$\frac{dX_I(t)}{dt} = \delta X_S(t)P(t) - \eta X_I(t) - DX_I(t), \tag{5.7b}$$

$$\frac{dP(t)}{dt} = -\delta X_S(t)P(t) + \beta\eta X_I(t) - \nu_p P(t) + D_P P_{in} - DP(t), \tag{5.7c}$$

$$\frac{dS(t)}{dt} = -\nu_s(\mu(S)X_S(t) - mX_I(t)) + D_S S_{in} - DS(t)). \tag{5.7d}$$

where P_{in} is the phage concentration on the phage flow input, D_S, and D_P are the substrate and phage dilution rates, respectively, each is denoted F_S/V and F_P/V, and the dilution rate is $D = D_S + D_P$.

The optimization problem is defined as follows:

- Find D_P that minimizes the total bacterial concentration, denoted as $X_T = X_S + X_I$, and the phage flow rate D_P, according to the following cost function:

  $$\min_{D_P} J \tag{5.8}$$

  where the cost function J is defined as

  $$J = \left(\sum_{i=1}^{N} X_T(t_i)^2 \right)^{1/2} + \lambda D_P \tag{5.9}$$

In this expression, $X_T(t_i)$ is the total bacterial concentration (the sum of susceptible and infected bacteria) at each discrete time point t_i of the simulation, N is the total number of time points, D_P is the (constant) phage inflow rate, and $\lambda = 2$ is a weighting parameter.

In the numerical implementation, the first term is computed using the Matlab *norm* function applied to the vector of total bacterial concentrations throughout the simulated time horizon, while the second term penalizes the magnitude of D_P.

In this context, λ is a weighting parameter introduced in the cost function J to balance the relative importance of the two terms being minimized: the total biomass X_T and the flow rate D_P. Specifically, λ determines the degree to which changes in D_P influence the overall cost

compared to changes in X_T. The value λ implies that the contribution of the flow rate D_P to the cost function is weighted twice as heavily as that of the total biomass X_T. This allows the optimization process to prioritize the minimization of D_P accordingly, depending on the specific objectives of the problem.

The optimal control was executed for a reactor volume (V) of $10\,m^3$ with the parameters in Table 3.1. The *fminunc* function from MATLAB was implemented to estimate the D_P that minimizes the cost function. Different control strategies were studied, and the evolution of the variables for these scenarios has been presented in this section.

5.2.1 Constant Phage-flow

The most straightforward optimization study involves operating the system with constant phage feeding. Regarding operationality, it represents the valve opening to feed a determined flow. To avoid the washout, the problem was constrained as $D < D_{washout}$. From section 4.1 it is known that $D_{washout} = 0.3901$. Phage flow was constraines as $D_P \leq 0.28\,h^{-1}$. At $P_{in} = 1 \cdot 10^8\ PFU\ mL^{-1}$, the optimization problem was solved, and the dilution rate that minimizes the cost function is $D_P = 0.28\,h^{-1}$, which corresponds to $F_P = 28\,m^3\,h^{-1}$. The phage input flow is more than double compared to F_S, suggesting that phage elimination may occur in this case due to the high dilution rate.

To evaluate the dilution rate effect, a scenario with constant flow and phage concentration $P_{in} = 0$. The system response was modeled using MATLAB, and the results are presented in figure 5.10.

The results show that the bacteria were eliminated when the phages were applied. Regardless of whether phage was present or absent in the input flow, the bacterial concentration decreased, by approximately $20\,h$ with phage addition and more than $50\,h$ without them. The constant-flow strategy is impractical, as in real-world applications, the required phage flow is unrealistically high and therefore not viable. Maintaining a continuous phage reservoir to supply such a flow is costly, making it non-competitive compared to chemical strategies such as chlorine. However, the elimination of bacteria was primarily driven by the dilution rate rather than phage infection, indicating that the phage flow should be limited, and its application strategies should be studied.

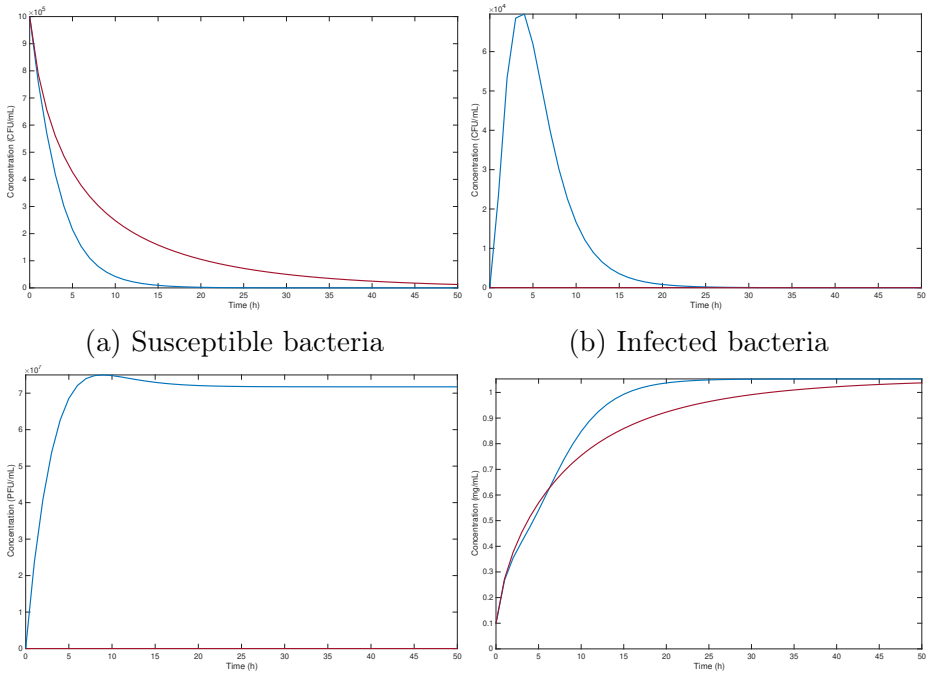

(a) Susceptible bacteria (b) Infected bacteria

(c) Phages (d) Substrate

Figure 5.10: Time evolution with constant phage-flow. The blue and red lines are cases with and without phage addition, respectively.

5.2.2 Variable Phage-flow

Continuing the study, and in an effort to approximate the scenario to a more realistic context, a variable-flow strategy was proposed. This approach was implemented as a sequence of discrete steps, simulating the process of opening and closing a valve to introduce phages—analogous to monitoring scenarios in which a sensor measures a variable of interest and an operator adjusts the valve accordingly.

Ten time intervals were defined, each lasting 10 hours, and a new D_P was recalculated for each interval. Figure 5.11 presents the temporal evolution of the system states, while figure 5.12 displays the corresponding phage flow profile. In the second, fourth, fifth, and seventh intervals, the phage flow reached $F_P = 28\, m^3\, h^{-1}$, which remains excessively high, similar to the constant-flow scenario. As a result, the susceptible bacte-

ria are eliminated between the fourth and fifth intervals, primarily due to the high dilution rates. To address this behavior, the phage flow was subsequently constrained to not exceed 10% of the substrate flow (i.e., $F_P \leq 10\% F_S$). The updated time evolutions under this constraint are compared in figures 5.12, and 5.11.

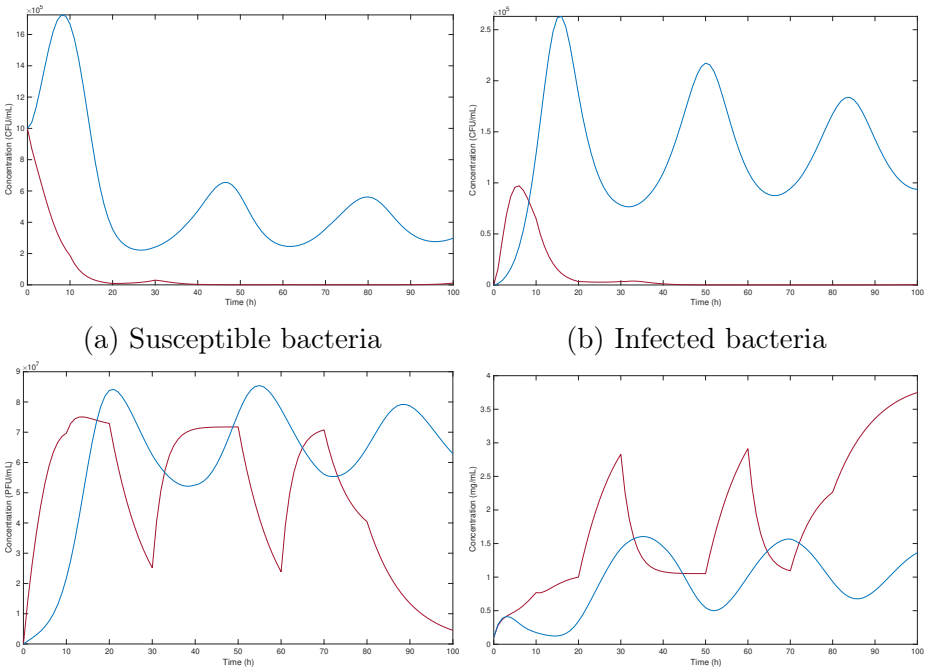

(a) Susceptible bacteria (b) Infected bacteria

(c) Phages (d) Substrate

Figure 5.11: Time evolution of variables with constraints on phage input flow (F_P). $P_{in} = 1 \cdot 10^8\ PFU\ mL^{-1}$. The red line is a scenery where $D < D_{washout}$, and the blue line is a scenery where $F_P \leq 10\% F_{Sin}$.

The constrained scenario aligns with industrial applications, as the phage flow is not high enough to create a dilution rate effect or render the process economically unfeasible due to the substantial phage production required. Under these conditions, the bacteria are not entirely eliminated; however, their concentration remains between $2 \cdot 10^5$ and $6 \cdot 10^5\, CFU\, mL^{-1}$, indicating their oscillatory behavior around their equilibrium point (section 4.1). Thus, the bacterial population does not grow uncontrollably to the point of causing operational issues, while still fulfilling its intended function within the system.

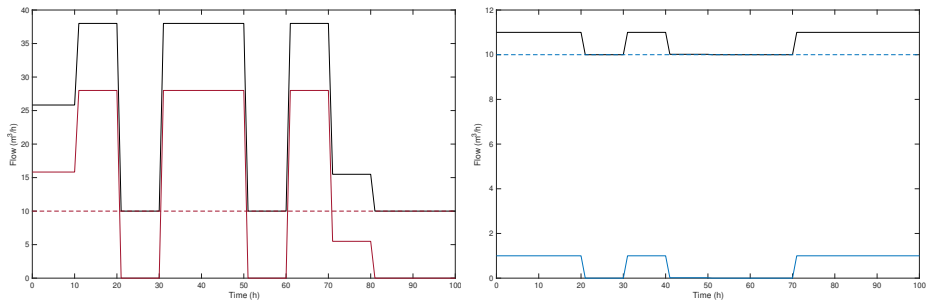

(a) $D < D_{washout}$ (b) $F_P \leq 10\% F_{Sin}$

Figure 5.12: Flow profiles for scenarios with constraints on F_P. The dashed line is F_S, the continuous line is F_P, and the black line is total flow ($F = F_S + F_P$).

An important aspect to highlight is the number of intervals considered in the study. This selection was based on the assumption that a control system involving a manually operated valve would require intervention by an operator. The operator would either rely on offline measurements of the variable of interest or, based on system observation and operational experience, anticipate an emerging issue and respond accordingly regarding the application or suspension of phage control. Consequently, a 10-hour interval was deemed a reasonable timeframe for operating the control valve. In contrast, a more robust control system equipped with sensors and automated technology would enable faster response times, thus allowing for shorter and more frequent control intervals.

Until now, the phage concentration in the input flow was maintained at $P_{in} = 1 \cdot 10^8\ PFU\ mL^{-1}$. However, understanding the system's behavior in response to variations in phage concentration in the feed is essential to determine the minimum effective concentration that ensures the phage reservoir remains effective for bacterial control. Figure 5.13 presents the system's response to different P_{in} values, while figure 5.14 shows the corresponding phage flow profiles for each input concentration.

The results indicate that a $P_{in} \geq 1 \cdot 10^{10}\ PFU\ mL^{-1}$ represents a phage concentration capable of eliminating the bacteria in a very short time. Conversely, a $P_{in} \leq 1 \cdot 10^8\, PFU\, mL^{-1}$ does not eliminate the bacterial population and instead results in an oscillatory behavior of bacterial concentration, indicating a coexistence of the bacteria-phage pair (section 4.1).

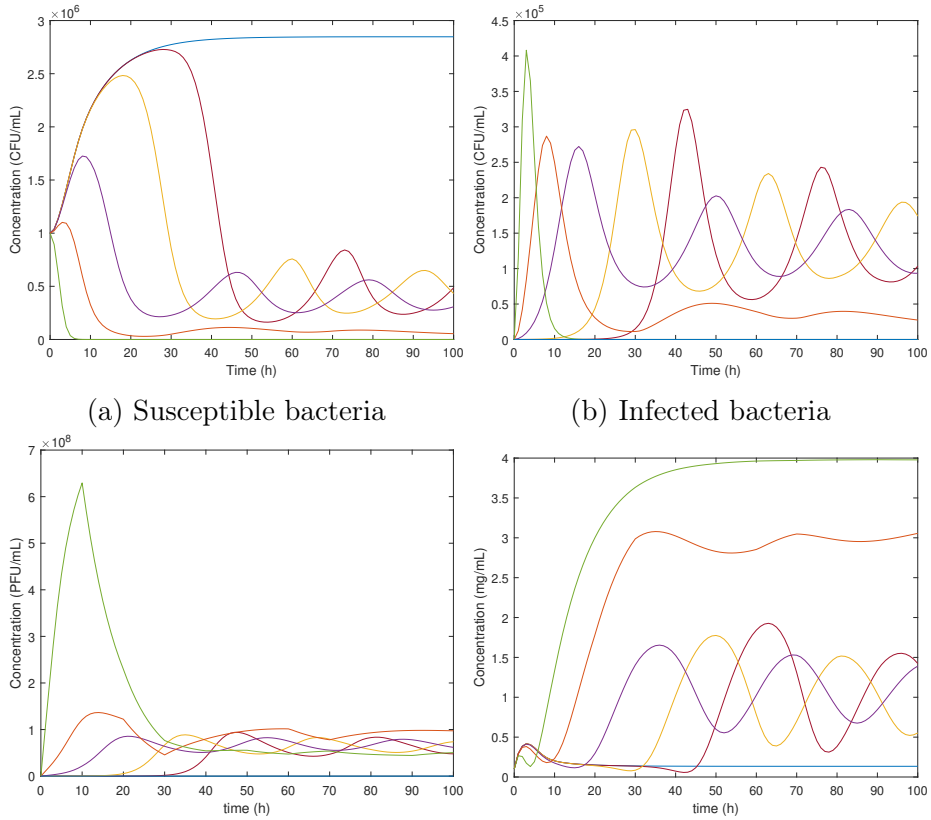

(a) Susceptible bacteria (b) Infected bacteria

(c) Phages (d) Substrate

Figure 5.13: Time evolution of variables for different initial phage concentrations. The color lines in order blue, red, yellow, purple, orange, and green correspond to initial phage concentrations $0, 1 \cdot 10^4, 1 \cdot 10^6, 1 \cdot 10^8, 1 \cdot 10^9, 1 \cdot 10^{10}$ $PFU\ mL^{-1}$, respectively.

Detailing the flow profiles for P_{in} $1 \cdot 10^9$ and $1 \cdot 10^{10}$ $PFU\ mL^{-1}$, in the former case, the phage flow remains mostly constant and close to the imposed constraint value. However, in the latter case, the flow profile is nearly constant and significantly below the constraint, which represents a noteworthy behavior from the perspective of system control and operation. This suggests that the process could be operated at very low phage flow rates, making it more practical and cost-effective—with smaller, more easily operated and maintained pumps, tanks, and associated equipment.

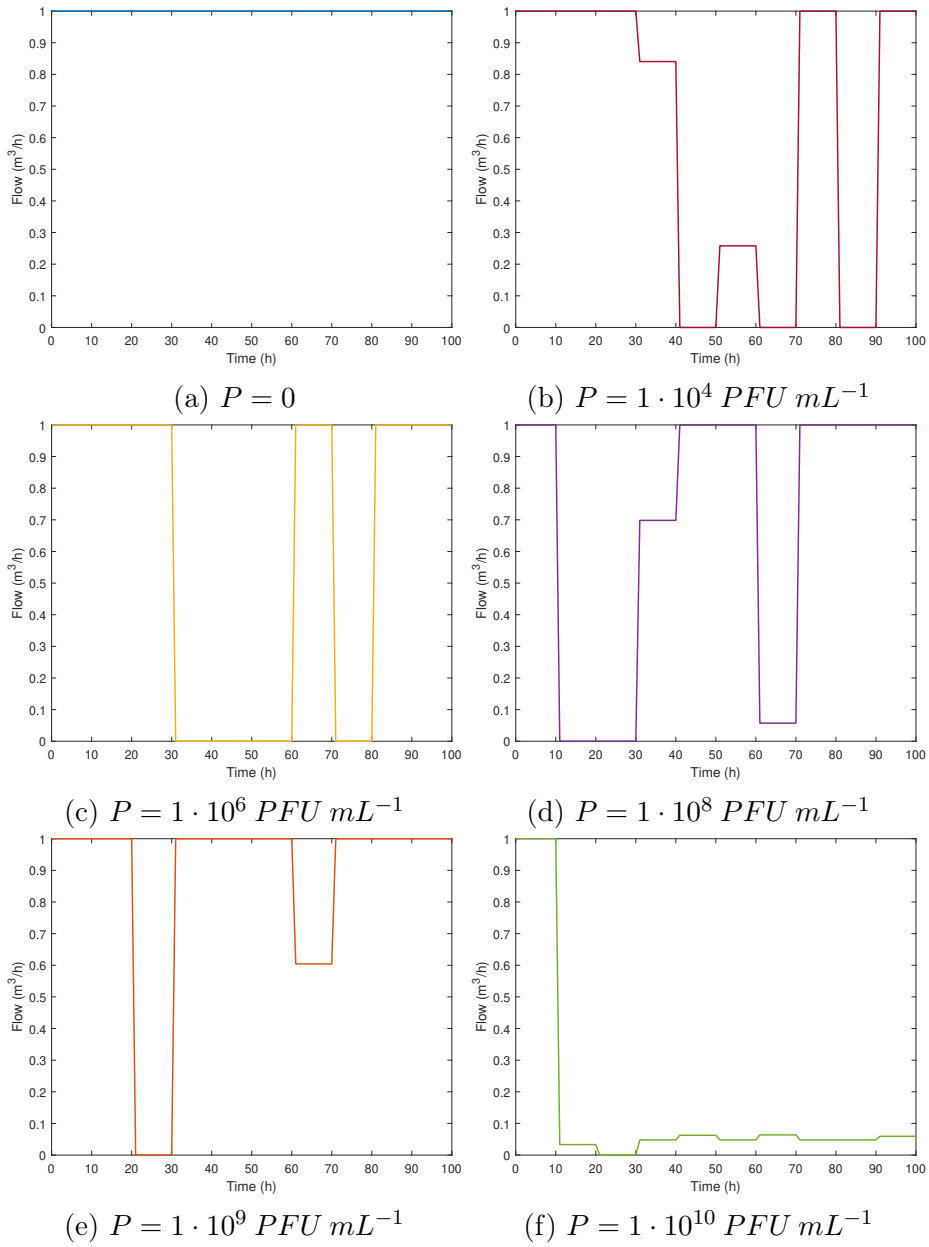

(a) $P = 0$

(b) $P = 1 \cdot 10^4\ PFU\ mL^{-1}$

(c) $P = 1 \cdot 10^6\ PFU\ mL^{-1}$

(d) $P = 1 \cdot 10^8\ PFU\ mL^{-1}$

(e) $P = 1 \cdot 10^9\ PFU\ mL^{-1}$

(f) $P = 1 \cdot 10^{10}\ PFU\ mL^{-1}$

Figure 5.14: Flow profiles for different initial phage concentrations.

A continuous or on-off control strategy is considered to conclude the optimal control study. Based on the previous analysis, P_{in} should range between P_{in} $1 \cdot 10^9$ and $1 \cdot 10^{10}\ PFU\ mL^{-1}$, and the phage flow should

not exceed 10% of F_S. However, the question at this point is whether ten intervals are sufficient to effectively control bacterial proliferation, and whether phage addition can be discontinued after these intervals, or if phage control must remain constant throughout plant operation. To address this, a new analysis was conducted by extending the simulation beyond the ten optimal control steps. In the first scenario, the valve was closed, and no additional phage was added; in the second, phage feeding was maintained at the last calculated flow rate. The bacterial response and corresponding flow profiles are presented in figure 5.15.

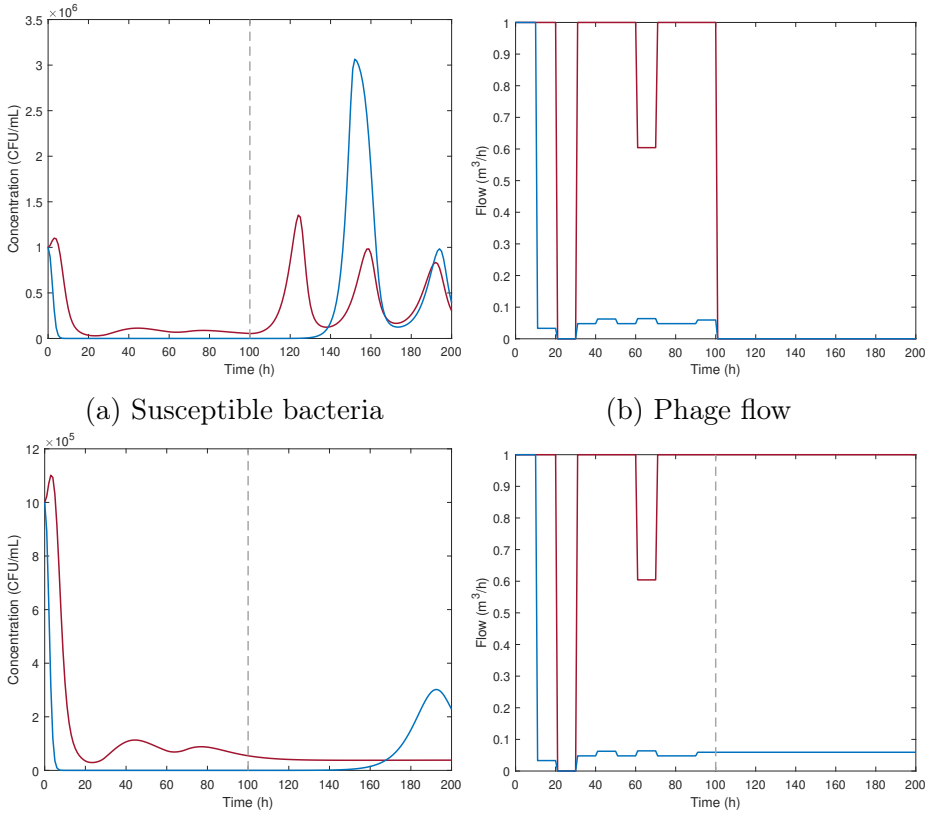

(a) Susceptible bacteria

(b) Phage flow

(c) Susceptible bacteria

(d) Phage flow

Figure 5.15: Time evolution if stops or continues the phage control. (a) and (b) the control stops, (c) and (d) the control remains at the last calculated flow. The red line is $P_{in} = 1 \cdot 10^9\ PFU\ mL^{-1}$, and the blue line is $P_{in} = 1 \cdot 10^{10}\ PFU\ mL^{-1}$.

The simulations show that the bacteria begin to proliferate either when the valve is closed (i.e., phage addition is stopped) or when the phage flow is insufficiently low. This indicates that the phage-based control strategy provides only a temporary solution. Therefore, periodic monitoring of bacterial concentration is essential to prevent overgrowth that could lead to operational issues and to initiate control measures in a timely manner. This behavior can be further understood by analyzing the model equations to identify their equilibrium points. A theoretical analysis revealed five equilibrium points in the system: one trivial point, three complex (non-real) solutions, and one point involving negative state values, which are not physically meaningful (section 4.1). Consequently, the equilibrium points were determined through numerical methods. The average values of the system states are presented in table 5.2, and the variables oscillate around these values when control is maintained.

Table 5.2: Equilibrium points for extended control. Numerical solution

$P_{in}(PFU\ mL^{-1})$	$1 \cdot 10^9$	$1 \cdot 10^{10}$
$X_S(CFU\ mL^{-1})$	$4.22 \cdot 10^{-8}$	$1.1 \cdot 10^{-9}$
$X_I(CFU\ mL^{-1})$	$2.0 \cdot 10^{-8}$	$7.80 \cdot 10^{-10}$
$P(PFU\ mL^{-1})$	$8.31 \cdot 10^7$	$5.35 \cdot 10^7$
$S(mg\,mL^{-1})$	3.63	3.97

Note that under the condition of maintaining a continuous phage flow at a concentration of $P_{in} = 1 \cdot 10^{10}$, an increase in bacterial concentration is observed at the end of the studied time interval (approximately $180\,h$). This phenomenon can be explained by the fact that, at such a high phage concentration, the bacteria are rapidly eliminated from the system, and the viral particles—which can only proliferate in the presence of susceptible bacteria—subsequently begin to be removed from the system due to their natural decay. Therefore, in an environment where there are not enough bacteria to support phage replication, the introduced phages become inactivated and are washed out of the system, which ultimately allows for a slight regrowth of bacteria within the reactor. This outcome does not occur under the condition of maintaining a continuous phage flow at a concentration of $P_{in} = 1 \cdot 10^9$, since the persistent presence of a threshold bacterial concentration in the system ensures that there is

always a probability for infection to occur.

From an operational standpoint, the implementation of the optimal control strategy could be facilitated by incorporating control parameters such as the Sludge Volume Index (VSI). When VSI values exceed 150 $mL\ g^{-1}$, it indicates poor sludge settleability, typically associated with the occurrence of bulking. In the case of foaming, control can be achieved by monitoring foam height or volume, ensuring it does not exceed the maximum permissible limits in secondary clarifiers or aeration tanks.

Both optimal control strategies and the Extended Kalman Filter (EKF) were studied in a controlled environment involving a bacteria and a phage; however, the activated sludge (AS) system represents a significantly more complex scenario. The next chapter will focus on validating the model under more realistic conditions. To this end, the proposed model will be integrated into the well-established ASM1 (Activated Sludge Model No. 1) framework.

Chapter 6

Case studies: application to the ASM1 model

The previous chapters involved developing and analyzing a bacteria-phage model, studying its properties, and using it for control purposes. This last chapter focuses on studying a more realistic environment; bulking and foaming are operative problems that affect activated sludge processes. In that sense, the well-known model ASM1 (Activated Sludge Model No.1) has been selected to evaluate the bacteria-phage behavior in a real wastewater treatment system.

The Activated Sludge Model No. 1 was the result of five years of development, during which many researchers and practitioners spent time to get a solid platform for activated sludge processes. The ASM1 is a model of minimal complexity that was well-received and has been widely used as a basis for further model development. ASM1 has been the core of numerous models, with supplementary details added in almost every case. Matrix notation, introduced alongside ASM1, facilitates the communication of complex models, allowing discussions to focus on the essential aspects of biokinetic modeling (Henze et al., 2006). Therefore, it is a proper option to incorporate the model that has been developed for phage therapy.

6.1 Activated Sludge Model No. 1

The ASM1 formulation brings together the most critical processes of WWT. Below is a brief description of the components and phenomena that constitute it.

The Chemical Oxygen Demand (COD) provides a link between electron equivalents in the organic substrate, the biomass, and the oxygen utilized. Thus, a mass balance can be expressed in terms of COD. Consequently, the concentrations of all organic materials, including biomass, are in COD units in the ASM1 model.

The organic matter in wastewater can be subdivided into several categories. The first important subdivision is based on biodegradability.

Non-biodegradable organic matter is biologically inert, is not involved in any conversion processes, and passes through an activated sludge system unchanged in form. Nevertheless, it is included because it is crucial to the process performance. Two fractions, depending on their physical state, can be identified: soluble and particulate.

- Inert soluble organic matter, S_I, leaves the system at the same concentration that it enters. Soluble inert organic matter contributes to the effluent COD.

- Inert suspended organic matter, X_I, becomes enmeshed in the activated sludge and becomes a part of the volatile suspended solids in the activated sludge system, and is removed from the system through sludge wastage.

Biodegradable organic matter may be divided into two fractions: readily biodegradable and slowly biodegradable.

- The readily biodegradable material, S_s, consists of relatively simple molecules generated through the hydrolysis of particulate organic matter entrapped in the biofloc. These molecules can be directly taken up by heterotrophic bacteria under either aerobic or anoxic conditions and utilized for the growth of new biomass (is treated as if it were soluble).

- The slowly biodegradable material, X_s, consisting of relatively complex molecules formed by the decay of both heterotrophic and autotrophic biomass, must be acted upon extracellularly and con-

verted into a readily biodegradable substrate by hydrolysis before it can be used (is treated as if it were particulate).

The biomass in the system is represented by the heterotrophic biomass, X_{BH}, and the autotrophic biomass, X_{BA}. Both heterotrophic and autotrophic biomass may be present in the wastewater itself, thereby significantly impacting system performance. Heterotrophic biomass can be formed by growth under either aerobic or anoxic conditions. Meanwhile, autotroph development only occurs under aerobic conditions. Both heterotrophic and autotrophic biomass are destroyed by decay.

Heterotrophic biomass, denoted as X_{BH}, forms from growth on readily biodegradable substrates in aerobic or anoxic environments, but is presumed to halt in anaerobic conditions. Biomass loss occurs through decay, which encompasses a range of mechanisms, including endogenous metabolism, death, predation, and lysis. This decay is believed to convert biomass into slowly biodegradable substrates and particulate byproducts. Heterotrophic biomass plays a crucial role in phage therapy because it comprises the bacteria that are targeted for elimination.

In the ASM1, it recognizes that not all biomass in an activated sludge system is active, as is the case with particulate products X_p. This product is formed by the decay of both heterotrophic and autotrophic biomass, yet it is not destroyed. Its rate of destruction is so low that, for all practical purposes, it appears inert within the SRTs commonly encountered in activated sludge systems.

Nitrogenous matter in wastewater, like carbonaceous matter, can be categorized into two types: non-biodegradable and biodegradable. Concerning the non-biodegradable fraction,

- The particulate portion is that associated with the non-biodegradable particulate COD,
- The soluble portion is usually negligibly small and is not incorporated into the model.

The biodegradable nitrogenous matter may be subdivided into:

- Ammonia (both the free compound and its salts), S_{NH}, arises from the ammonification of soluble biodegradable organic nitrogen and is eliminated through the growth of biomass. The primary use of

ammonia nitrogen is as an energy source for the aerobic development of autotrophic biomass. Additionally, nitrogen is integrated into biomass during cell synthesis.

- Soluble organic nitrogen, S_{ND}, results from the hydrolysis of particulate organic nitrogen and is transformed into ammonia nitrogen through ammonification.

- Particulate organic nitrogen, X_{ND}, is generated from the decay of both heterotrophic and autotrophic biomass.

The model also features nitrate nitrogen, S_{NO}, which originates from the aerobic growth of autotrophic bacteria and is depleted during the anoxic growth of heterotrophic biomass. While nitrite nitrogen is an intermediate that forms during nitrification, for the sake of simplicity in modeling, it is assumed that nitrate is the sole oxidized form of nitrogen present.

The volatile solids concentration (in COD units) in the activated sludge system is the sum of the five particulate terms: X_S, X_{BH}, X_{BA}, X_P, and X_I.

The concentration of dissolved oxygen (DO), denoted as S_o, is measured within the reactor. The processes outlined in this model focus solely on removing oxygen from the solution, with no processes included for its addition; thus, the matrix comprises entirely biological processes. The oxygen balance equation determines the quantity of oxygen necessary for the metabolic requirements of the bacteria. Oxygen consumption is closely linked to the aerobic growth of both heterotrophic and autotrophic biomass. To represent changes in dissolved oxygen (DO) concentration, suitable oxygen transfer relations must be incorporated.

The twelve components outlined are viewed as the minimum necessary for accurately modeling an activated sludge system that facilitates carbon oxidation, nitrification, and denitrification. Nevertheless, a thirteenth element, total alkalinity, represented as $S_{A,L,K}$, exists. While adding alkalinity to the model isn't crucial, including it is beneficial as it offers insights for predicting significant pH fluctuations.

The model incorporates four key processes: biomass growth, biomass decay, ammonification of organic nitrogen, and the hydrolysis of particulate organics trapped within the biofloc.

6.2 Application of phage control to ASM1

Until now, our proposed model has considered a scenario in which heterotrophic bacteria grow in an environment utilizing a soluble carbon-based energy substrate. In a straightforward conceptualization of this situation, two fundamental processes occur: biomass increases through cell growth and decreases through lysis caused by a phage. However, not all heterotrophic bacteria are infected by the phage, a fact that makes them non-susceptible to the phage. Non-susceptible, susceptible, and infected bacteria compound the total heterotrophic bacteria population of the system. In table 6.1 find all the states of the ASM1 and the new variables added associated with phage control with their respective notations.

Table 6.1: ASM1 modified model variables

S_I	Soluble inert organic matter
S_S	Readily biodegradable substrate
X_I	Particulate inert organic matter
X_S	Slowly biodegradable substrate
X_{BH}	Active heterotrophic biomass
$X_{BH,NS}$	Non-susceptible heterotrophic biomass
$X_{BH,S}$	Susceptible heterotrophic biomass
$X_{BH,I}$	Infected heterotrophic biomass
P	Bacteriophage
X_{BA}	Active autotrophic biomass
X_P	Particulate products arising from biomass decay
S_O	Oxygen
S_{NO}	Nitrate and nitrite nitrogen
S_{NH}	$NH_4^+ + NH_3$ nitrogen
S_{ND}	Soluble biodegradable organic nitrogen
X_{ND}	Particulate biodegradable organic nitrogen
S_{ALK}	Alkalinity - Molar units

ASM1, which incorporates phenomena such as carbon oxidation, nitrification, and denitrification, accounts for many reactions between many components. The growth of heterotrophic biomass decreases as a reactor solids retention time increases. This phenomenon is thought to be due

to many mechanisms, including predation, lysis, and the need for maintenance energy. The presence of bacteriophage in an activated sludge system and, therefore, infection is a natural phenomenon that exists in the real system; nevertheless, it has always been neglected.

To have a mathematically tractable model while providing realistic predictions, the reactions must represent the most essential fundamental processes occurring within the system. To use the model for phage treatment, the bacteriophage infection is not a secondary process; on the contrary, it plays an essential role in the bacteria population that impacts the system operation.

The term process means a distinct event acting upon one or more system components. The components in the model are shown across the top of table 6.2, and the fundamental processes incorporated into the model are listed in the leftmost column of the table, while the rate expression is listed in the table 6.3.

Figure 6.1 shows the scheme for the activated sludge system to study in this chapter. This consists of an aerobic reactor followed by a settler. The clarified water of the settler is the wastewater treated (solid-free and COD low), and a part of the sludge of the settler is recirculated to the reactor. The equipment volumes and operational conditions are shown in Table 6.4.

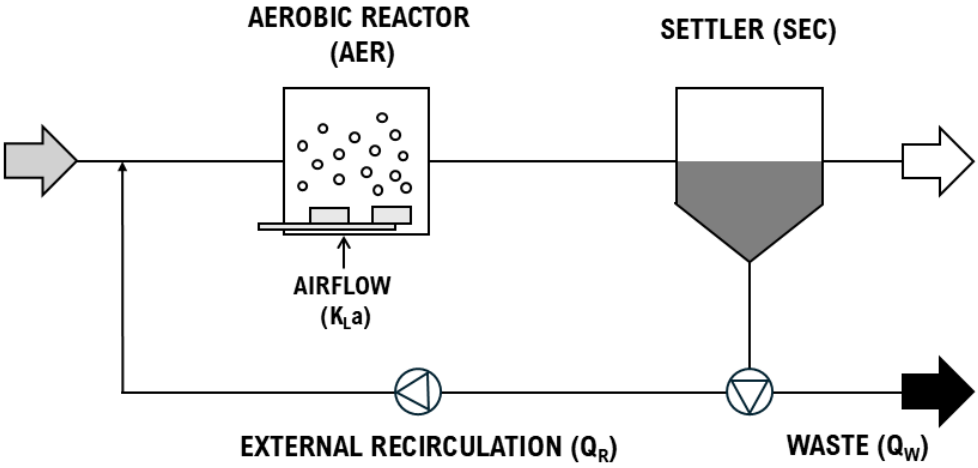

Figure 6.1: Activated sludge system scheme

Table 6.2: Process kinetics and stoichiometry ASM1 model incorporating bacteria-phage control.

	Process	Component S_I	S_S	X_I	X_S	$X_{BH,NS}$	$X_{BH,S}$	$X_{BH,I}$	P	X_{BA}	X_P	S_O	S_{NO}	S_{NH}	S_{ND}	X_{ND}	S_{ALK}
1	Aerobic growth of heterotrophs		$-1/Y_H$			1	1					$-\frac{1-Y_H}{Y_H}$		$-i_{XB}$			$-\frac{i_{XB}}{14}$
2	Anoxic growth of heterotrophs		$-1/Y_H$			1	1						$-\frac{1-Y_H}{2.86Y_H}$	$-i_{XB}$			$-\frac{1-Y_H}{14\cdot 2.86Y_H}-\frac{i_{XB}}{14}$
3	Aerobic growth of autotrophs									1		$-\frac{4.57-Y_A}{Y_A}$	$\frac{1}{Y_A}$	$-i_{XB}-\frac{1}{Y_A}$			$-\frac{i_{XB}}{14}-\frac{1}{7Y_A}$
4	'Decay' of autotrophs				$1-f_P$	-1					f_P					$i_{XB}-f_P i_{XP}$	
5	'Hydrolysis' of entrapped organics				$1-f_P$					-1	f_P					$i_{XB}-f_P i_{XP}$	
6	Ammonification of soluble organic nitrogen													1	-1		$\frac{1}{14}$
7	'Hydrolysis' of entrapped organics		1		-1												
8	'Hydrolysis' of entrapped organic nitrogen														1	-1	
9	Infection						-1	1	-1								
10	Lysis (Infection)							-1	β								
11	'Decay' of phages								-1								

Table 6.3: Process kinetics and stoichiometry ASM1 model incorporating bacteria-phage control.

	Process	Process Rate
1	Aerobic growth of heterotrophs	$\hat{\mu_H}(\frac{S_S}{K_S+S_S})(\frac{S_O}{K_{O,H}+S_O})(X_{BH,NS}+X_{BH,S})$
2	Anoxic growth of heterotrophs	$\hat{\mu_H}(\frac{S_S}{K_S+S_S})(\frac{K_O}{K_{O,H}+S_O})(\frac{S_{NO}}{K_{NO}+S_{NO}})\eta_b(X_{BH,NS}+X_{BH,S})$
3	Aerobic growth of autotrophs	$\hat{\mu_A}(\frac{S_{NH}}{K_{NH}+S_{NH}})(\frac{S_O}{K_{O,A}+S_O})X_{BA})$
4	'Decay' of autotrophs	$b_H(X_{BH,NS}+X_{BH,S})$
5	'Hydrolysis' of entrapped organics	$b_A X_{BA}$
6	Ammonification of soluble organic nitrogen	$k_a S_{ND} X_{BH,NS}$
7	'Hydrolysis' of entrapped organics	$k_h \frac{X_S/X_{BH,NS}}{K_x+(X_S/X_{BH,NS}}[(\frac{S_O}{K_{O,H}+S_O})+\eta_g(\frac{K_O}{K_{O,H}+S_O})(\frac{S_{NO}}{K_{NO}+S_{NO}})]X_{BH,NS}$
8	'Hydrolysis' of entrapped organic nitrogen	$\rho_7(X_{ND}/X_S)$
9	Infection	$\delta X_{BH,S} P$
10	Lysis (Infection)	$\eta_P X_{BH,I}$
11	'Decay' of phages	$\nu_P P$

For a model to have utility in the operation and control of wastewater treatment systems, it must be possible to evaluate wastewater-specific parameter values and estimate concentrations of essential components in the influent. In this case, all the values to the simulation were taken from the work of Flores-Alsina et al. (2012). This work examines the effect of a reactive settler on biological nutrient removal as described by the activated sludge models (ASM) 1, 2d, and 3. The values are presented in table 6.4.

Table 6.4: ASM1 modified model parameter values.

Parameter		**Value**
Operational parameters		
Input flow rate	$Q_{in}(m^3\,day^{-1})$	4611
Recirculation flow rate	$Q_r(m^3\,day^{-1})$	18446
Waste flow rate	$Q_w(m^3\,day^{-1})$	385
Reactor volume	$V_R(m^3)$	6000
Settler volume	$V_S(m^3)$	6000
Kinetic parameters		
Heterotrophic growth and decay	$\hat{\mu_H}(day^{-1})$	4
	$K_S(COD\,m^{-3})$	10
	$K_{OH}(-COD\,m^{-3})$	0.2
	$K_{NO}(N\,m^{-3})$	0.5
	$b_H(day^{-1})$	0.3
Autotrophic growth and decay	$\hat{\mu_A}(day^{-1})$	0.5
	$K_{NH}(N\,m^{-3})$	1
	$K_{OA}(-COD\,m^{-3})$	0.4
	$b_A(day^{-1})$	0.05
Correction factor for anoxic growth of heterotrophs	η_g	0.8
Ammonification	$k_a(m^3\,COD^{-1}\,day^{-1})$	0.05
Hydrolysis	$K_X((COD\,m^{-3})\,(COD\,m^{-3})^{-1})$	0.1
	$k_h(COD\,COD^{-1}\,day^{-1})$	3
Correction factor for anoxic hydrolysis	η_h	0.8
Stoichiometric parameters		
Heterotrophic yield	$Y_H(COD\,COD^{-1})$	0.67
Autotrophic yield	$Y_A(COD\,COD^{-1})$	0.24
Fraction of biomass yielding particulate products	$f_P(COD\,COD^{-1})$	0.08
Mass N/Mas COD in biomass	$i_{XB}(N\,COD^{-1})$	0.08
Mass N/Mas COD in products from biomass	$i_{XP}(N\,COD^{-1})$	0.06
Infection parameters		
Adsorption rate	$\delta(mL\,COD^{-1}COD_P^{-1}\,day^{-1})$	$3.02 \cdot 10^{-3}$
Burst size	$\beta(COD_P\,COD^{-1})$	110
Lysis rate	$\eta_P(day^{-1})$	0.5
Natural phage inactivation rate	$\nu_P(day^{-1})$	$1 \cdot 10^5$
Other parameters		
Volumetric oxygen transfer coefficient	$K_La(day^{-1})$	240
Oxygen saturation concentration	$SO_{sat}(COD\,m^{-3})$	8

The first study compared the behavior of the ASM1-modified model with and without phages in the system. For calculation purposes, the susceptible bacteria was assumed a 40% of the total heterotrophic bacteria. Figure 6.3 presents the heterotrophic bacteria and phage evolution in the reactor effluent. In addition, figure 6.2 shows all the nutrient concentrations in the reactor effluent. Note that all the values are given as COD units.

It is observable and expected that the concentration of heterotrophic bacteria decreases in the presence of the bacteriophage. However, this decrease in the heterotrophic bacteria population does not affect the nutrient concentration. This is consistent with the fact that COD is degraded not only by one type of microorganism. If one population decreases its concentration in an activated sludge system, another can proliferate and consume the remaining COD. The interactive nature of the AS system presents an opportunity to apply phage control to a specific microorganism, rather than a chemical treatment that indiscriminately eliminates all populations.

The percentage of susceptible bacteria was modified to analyze the system behavior. Figure 6.4 shows the results, allowing us to distinguish the decrease in heterotrophic susceptible bacteria concentration based on the percentage of their presence. The distinction is the time required to control the susceptible bacteria, which is approximately between 3 and 6 days, depending on the bacterial concentration. This result is significant because it is necessary to ensure the continuity of the AS process, as operational problems can take days and could be critical to the plant's performance.

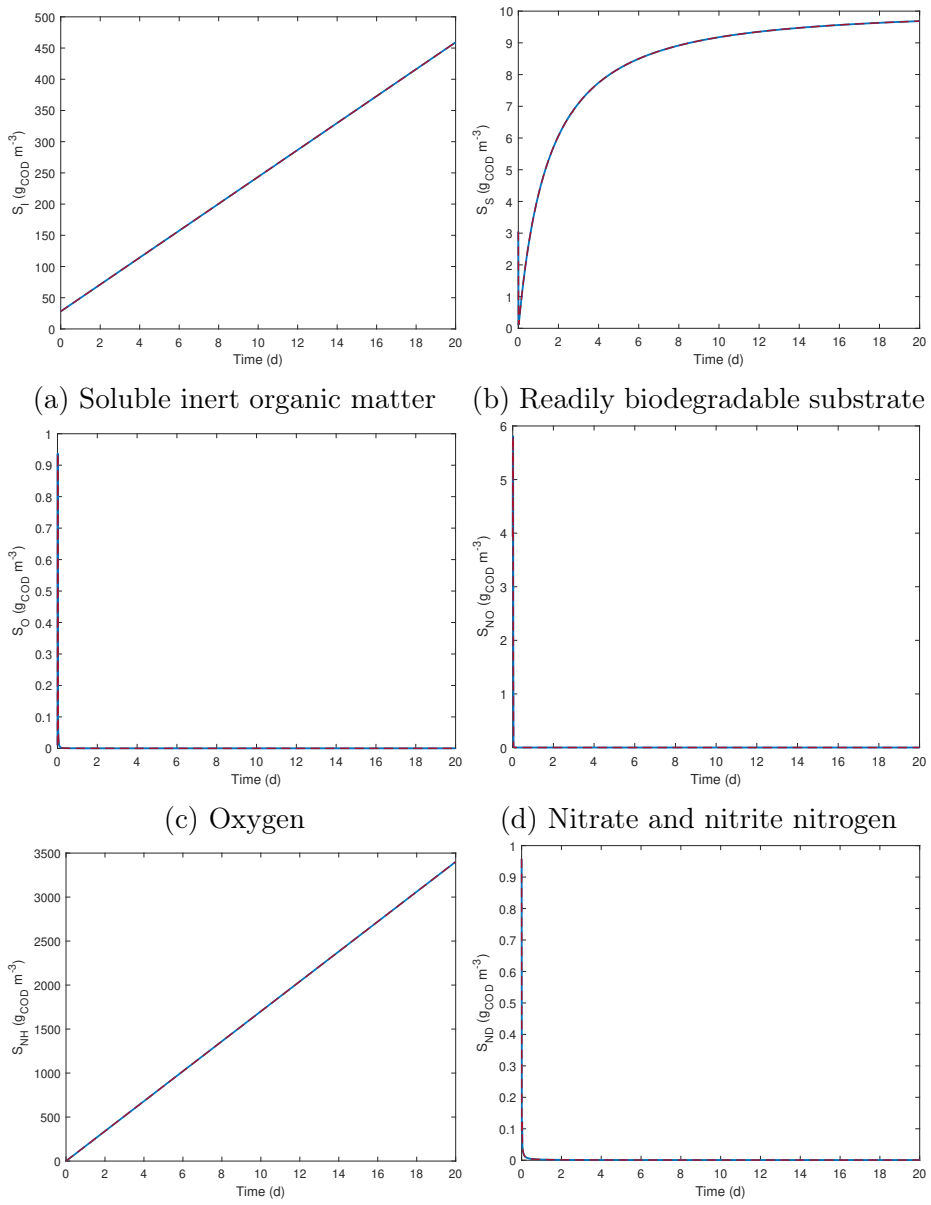

(a) Soluble inert organic matter

(b) Readily biodegradable substrate

(c) Oxygen

(d) Nitrate and nitrite nitrogen

(e) NH_4^++NH_3 nitrogen

(f) Soluble biodegradable organic nitrogen

Figure 6.2: Nutrients in the Reactor effluent. The red line is with phages, and the blue line is without phages.

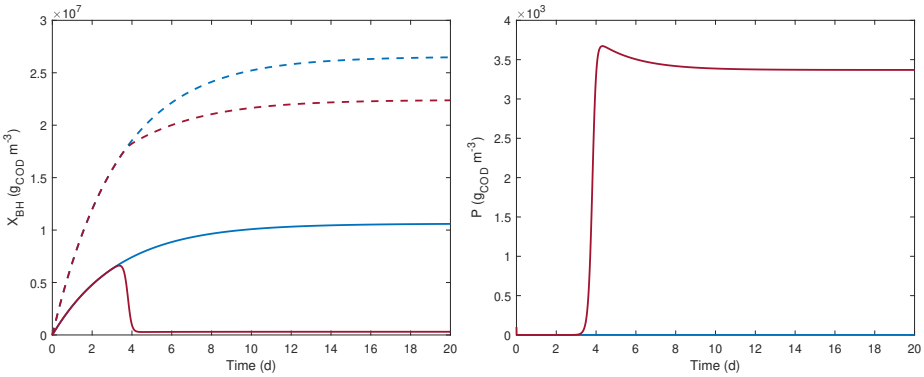

(a) Heterotrophic biomass (b) Phage

Figure 6.3: Reactor effluent. The red line is with phages, and the blue line is without phages. The continuous line represents susceptible bacteria, and the dashed line represents the total active heterotrophic biomass.

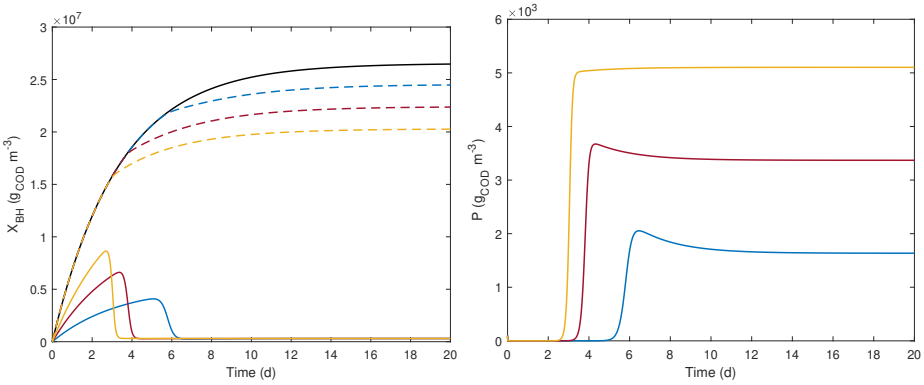

(a) Heterotrophic biomass (b) Phage

Figure 6.4: Reactor outputs. The blue, red, and yellow lines are in order 20%, 40%, and 60% of active heterotrophic susceptible biomass, respectively. The continuous line is a susceptible bacteria, and the dashed line is the total active heterotrophic biomass. The black line is the total active heterotrophic biomass if no susceptible bacteria are present.

6.3 Discussion

The enhancement of the Activated Sludge Model No. 1 (ASM1) to explicitly include bacteriophage-mediated infection marks a major step forward in modeling biological wastewater treatment processes. In the past, ASM1 and its variations have accounted for biomass decay using general mechanisms like endogenous respiration, predation, and lysis, often overlooking the significant role of bacteriophages within activated sludge systems. By incorporating bacteriophage dynamics—including the distinctions among non-susceptible, susceptible, and infected heterotrophic biomass—this revised model offers a more accurate and mechanistic representation of biomass populations dynamics.

The simulations show that introducing phage infection mechanisms significantly reduces the levels of susceptible heterotrophic bacteria while not negatively impacting nutrient removal efficiency. This result is crucial, as it indicates that targeted phage therapy can manage specific problematic bacterial populations, like filamentous bacteria that contribute to sludge bulking and foaming, without compromising the overall stability and effectiveness of the wastewater treatment process. In contrast to traditional chemical control methods, which tend to have broad-spectrum toxicity, phage control provides a selective approach that complies with the increasing environmental regulations on chemical use in wastewater treatment.

The findings further underscore the resilience of the activated sludge system: even with reduced susceptible heterotrophic biomass, the overall chemical oxygen demand (COD) removal stays consistent. This consistency is due to functional redundancy in microbial communities, where resilient organisms take over for the lost susceptible ones. These ecological insights, now integrated into a modeling framework, open doors to more sophisticated operational strategies, such as the deliberate alteration of microbial community structures via phage addition.

Moreover, varying the proportion of susceptible biomass in the simulations revealed that the time required for phage-mediated control ranged between three to six days, depending on initial concentrations. This timescale is particularly important for real-world applications, as operational upsets or microbial shifts often occur over similar periods. The ability to predict and manage bacterial populations proactively within this timeframe could significantly enhance the robustness of wastewater

treatment plants.

Notably, this modeling framework establishes a foundation for future work on dynamic control strategies, in which real-time monitoring and adjustment of phage dosing can be integrated into supervisory control systems. The explicit inclusion of phage kinetics—adsorption rate, burst size, lysis rate, and inactivation rate—provides new degrees of freedom for model calibration and opens avenues for optimization under various operational conditions.

In summary, incorporating bacteriophage infection into ASM1 enhances the biological accuracy of wastewater modeling and opens up opportunities for targeted, sustainable microbial management in activated sludge systems. This advancement creates a connection between the observed microbial ecology in wastewater systems and its mathematical modeling, thus enriching both theoretical understanding and practical applications in wastewater engineering

Chapter 7

Conclusions & Perspectives

7.1 Conclusions

The bulking and foaming processes are phenomena that occur in both aquaculture and WWTP. Both bulking and foaming represent some of the most challenging problems to solve, as they result from the growth of a range of filamentous microorganisms (bacteria and fungi) whose growth and development factors remain poorly understood. The control strategies commonly employed in WWTPs aim to eradicate or eliminate filamentous bacteria through chemical processes or methods, such as chlorination, zonation, or the addition of hydrogen peroxide (H_2O_2), alum, or ferrous salts.

These operational problems treated with physicochemical treatments are considered "effective"; however, this assessment is far from reality. The corrective measures applied, generally chlorination, are not a specific solution and require control and monitoring. Doses must be tied to cell viability. If chlorine application is not controlled, the dose may be too low, leading to waste of product, or too high, resulting in disruption of the purification process (with the appearance of white foams). Many studies have shown that phage therapy is desirable since it is highly specific, environmentally friendly, and generally safe.

In recent years, researchers have studied the ecophysiological details of its relationship with host cells and its method of host cell synthesis. This information is necessary before its potential as an antifoam agent can be appropriately tested.

Zornoza (2017) list in their work the most common mistakes made when faced with problems caused by the excessive proliferation of filamentous bacteria in activated sludge. The first serious mistake is not identifying the leading cause of the foaming and/or bulking episode. If the filamentous bacteria are not identified, one will be "walking" blindly, with very low chances of success.

Using non-specific corrective measures without first considering control strategies based on the in situ ecophysiology and ecology of filamentous bacteria can be problematic. Some WWTP managers opt for non-specific control measures as their primary choice, such as chlorination, surface ozone application, or other physicochemical treatments, which carry greater risks and operational costs. The initial approach should always involve selecting control strategies based on the most recent data available on the in situ ecophysiology and ecology of the dominant filamentous bacteria. This data will help determine the logical order of the measures to be applied, utilizing the best tools to control the effectiveness of these measures. When all attempts at corrective measures based on in situ ecology and ecophysiology have been exhausted, it is time to resort to non-specific treatments.

Large-scale studies must be conducted to utilize bacteriophage as a biocontrol mechanism in WWTP. To date, all studies have focused on identifying, isolating, and sequencing numerous phage-lytic populations capable of lysing certain strains, particularly Gordonia amarae and Gordonia pseudoamarae, members of the Mycolata, a principal group responsible for bulking and foaming. All these studies have demonstrated the effectiveness of phages in lysing bacterial populations. However, WWTPs worldwide are particularly well endowed with bacteria possessing genes encoding antiviral defense mechanisms.

At the pilot scale, involving specifically targeted bacteria, the real-life scenario includes a complex community of microorganisms and certain environmental stress factors that may affect the performance of bacteriophages used for phage therapy. To address these factors, a thorough study of the treatment plant parameters and the involvement of the microbial community must be conducted to enable a large-scale study of phage therapy. To utilize bacteriophage as a microbial control agent, new infrastructure needs to be developed, and new practices must be implemented. Phage banks must be created to house phages specific to

the most critical targets in a WWTP system. A high concentration of phage cocktails must be applied for successful biocontrol. Understanding the necessary concentration of phage cocktail to treat the wastewater in a WWTP is essential.

Computational modeling of reactor systems regarding the impact that phage treatment can have on a wastewater treatment plant is essential to initiate phage-based strategies aimed at addressing bulking and foaming caused by an overgrowth of activated sludge microorganisms. The models must be carefully formulated and evaluated for their properties. This thesis adopted this approach as the chosen method to achieve the objectives.

There are many infection models in the literature. These function effectively in straightforward situations, but due to the complex nature of the activated sludge system, a simple model to study its behavior is essential. This work proposes a specific model that considers the most relevant phenomena and is easy to implement from a computational perspective.

Models can be used for various purposes. They can help operate the plant (avoid problems), optimize phage production on an industrial scale, support phage operation and control design, and reconstruct non-measured variables. Studying a model properties is fundamental for using it for different purposes. The equilibrium and stability analyses provided insight into the operational conditions, such as initial conditions and stability. The identifiability and observability analyses determined that the model can identify unknown parameters or states with a minimum number of online measurements or critical known parameters. These properties are essential for controlling purposes.

A vital advancement necessary is the development of software sensors that utilize information from the models, enabling significant progress in monitoring various biological variables. This complements the shortfall of online hardware sensors capable of performing these tasks. The EKF, as a state observer, facilitated the estimation of unknown variables, which greatly aids this type of system where online measurement instruments are lacking or absent. Consequently, monitoring and controlling the treatment become more complex.

In a different method, optimal control facilitated the investigation of a phage application strategy in an open loop. Furthermore, this research

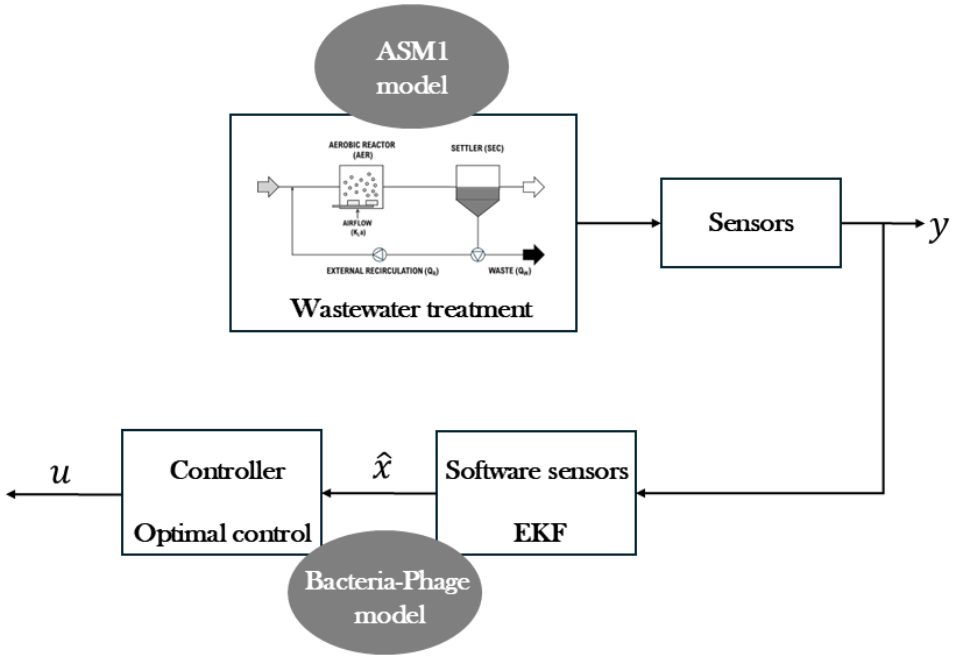

Figure 7.1: Thesis scheme. Open Loop

enables the assessment of concentrations, doses, and system response times. Figure 7.1 presents the scheme that summarizes the work performed in an open-loop control. A frequent error is expecting biological changes to occur right after implementing corrective actions. Activated sludge systems, being biological cultures, require time for modifications to manifest at a macroscopic level. Understanding response times empowers plant managers to implement timely corrective actions.

This research greatly enhances our insight into the application of phage therapy for tackling bulking and foaming in activated sludge systems. It offers vital resources for understanding and applying phage treatments in wastewater treatment facilities aimed at controlling these issues. Coupled with studies on the system's ecological and physiological dynamics, this approach positions bacteriophage treatment as a more effective, cost-efficient, and sustainable alternative to traditional chemical methods.

7.2 Perspectives

This doctoral thesis establishes a scientific foundation for the rational application of bacteriophages in controlling filamentous bacteria within activated sludge systems. The research not only addresses a critical operational challenge in wastewater treatment plants but also generates a methodological and conceptual platform upon which future technological developments can be built. Moving forward, the following steps aim to close the loop with feedback control and, ideally, validate it with improved and sufficient data.

Given the inherent variability and frequent disturbances present in wastewater treatment systems, implementing a closed-loop control strategy is essential to ensure robust and reliable process performance. Unlike open-loop approaches, closed-loop control enables the real-time adjustment of operating parameters in response to deviations from the desired system behavior, thereby improving disturbance rejection and maintaining target performance despite fluctuations in influent characteristics or unexpected process upsets. Model Predictive Control (MPC), in particular, is well suited for such complex biological systems, as it utilizes a dynamic model to predict future system states and optimize control actions over a receding horizon. This predictive capability enables anticipatory adjustments that account for process delays and nonlinearities, thereby enhancing system stability and efficiency under variable conditions. Figure 7.2 presents the proposed closed-loop scheme.

Therefore, the thesis lays the groundwork for implementing closed-loop control strategies, enabling the real-time regulation of filamentous bacteria in activated sludge systems through the dynamic adjustment of phage dosing. Experimental work is dedicated to validating protocols for large-scale phage production, purification, and storage, ensuring a consistent supply of stable and effective phage preparations suitable for automated dosing systems. By integrating process monitoring with mathematical modeling, the thesis demonstrates how feedback control can be applied to maintain optimal sludge characteristics—such as the sludge volume index—by continuously adjusting phage application in response to measured process variables. This approach not only enhances the efficacy and robustness of biocontrol interventions but also establishes a technological foundation for advanced process automation in wastewater treatment plants.

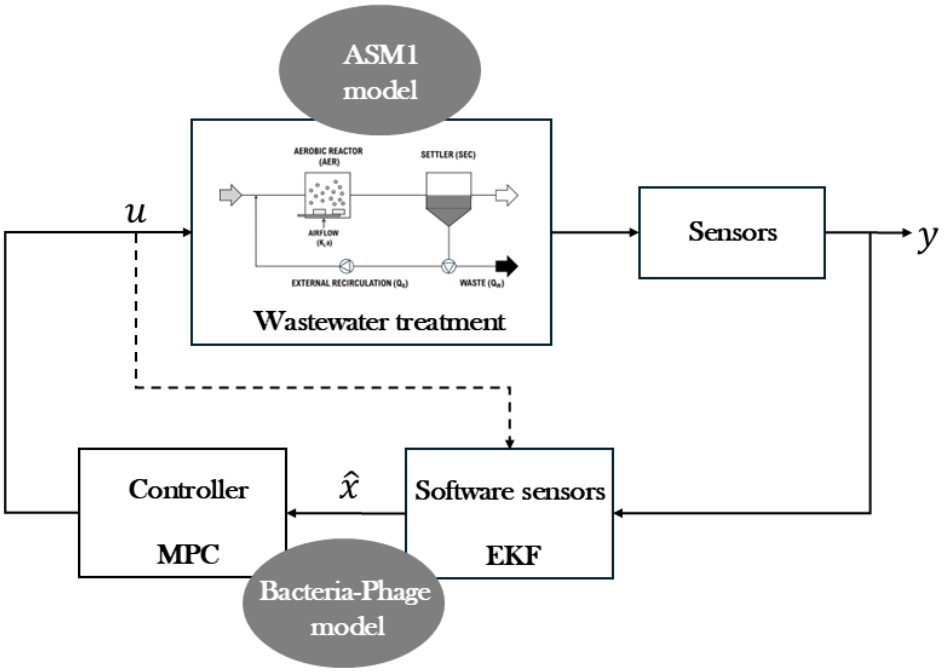

Figure 7.2: Control proposal. Closed Loop

A central perspective of the thesis is its integration of experimental and modeling work. Laboratory-scale experiments could be designed to isolate, characterize, and select bacteriophages with high lytic activity and stability under realistic wastewater conditions. These experimental efforts should include evaluating phage performance in the presence of environmental stressors commonly encountered in activated sludge, such as variable pH levels, temperature fluctuations, and exposure to chemical agents. The data generated would provide a robust basis for assessing the feasibility and reliability of phage-based interventions under practical conditions.

To advance the validation of the model, the thesis develops a mathematical model, the calibration of which is crucial for describing the infection dynamics between bacteriophages and filamentous bacteria. By combining experimental observations with computational modeling, the work enables the prediction and optimization of dosing strategies, supporting the practical application of phages to mitigate bulking and foaming. These models not only facilitate the design of future experiments

but also inform the scaling of laboratory findings to pilot and full-scale treatment systems.

Overall, the doctoral thesis serves as both a reference and a methodological guide for future studies aiming to refine and deploy phage-based solutions in wastewater treatment. Its combination of rigorous experimentation and advanced modeling provides a framework for further research, optimization, and potential industrial application. The outcomes of this work thus have the potential to influence not only scientific understanding but also the practical management of activated sludge systems, laying the groundwork for innovation in biological control strategies.

Bibliography

Abedon, S. T. (2023). Bacteriophage adsorption: Likelihood of virion encounter with bacteria and other factors affecting rates. *Antibiotics*, 12(4):723.

Abedon, S. T., Herschler, T. D., and Stopar, D. (2001). Bacteriophage latent-period evolution as a response to resource availability. *Applied and Environmental Microbiology*, 67(9):4233–4241.

Abedon, S. T., Hyman, P., and Thomas, C. (2003). Experimental examination of bacteriophage latent-period evolution as a response to bacterial availability. *Applied and Environmental Microbiology*, 69(12):7499–7506.

Abedon, S. T., Kuhl, S. J., Blasdel, B. G., and Kutter, E. M. (2011a). Phage treatment of human infections. *Bacteriophage*, 1(2):66–85.

Abedon, S. T., Thomas-Abedon, C., Thomas, A., and Mazure, H. (2011b). Bacteriophage prehistory: is or is not hankin, 1896, a phage reference? *Bacteriophage*, 1(3):174–178.

Acevedo, F., M., J. C. G., and Illanes, A. (2004). *Fundamentos de ingeniería bioquímica*. Eds. Universitarias de Valparaíso de la Pontificia Universidad Católica de Valparíso.

Alexander, R., Campani, G., Dinh, S., and Lima, F. V. (2020). Challenges and opportunities on nonlinear state estimation of chemical and biochemical processes. *Processes*, 8(11):1462.

Alexander, R., Dinh, S., Schultz, G., Ribeiro, M. P., and Lima, F. V. (2023). State and covariance estimation of a semi-batch reactor for bioprocess applications. *Computers & Chemical Engineering*, 172:108180.

Anderson, R. M. and May, R. M. (1981). The population dynamics of microparasites and their invertebrate hosts. *Philosophical Transactions of the Royal Society of London. B, Biological Sciences*, 291(1054):451–524.

Arber, W. and Dussoix, D. (1962). Host specificity of dna produced by escherichia coli: I. host controlled modification of bacteriophage λ. *Journal of molecular biology*, 5(1):18–36.

Audoly, S., Bellu, G., D'Angio, L., Saccomani, M. P., and Cobelli, C. (2001). Global identifiability of nonlinear models of biological systems. *IEEE Transactions on Biomedical Engineering*, 48(1):55–65.

Aw, T. G., Howe, A., and Rose, J. B. (2014). Metagenomic approaches for direct and cell culture evaluation of the virological quality of wastewater. *Journal of virological methods*, 210:15–21.

Ayyaru, S., Choi, J., and Ahn, Y.-H. (2018). Biofouling reduction in a mbr by the application of a lytic phage on a modified nanocomposite membrane. *Environmental Science: Water Research & Technology*, 4(10):1624–1638.

Baldassarre, A., Dion, J.-L., Peyret, N., and Renaud, F. (2024). Digital twin with augmented state extended kalman filters for forecasting electric power consumption of industrial production systems. *Heliyon*, 10(6).

Bastías, R., Higuera, G., Sierralta, W., and Espejo, R. T. (2010). A new group of cosmopolitan bacteriophages induce a carrier state in the pandemic strain of vibrio parahaemolyticus. *Environmental Microbiology*, 12(4):990–1000.

Bastin, G. and Dochain, D. (1990). *On-line Estimation and Adaptive Control of Bioreactors*. Elsevier.

Benzer, S. (1955). Fine structure of a genetic region in bacteriophage. *Proceedings of the National Academy of Sciences*, 41(6):344–354.

Beretta, E. and Kuang, Y. (1998). Modeling and analysis of a marine bacteriophage infection. *Mathematical Biosciences*, 149(1):57–76.

Bernard, O. and Gouzé, J.-L. (2002). State estimation for bioprocesses. Technical report.

Bertanza, G., Menoni, L., and Baroni, P. (2020). Energy saving for air supply in a real wwtp: application of a fuzzy logic controller. *Water Science and Technology*, 81(8):1552–1557.

Blackall, L., Hayward, A., Pettigrew, A., and Greenfield, P. (1985). Biological foam and scum formation in activated sludge treatment systems. *Australian Water and Wastewater Association, 11th Federal Convention*, pages 338–345.

Boehm, A. B. (2019). Risk-based water quality thresholds for coliphages in surface waters: effect of temperature and contamination aging. *Environmental Science: Processes & Impacts*, 21(12):2031–2041.

Bogaerts, P. and Wouwer, A. V. (2003). Software sensors for bioprocesses. *ISA Transactions*, 42(4):547–558.

Buttimer, C., Mcauliffe, O., Ross, R. P., Hill, C., Mahony, J. O., Coffey, A., Abedon, S. T., and Chan, B. K. (2017). Bacteriophages and bacterial plant diseases. *Frontiers in microbiology*.

Cairns, B. J., Timms, A. R., Jansen, V. A. A., Connerton, I. F., and Payne, R. J. H. (2009). Quantitative models of in vitro bacteriophage–host dynamics and their application to phage therapy. *PLoS Pathog*, 5(1):e1000253.

Campbell, A. (1961). Conditions for the existence of bacteriophage. *Evolution*, 15(2):153–165.

Carlton, R. M. (1999). Phage therapy: past history and future prospects. *Archivum Immunologiae Et Therapiae Experimentalis-English Edition-*, 47:267–274.

Chen, K., Wang, H., Valverde-Pérez, B., Zhai, S., Vezzaro, L., and Wang, A. (2021). Optimal control towards sustainable wastewater treatment plants based on multi-agent reinforcement learning. *Chemosphere*, 279:130498.

Choi, J., Kotay, S. M., and Goel, R. (2011). Bacteriophage-based biocontrol of biological sludge bulking in wastewater. *Bioengineered Bugs*, 2(4):214–217.

de Leeuw, M., Brenner, A., and Kushmaro, A. (2017). Modelling Phage - Bacteria Interaction in Micro-Bioreactors. *CLEAN–Soil, Air, Water*, 45(8):1600702.

Delbrück, M. (1940a). Adsorption of bacteriophage under various physiological conditions of the host. *The Journal of general physiology*, 23(5):631.

Delbrück, M. (1940b). The growth of bacteriophage and lysis of the host. *The journal of general physiology*, 23(5):643.

d'Herelle, F. (1926). *The bacteriophage and its behavior*. Williams & Wilkins.

d'Herelle, M. (1961). Sur un microbe invisible antagoniste des bacilles dysentériques. *Acta Kravsi*.

Ding, Y., Tian, Y., Li, Z., Zuo, W., and Zhang, J. (2015). Bioresource Technology A comprehensive study into fouling properties of extracellular polymeric substance (EPS) extracted from bulk sludge and cake sludge in a mesophilic anaerobic membrane bioreactor. *Bioresource Technology*, 192:105–114.

Dochain, D. (2003). State and parameter estimation in chemical and biochemical processes: a tutorial. *Journal of process control*, 13(8):801–818.

Doss, J., Culbertson, K., Hahn, D., Camacho, J., and Barekzi, N. (2017). A review of phage therapy against bacterial pathogens of aquatic and terrestrial organisms.

Dublanchet, A. and Fruciano, E. (2008). A short history of phage therapy. *Médecine et maladies infectieuses*, 38(8):415–420.

Dyson, Z. A., Tucci, J., Seviour, R. J., and Petrovski, S. (2015). Lysis to kill: evaluation of the lytic abilities, and genomics of nine bacteriophages infective for Gordonia spp. and their potential use in activated sludge foam biocontrol. *PLoS ONE*, 10(8):e0134512.

d'Herelle, F. (1925). Essai de traitement de la peste bubonique par le bacteriophage. *Presse Med*, 33:1393–4.

Eikelboom, D. (1991). The role of competition between floc-forming and filamentous bacteria in bulking of activated sludge. *Biological approach to sewage treatment process: current status and perspectives/Ed. P. Madoni.–Luigi Bazzucchi Auter, Perugia*, pages 143–149.

Ellis, E. L. and Delbruck, M. (1939). The growth of bacteriophage. *Journal of General Physiology*, 22(3):365–384.

Endersen, L., Mahony, J. O., Hill, C., Ross, R. P., Mcauliffe, O., and Coffey, A. (2014). Phage Therapy in the Food Industry. *Annual review of food science and technology*, 5(1):327–349.

Epstein, R., Bolle, A., Steinberg, C. M., Kellenberger, E., De La Tour, E. B., Chevalley, R., Edgar, R., Susman, M., Denhardt, G., and Lielausis, A. (1963). Physiological studies of conditional lethal mutants of bacteriophage t4d. In *Cold Spring Harbor Symposia on Quantitative Biology*, volume 28, pages 375–394. Cold Spring Harbor Laboratory Press.

Fan, N., Qi, R., Rossetti, S., Tandoi, V., Gao, Y., and Yang, M. (2017). Factors affecting the growth of Microthrix parvicella : Batch tests using bulking sludge as seed sludge. *Science of the Total Environment*, 609:1192–1199.

Flores-Alsina, X., Gernaey, K. V., and Jeppsson, U. (2012). Benchmarking biological nutrient removal in wastewater treatment plants: influence of mathematical model assumptions. *Water Science and Technology*, 65(8):1496–1505.

García, R., Latz, S., Romero, J., Higuera, G., García, K., and Bastías, R. (2019). Bacteriophage production models: An overview. *Frontiers in Microbiology*, 10:1187.

Garikiparthy, P. S. N., Lee, S. C., Liu, H., Kolluri, S. S., Esfahani, I. J., and Yoo, C. K. (2016). Evaluation of multiloop chemical dosage control strategies for total phosphorus removal of enhanced biological nutrient removal process. *Korean Journal of Chemical Engineering*, 33:14–24.

Gefter, M., Hausmann, R., Gold, M., and Hurwitz, J. (1966). The enzymatic methylation of ribonucleic acid and deoxyribonucleic acid: X. bacteriophage t3-induced s-adenosylmethionine cleavage. *Journal of Biological Chemistry*, 241(9):1995–2006.

Goffaux, G. and Vande Wouwer, A. (2005). Bioprocess state estimation: Some classical and less classical approaches. In *Control and Observer Design for Nonlinear Finite and Infinite Dimensional Systems*, pages 111–128. Springer Berlin Heidelberg.

Golec, P., Karczewska-Golec, J., Łoś, M., and Węgrzyn, G. (2014). Bacteriophage T4 can produce progeny virions in extremely slowly growing Escherichia coli host: Comparison of a mathematical model with the experimental data. *FEMS Microbiology Letters*, 351(2):156–161.

Goode, D., Allen, V., and Barrow, P. (2003). Reduction of experimental salmonella and campylobacter contamination of chicken skin by application of lytic bacteriophages. *Applied and environmental microbiology*, 69(8):5032–5036.

Grasso, C. R., Pokrzywinski, K. L., Waechter, C., Rycroft, T., Zhang, Y., Aligata, A., Kramer, M., and Lamsal, A. (2022). A review of cyanophage–host relationships: Highlighting cyanophages as a potential cyanobacteria control strategy. *Toxins*, 14(6):385.

Hadas, H., Einav, M., Fishov, I., and Zaritsky, A. (1997). Bacteriophage T4 development depends on the physiology of its host Escherichia coli. *Microbiology*, 143(1):179–185.

Hankin, E. (1896). L'action bactericide des eaux de la jumna et du gange sur le vibrion du cholera. *Ann Inst Pasteur*, 10:511.

Hao, X., Wang, Q., Cao, Y., and van Loosdrecht, M. C. M. (2011). Evaluating sludge minimization caused by predation and viral infection based on the extended activated sludge model No. 2d. *Water Research*, 45(16):5130–5140.

Harper, D. R., Abedin, S., Burrowes, B. H., and McConville, M. L. (2021). *Bacteriophages*. Springer.

Henze, M., Gujer, W., Mino, T., and Van Loosedrecht, M. (2006). *Activated sludge models ASM1, ASM2, ASM2d and ASM3*. IWA publishing.

Hershey, A. and Rotman, R. (1949). Genetic recombination between host-range and plaque-type mutants of bacteriophage in single bacterial cells. *Genetics*, 34(1):44.

Hong, H., Ovchinnikov, A., Pogudin, G., and Yap, C. (2020). Global identifiability of differential models. *Communications on Pure and Applied Mathematics*, 73(9):1831–1879.

Hongyang, X., Pedret, C., Santin, I., and Vilanova, R. (2018). Decentralized model predictive control for n and p removal in wastewater treatment plants. In *2018 22nd International Conference on System Theory, Control and Computing (ICSTCC)*, pages 224–230. IEEE.

Hreiz, R., Latifi, M. A., and Roche, N. (2015). Optimal design and operation of activated sludge processes: State-of-the-art. *Chemical Engineering Journal*, 281:900–920.

Hyman, P. and Abedon, S. T. (2009). Practical methods for determining phage growth parameters. *Methods in molecular biology (Clifton, N.J.)*, 501:175–202.

Isoko, K., Cordiner, J. L., Kis, Z., and Moghadam, P. Z. (2024). Bioprocessing 4.0: a pragmatic review and future perspectives. *Digital Discovery*, 3(9):1662–1681.

Jenkins, D., Richard, M. G., and Daigger, G. T. (2004). *Manual on the causes and control of activated sludge bulking, foaming, and other solids separation problems*.

Jeon, G. and Ahn, J. (2021). Evaluation of phage adsorption to salmonella typhimurium exposed to different levels of ph and antibiotic. *Microbial pathogenesis*, 150:104726.

Ji, M., Liu, Z., Sun, K., Li, Z., Fan, X., and Li, Q. (2021). Bacteriophages in water pollution control: Advantages and limitations. *Frontiers of Environmental Science & Engineering*, 15(5):1–15.

Jiang, X., Ma, M., Li, J., LU, A., and Zhong, Z. (2008). Bacterial diversity of active sludge in wastewater treatment plant. *Earth Science Frontiers*, 15(6):163–168.

Kadlec, P., Gabrys, B., and Strandt, S. (2009). Data-driven soft sensors in the process industry. *Computers & Chemical Engineering*, 33(4):795–814.

Kalatzis, P. G., Bastías, R., Kokkari, C., and Katharios, P. (2016). Isolation and characterization of two lytic bacteriophages, φst2 and φgrn1; phage therapy application for biological control of vibrio alginolyticus in aquaculture live feeds. *PloS one*, 11(3):e0151101.

Kannoly, S., Singh, A., and Dennehy, J. J. (2022). An optimal lysis time maximizes bacteriophage fitness in quasi-continuous culture. *MBio*, 13(3):e03593–21.

Kokkari, C., Sarropoulou, E., Bastias, R., Mandalakis, M., and Katharios, P. (2018). Isolation and characterization of a novel bacteriophage infecting vibrio alginolyticus. *Archives of microbiology*, 200:707–718.

Kotay, S. M., Datta, T., Choi, J., and Goel, R. (2011). Biocontrol of biomass bulking caused by Haliscomenobacter hydrossis using a newly isolated lytic bacteriophage. *Water Research*, 45(2):694–704.

Krausfeldt, L. E., Shmakova, E., Lee, H. W., Mazzei, V., Loftin, K. A., Smith, R. P., Karwacki, E., Fortman, P. E., Rosen, B. H., Urakawa, H., et al. (2024). Microbial diversity, genomics, and phage–host interactions of cyanobacterial harmful algal blooms. *MSystems*, 9(7):e00709–23.

Krysiak-Baltyn, K., Martin, G. J. O., and Gras, S. L. (2018). Computational modelling of large scale phage production using a two-stage batch process. *Pharmaceuticals*, 11(2):31.

Krysiak-Baltyn, K., Martin, G. J. O., Stickland, A. D., Scales, P. J., and Gras, S. L. (2017). Simulation of phage dynamics in multi-reactor models of complex wastewater treatment systems. *Biochemical Engineering Journal*, 122:91–102.

Kutter, E. and Sulakvelidze, A. (2004). *Bacteriophages: biology and applications*. Crc press.

Lafitte, I. (2019). Producción de bacteriófagos para el biocontrol de bacterias filamentosas. Master's thesis, Pontificia Universidad Católica de Valparaíso.

Lam, N. N., Docherty, P. D., and Murray, R. (2022). Practical identifiability of parametrised models: A review of benefits and limitations of various approaches. *Mathematics and Computers in Simulation*, 199:202–216.

Levin, B. R., Stewart, F. M., and Chao, L. (1977). Resource-Limited growth, competition, and predation: A model and experimental studies with bacteria and bacteriophage. *The American Naturalist*, 111(977):3–24.

Lin, D. M., Koskella, B., and Lin, H. C. (2017). Phage therapy: An alternative to antibiotics in the age of multi-drug resistance. *World journal of gastrointestinal pharmacology and therapeutics*, 8(3):162.

Liu, M., Gill, J. J., Young, R., and Summer, E. J. (2015). Bacteriophages of wastewater foaming-associated filamentous Gordonia reduce host levels in raw activated sludge. *Scientific Reports*, 5(1):13754.

Ljung, L. and Glad, T. (1994). On global identifiability for arbitrary model parametrizations. *Automatica*, 30(2):265–276.

Lotka, A. J. (1925). *Elements of physical biology*. Williams & Wilkins.

Madhusudana Rao, B. and Lalitha, K. (2015). Bacteriophages for aquaculture: Are they beneficial or inimical.

Madoni, P., Davoli, D., and Gibin, G. (2000). Survey of filamentous microorganisms from bulking and foaming activated-sludge plants in Italy. *Water Research*, 34(6):1767–1772.

Malthus, T. R. (1798). *An essay on the principle of population (1798)*, volume 1.

Mamais, D., Kalaitzi, E., and Andreadakis, A. (2011). Foaming control in activated sludge treatment plants by coagulants addition. *Global NEST Journal*, 13(3):237–245.

Marčuk, L., Nikiforov, V., Ščerbak, J. F., Levitov, T., Kotljarova, R., Naumšina, M., Davydov, S., Monsur, K., Rahman, M., Latif, M., et al. (1971). Clinical studies of the use of bacteriophage in the treatment of cholera. *Bulletin of the World Health Organization*, 45(1):77.

Maura, D. and Debarbieux, L. (2011). Bacteriophages as twenty-first century antibacterial tools for food and medicine. *Applied microbiology and biotechnology*, 90(3):851–859.

Moeller, L., Zehnsdorf, A., Pokorná, D., and Zábranská, J. (2018). volume 3, chapter Foam Formation in Anaerobic Digesters, pages 1–42. Elsevier.

Monod, J. (1950). The growth of bacterial cultures. *Annual Reviews in Microbiology*, 3(1):371–394.

Monsur, K., Rahman, M., Huq, F., Islam, M., Northrup, R., and Hirschhorn, N. (1970). Effect of massive doses of bacteriophage on excretion of vibrios, duration of diarrhoea and output of stools in acute cases of cholera. *Bulletin of the World Health Organization*, 42(5):723.

Nabergoj, D., Modic, P., and Podgornik, A. (2018). Effect of bacterial growth rate on bacteriophage population growth rate. *MicrobiologyOpen*, 7(2):e00558.

Nachimuthu, R., Madurantakam Royam, M., Manohar, P., and Leptihn, S. (2021). Application of bacteriophages and endolysins in aquaculture as a biocontrol measure.

Nielsen, P. H., Kragelund, C., Nielsen, J. L., Tiro, S., Lebek, M., Rosenwinkel, K. H., and Gessesse, A. (2005). Control of Microthrix parvicella in activated sludge plants by dosage of polyaluminium salts: Possible mechanisms. *Acta Hydrochimica et Hydrobiologica*, 33(3):255–261.

Noutsopoulos, C., Mamais, D., and Andreadakis, A. (2006). Effect of solids retention time on Microthrix parvicella growth. *Water SA*, 32(3):315–321.

Ostace, G. S., Baeza, J. A., Guerrero, J., Guisasola, A., Cristea, V. M., Agachi, P. Ş., and Lafuente, J. (2013). Development and economic assessment of different wwtp control strategies for optimal simultaneous removal of carbon, nitrogen and phosphorus. *Computers & Chemical Engineering*, 53:164–177.

Pallavali, R., Shin, D., and Choi, J. (2023). Phage-based biocontrol of antibiotic-resistant bacterium isolated from livestock wastewater treatment plant. *Water*, 15(8):1616.

Paris, S., Lind, G., Lemmer, H., and Wilderer, P. A. (2005). Dosing aluminum chloride to control Microthrix parvicella. *Acta Hydrochimica et Hydrobiologica*, 33(3):247–254.

Payne, R. J. H. and Jansen, V. A. A. (2001). Understanding bacteriophage therapy as a density-dependent kinetic process. *Journal of Theoretical Biology*, 208(1):37–48.

Petrovski, S., Dyson, Z. A., Quill, E. S., Mcilroy, S. J., Tillett, D., and Seviour, R. J. (2011). An examination of the mechanisms for stable foam formation in activated sludge systems. *Water Research*, 45(5):2146–2154.

Pirt, S. (1965). The maintenance energy of bacteria in growing cultures. *Proceedings of the Royal Society of London. Series B. Biological Sciences*, 163(991):224–231.

Plaza, N., Castillo, D., Pérez-Reytor, D., Higuera, G., García, K., and Bastías, R. (2018). Bacteriophages in the control of pathogenic vibrios. *Electronic Journal of Biotechnology*, 31:24–33.

Podgornik, A., Janež, N., Smrekar, F., and Peterka, M. (2015). Continuous production of bacteriophages. 297-338. In Subramanian, G., editor, *Continuous Processing in Pharmaceutical Manufacturing*, chapter 12, pages 297–338. First edition.

Pradeep, A., Ramasamy, S., Veniemilda, J., and Kumar, C. (2022). Effect of ph & temperature variations on phage stability-a crucial prerequisite for successful phage therapy. *Int. J. Pharm. Sci. Res*, 13:5178–5182.

Rawlings, J. B., Mayne, D. Q., Diehl, M., et al. (2017). *Model predictive control: theory, computation, and design*, volume 2. Nob Hill Publishing Madison, WI.

Reisoglu, Ş. and Aydin, S. (2023). Bacteriophages as a promising approach for the biocontrol of antibiotic resistant pathogens and the reconstruction of microbial interaction networks in wastewater treatment systems: A review. *Science of the Total Environment*, 890:164291.

Revollar, S., Vilanova, R., Vega, P., Francisco, M., and Meneses, M. (2020). Wastewater treatment plant operation: simple control schemes with a holistic perspective. *Sustainability*, 12(3):768.

Richard, M., Brown, S., and Collins, F. (2003). Activated sludge microbiology problems and their control. In *20th Annual USEPA National Operator Trainers Conference*, volume 8, pages 1–21.

Richard, M. G., Shimizu, G. P., and Jenkins, D. (1985). The growth physiology of the filamentous organism type 021n and its significance to activated sludge bulking. *Journal of Water Pollution Control Federation*, 57:1152–1162.

Roels, T., Dauwe, F., Van Damme, S., De Wilde, K., and Roelandt, F. (2002). The influence of PAX-14 on activated sludge systems and in particular on Microthrix parvicella. In *Water Science and Technology*, volume 46, pages 487–490.

Runa, V., Wenk, J., Bengtsson, S., Jones, B. V., and Lanham, A. B. (2021). Bacteriophages in biological wastewater treatment systems: occurrence, characterization, and function. *Frontiers in microbiology*, 12:730071.

Santín, I., Meneses, M., Pedret, C., Barbu, M., and Vilanova, R. (2023). Nitrous oxide reduction in wastewater treatment plants by the regulation of the internal recirculation flow rate with a fuzzy controller. *Journal of Water Process Engineering*, 53:103802.

Santos, S. B., Carvalho, C., Azeredo, J., and Ferreira, E. C. (2014). Population dynamics of a Salmonella lytic phage and its host: Implications of the host bacterial growth rate in modelling. *PLoS ONE*, 9(7):e102507.

Séka, M. A., Kalogo, Y., Hammes, F., Kielemoes, J., and Verstraete, W. (2001). Chlorine-susceptible and chlorine-resistant type 021N bacteria occurring in bulking activated sludges. *Applied and Enviromental Microbiology*, 67(11):5303–5307.

Shao, Y. and Wang, I. N. (2008). Bacteriophage adsorption rate and optimal lysis time. *Genetics*, 180(1):471–482.

Shao, Y. J., Starr, M., Kaporis, K., Kim, H. S., and Jenkins, D. (1997). Polymer addition as a solution to Nocardia foaming problems. *Water Environment Research*, 69(1):25–27.

Shapiro, J., Machattie, L., Eron, L., Ihler, G., Ippen, K., and Beckwith, J. (1969). Isolation of pure lac operon dna. *Nature*, 224(5221):768–774.

Sharma, S., Chatterjee, S., Datta, S., Prasad, R., Dubey, D., Prasad, R. K., and Vairale, M. G. (2017). Bacteriophages and its applications: an overview.

Sharp, R. (2001). Bacteriophages: biology and history. *Journal of Chemical Technology & Biotechnology*, 76(7):667–672.

Sheik, A. G., Machavolu, V. R. K., Seepana, M. M., and Ambati, S. R. (2022). Integrated supervisory and override control strategies for effective biological phosphorus removal and reduced operational costs in wastewater treatment processes. *Chemosphere*, 287:132346.

Shivaram, K. B., Bhatt, P., Applegate, B., and Simsek, H. (2023). Bacteriophage-based biocontrol technology to enhance the efficiency of wastewater treatment and reduce targeted bacterial biofilms. *Science of The Total Environment*, 862:160723.

Sieiro, C., Areal-Hermida, L., Pichardo-Gallardo, Á., Almuiña-González, R., De Miguel, T., Sánchez, S., Sánchez-Pérez, Á., and Villa, T. G. (2020). A hundred years of bacteriophages: Can phages replace antibiotics in agriculture and aquaculture?

Siekmann, I., Malchow, H., and Venturino, E. (2008). An extension of the Beretta-Kuang model of viral diseases. *Mathematical Biosciences & Engineering*, 5(3):549–565.

Silverman, A. I., Peterson, B. M., Boehm, A. B., McNeill, K., and Nelson, K. L. (2013). Sunlight inactivation of human viruses and bacteriophages in coastal waters containing natural photosensitizers. *Environmental science & technology*, 47(4):1870–1878.

Simpson, J., List, E., and Dunbar, J. (1991). Bulking sludge: A theory and successful case histories. *Water and Environment Journal*, 5(3):302–311.

Soddell, J. A. and Seviour, R. J. (1990). Microbiology of foaming in activate sludge plants. *Journal of applied Bacteriology*, 69(2):145–176.

Stefanakis, A., Bardiau, M., Trajano, D., Couceiro, F., Williams, J., and Taylor, H. (2019). Presence of bacteria and bacteriophages in full-scale trickling filters and an aerated constructed wetland. *Science of the total Environment*, 659:1135–1145.

Summers, W. C. (1999). *Felix dHerelle and the origins of molecular biology*. Yale University Press.

Suttle, C. A. (2007). Marine viruses — major players in the global ecosystem. *Nature reviews microbiology*, 5(10):801–812.

Svircev, A., Roach, D., and Castle, A. (2018). Framing the future with bacteriophages in agriculture.

Switzenbaum, M., Plante, T., and Woodworth, B. (1992). Filamentous bulking in massachusetts: extent of the problem and case studies. *Water Science and Technology*, 25(4-5):265–271.

Tandoi, V., Rossetti, S., and Wanner, J. (2017). *Activated sludge separation problems: theory, control measures, practical experiences*. IWA Publishing.

Tejaswini, E., Panjwani, S., and Rao, A. S. (2020). Design of hierarchical control strategies for biological wastewater treatment plants to reduce operational costs. *Chemical Engineering Research and Design*, 161:197–205.

Toledo, M. I. (2022). Determinación de los parámetros de operación en la producción de bacteriófagos para el control en procesos industriales. Master's thesis, Pontificia Universidad Católica de Valparaíso.

Twort, F. W. (1961). An investigation on the nature of ultra-microscopic viruses. *Acta Kravsi*.

United Nations, U. (2019). Water and Sanitation - Sustainable Development Goals.

United Nations, U. (2023). The sustainable development goals report 2023.

Verhulst, P.-F. (1838). Notice sur la loi que la population suit dans son accroissement. *Correspondence mathematique et physique*, 10:113–121.

Villaverde, A. F. (2019). Observability and structural identifiability of nonlinear biological systems. *Complexity*.

Villaverde, A. F., Tsiantis, N., and Banga, J. R. (2019). Full observability and estimation of unknown inputs, states and parameters of nonlinear biological models. *Journal of the Royal Society Interface*, 16(156):20190043.

Volterra, V. (1926). Fluctuations in the abundance of a species considered mathematically. *Nature*, 118:558–560.

Wagner, F. (1982). Study of the causes and prevention of sludge bulking in germany. *Bulking of activated sludge(edited by Chambers and Tomlinson). Ellis Horwood Ltd, Chichester*, pages 29–46.

Wang, I.-N. (2006). Lysis timing and bacteriophage fitness. *Genetics*, 172(1):17–26.

Wang, I.-N., Dykhuizen, D. E., and Slobodkin, L. B. (1996). The evolution of phage lysis timing. *Evolutionary Ecology*, 10:545–558.

Wang, L., Liu, Y., Li, J., Liu, X., Dai, R., Zhang, Y., Zhang, S., and Li, J. (2010). Effects of Ni 2 + on the characteristics of bulking activated sludge. *Journal of Hazardous Materials*, 181(1-3):460–467.

Weber-Dąbrowska, B., Mulczyk, M., and Górski, A. (2001). Bacteriophage therapy of bacterial infections: an update of our institute's experience. *Inflammation*, pages 201–209.

Weitz, J. S. (2016). *Quantitative viral ecology: dynamics of viruses and their microbial hosts*. Princeton University Press.

Withey, S., Cartmell, E., Avery, L. M., and Stephenson, T. (2005). Bacteriophages - Potential for application in wastewater treatment processes. *Science of the Total Environment*, 339(1-3):1–18.

Wu, C., Li, W., Wang, K., and Li, Y. (2015). Usage of pumice as bulking agent in sewage sludge composting. *Bioresource Technology*, 190:516–521.

Yahya, M., Hmaied, F., Jebri, S., Jofre, J., and Hamdi, M. (2015). Bacteriophages as indicators of human and animal faecal contamination in raw and treated wastewaters from tunisia. *Journal of applied microbiology*, 118(5):1217–1225.

Yang, Q., Zhao, H., and Du, B. (2017). Bacteria and bacteriophage communities in bulking and non-bulking activated sludge in full-scale municipal wastewater treatment systems. *Biochemical Engineering Journal*, 119:101–111.

Zambrano, J., Krustok, I., Nehrenheim, E., and Carlsson, B. (2016). A simple model for algae-bacteria interaction in photo-bioreactors. *Algal Research*, 19:155–161.

Zhen, G., Pan, Y., Lu, X., Li, Y.-Y., Zhang, Z., Niu, C., Kumar, G., Kobayashi, T., Zhao, Y., and Xu, K. (2019). Anaerobic membrane bioreactor towards biowaste biorefinery and chemical energy harvest: Recent progress, membrane fouling and future perspectives. *Renewable and Sustainable Energy Reviews*, 115:109392.

Zornoza, A. M. (2017). *Estudio de la dinámica poblacional de protistas, metazoos y bacterias filamentosas y su interpretación ecológica en fangos activos*. PhD thesis, Universitat Politècnica de València.